Measuring and Modeling Drainage in North Idaho Forest Water Reclamation Facilities

A Thesis
Presented in Partial Fulfillment of the Requirements for the
Degree of Master of Science
with a
Major in Environmental Science
in the
College of Graduate Studies
University of Idaho
by
Madeline R. Clark

Approved by:
Major Professor: Mark Coleman, Ph.D.
Committee Members: Erin Brooks, Ph.D.; Robert Heinse, Ph.D.
Department Administrator: Lee Vierling, Ph.D.

August 2022

Abstract

A growing human population requires sustainable options to regulate and dispose municipal wastewater. In northern Idaho, wastewater treatment facilities are permitted by the Idaho Department of Environmental Quality to apply reclaimed wastewater to areas of forest during the growing season. One of the intentions of this land application is to dispose the reclaimed wastewater while protecting the quality of nearby freshwaters. To avoid excess irrigation, the Idaho Department of Environmental Quality provides facilities with monthly hydraulic loading rates. Drainage measurements below the rooting zone provide quantifications of deep soil drainage, allowing for an assessment of drainage patterns during the growing and non-growing season. No drainage occurred throughout two months of the seasonal drought, but large magnitudes of drainage were recorded during the shoulder months of the growing season. To predict drainage in plots where drainage measurements were not possible, we quantified potential drainage in irrigated forests using hydrological models (Hydrus-1D and Water Erosion Prediction Project). Hydrus-1D and Water Erosion Prediction Project were successful at predicting observed and potential drainage during the growing season. There was not a statistically significant difference between the measured monthly drainage data and the predicted monthly drainage values during the growing season. However, the models were less effective or incapable of precise non-growing season drainage estimates. Annual measured drainage at control plots differed from measured drainage at effluent plots at some facilities. There was large variation in annual measured drainage between effluent plots at four of the facilities. As shown through the models, the estimated crop coefficient recommended by the Idaho Department of Environmental Quality is sufficient in avoiding drainage during the growing season in north Idaho forest systems. Potential drainage is predicted to begin following the treatment season and the start of the autumn wet-season. Drainage quantification is a necessary component to calculate the nutrient flux of forests irrigated with reclaimed wastewater. Based on the findings in this study, there is an elevated risk for nutrient leaching to nearby freshwaters with large magnitudes of drainage occurring during the shoulder months of the growing season and throughout the non-growing season.

Acknowledgments

A big thanks to all involved in this project: my advisor Dr. Mark Coleman, committee members Dr. Erin Brooks & Dr. Robert Heinse, Eureka Joshi, facility managers, neighboring landowners, undergraduate assistants. Thanks to the USDA for the grant that funded this project and METER Group for the gift of five drain gauges used in this project.

Dedication

A massive thanks to my wonderful family, fiancé, and friends for all the support during the last 2.5 years. Thank you to my mom, Yvonne, for frequently sending me pictures of our pets, my dad, Patrick, for words of support during challenging times and helping build the handmade drain gauges involved in this project, and my brothers, Anthony and Trevor, for our entertaining group chats and helping me install the prototype for the drain gauges used in this project. Thank you to my amazing fiancé, Eric, for constantly pouring confidence into me and being my #1 fan. Thank you to all of my friends who never wavered in their support, even if they didn't fully understand what my research was about. Even though she was a part of the official acknowledgements, Eureka became an amazing friend (and mind reader) – thanks for all the ice cream, coffee, and beer we've shared together. Finally, I rekindled my love for reading during the last year of this study, so thank you to the many books I read for leisure – you provided the escapism I needed.

Table of Contents

Abstract ii

Acknowledgments iii

Dedication iv

List of Tables vii

List of Equations viii

List of Figures ix

Chapter 1: Introduction and Background 1

Wastewater Land Application 2

Processes Involved with Water Uptake of Conifers 3

Measuring Drainage 3

IDEQ Regulations for the Land Application of Wastewater 4

Water Movement in Forest Soils 6

Effects of Wastewater on Soil Properties 7

Wastewater Irrigation of Forests 8

Hydrologic Models 10

Description of Project 13

Chapter 2: Measuring Drainage in North Idaho Water Reclamation Facilities 14

Introduction 14

Materials/Methods 16

Results 27

Simulated Model Runs 33

Discussion 35

Conclusion 40

Chapter 3: Conclusion 41

Appendix A: Average Soil Bulk Density Measurements & Three-Way ANOVA Test 44

Appendix B: Handmade Drain Gauge Construction 45

Appendix C: Install Data Loggers, Water Level Sensors, and Soil Water Potential Sensors...............47

Appendix D: Collect Data and Water Samples...49

Appendix E: Soil Water Potential and Temperature Measurements...50

Appendix F: Irrigation Distribution Heat Maps...58

Appendix G: Hydrus-1D and WEPP Analysis Table 66

Literature Cited 67

List of Tables

Table 1: Climate information for all five facilities. 17

Table 2: Soil descriptions and overstory and understory compositions for all five facilities. Joshi and Coleman unpublished data. 18

Table 3: Descriptive statistics for 10 cm and 50 cm depths at control and effluent drain gauge plots. Hourly soil temperature and soil water potential data for all drain gauge plots are found in Appendix E. Some soil water potential measurements exceeded the device's range of accuracy. Accurate soil water potential measurements for Terros 21 sensors ranged from -9 kPa to -100 kPa, and for MPS-2 sensors ranged from -10 kPa to -100 kPa. 28

Table 4: Monthly drainage totals (cm) collected in drain gauges during 2021. Values of "N/A" were missing data as a result of faulty water level sensors and/or dead batteries in data loggers that occurred during the entire month. Values containing ">" represent drainage that exceeded the capacity of the drain gauge, faulty water level sensors, and/or dead batteries in data loggers at some point during the month. "C" represents "control" non-irrigated plots and "E" represents "effluent" irrigated plots. The "C" plots contained handmade drain gauges. The first column under each "E" was an irrigated plot that contained a G3 drain gauge and the second column was an irrigated plot that contained a handmade drain gauge. A three-way ANOVA test revealed there was a statistically significant interaction between the effects of facility and treatment type on observed monthly drainage ($p = 0.01$), and a statistically significant effect of month on observed monthly drainage ($p < 0.05$). 31

List of Equations

Equation 1: Forest water balance equation calculation for drainage. 3
Equation 2: Nash-Sutcliffe efficiency equation. 26

List of Figures

Figure 1: Map of five wastewater facilities involved in study. 17

Figure 2: Average daily evapotranspiration (ET) rate of reference crop (alfalfa) per month in 2021. The red line refers to evapotranspiration rates for Cave Bay and Heyburn State Park, and the black line refers to evapotranspiration rates for Ellisport Bay, Bottle Bay, and Garfield Bay. 20

Figure 3: Diagram of a passive-wick drain gauge and its components. 21

Figure 4: Average measured LAI for control (C) and effluent-irrigated (E) plots at each facility. Two-way ANOVA test showed a significant interaction of facility and treatment type on LAI. 27

Figure 5: Irrigation distribution per irrigated plot over two week periods. Plot numbers in the 300's were located at Ellisport Bay, 400's were located at Bottle Bay, and 500's were located at Garfield Bay. Plots at Heyburn State Park were not irrigated at the time of measurement and measurements at Cave Bay were not able to be analyzed as the irrigation logs were not provided by the time of data analysis. The standard error for across all plots was +/- 0.35 cm. One-way ANOVA test produced a p-value <0.05 for the effect of site on plot irrigation distribution. 29

Figure 6: Irrigation distribution heat maps for two irrigated plots containing drain gauges at Garfield Bay. Black circles delineate the plot area, colored dots show locations of rain gauges, and black dots show locations of drain gauges. Irrigation distribution heat maps for all irrigated plots found in Appendix F. 30

Figure 7: The total daily difference in observed and predicted drainage during the growing season for all drain gauge plots using Hydrus-1D. The top heatmap compared the single-porosity van Genuchten-Mualem model drainage with observed daily drainage, and the bottom heatmap compared the Durner dual-porosity model drainage with observed daily drainage. Root water uptake and evapotranspiration were excluded from model predictions. 32

Figure 8: Observed and predicted values of monthly drainage during the growing season at all drain gauge plots except for two effluent irrigated drain gauge plots at Cave Bay due to lack of daily irrigation logs. Root water uptake and evapotranspiration were excluded from calibrated model predictions. Blue points are Hydrus-1D-predicted drainage and red points are WEPP-predicted drainage. The blue dotted line is best fit for the Hydrus-1D and the red dotted line is best fit for WEPP. Solid gray line is 1:1 line. A regression analysis revealed that there was not a statistically significant difference in monthly drainage values between the collected data and predicted values for each model. 33

Figure 9: Box-and-whiskers plot comparing all drain gauge observed monthly drainage (cm) and WEPP-predicted monthly drainage (cm) during the non-growing season months for all facilities.

Monthly drainage data for January, February, March, November, and December. Root water uptake and evapotranspiration were included in simulated model predictions. A regression analysis showed that there was a statistically significant difference in non-growing season monthly drainage values between the collected data and WEPP-predicted drainage values. A one-way ANOVA revealed that there was not a significant different in observed and WEPP-predicted monthly drainage values between facilities ($p = 0.353$). 34

Figure 10: Predicted monthly drainage (mm) from Hydrus-1D simulated runs. Root water uptake and evapotranspiration were included in simulated model predictions. A three-way ANOVA showed a significant interaction effect of facility location, treatment type, and month of growing season on predicted monthly drainage ($p < 0.05$)..35

Chapter 1: Introduction and Background

Wastewater is an unavoidable product of populated areas around the world. While the wastewater that humans produce is increasing every year, the amount of clean water needed for everyday tasks is diminishing. Treating municipal wastewater to return it to a healthy, drinkable state is costly and time consuming, which is why it is more economically-friendly for wastewater reclamation facilities to process this waste to a certain extent (EPA, 2012). Instead of irrigating crops with precious drinkable water, treated wastewater can be applied to agricultural land and supply not only water to the crops, but nutrients as well. This application has proven to be advantageous for many crops (Singh, Deshbhratar, & Ramteke, 2012). For water reclamation facilities, this land management practice is economically beneficial and practical (Al-Jamal, Sammis, Mexal, Picchioni, & Zachritz, 2002). The Idaho Department of Environmental Quality (IDEQ) has set regulations for wastewater reclamation facilities in Idaho to follow when planning to irrigate areas with treated municipal wastewater (IDEQ, 2007). Forests are another ecosystem that may be effective at taking up this wastewater safely and productively. The potential economic benefit from irrigating forests could be large, considering forestry products are in demand. However, there is limited information specifically on how this water flows through forest ecosystems at individual tree and watershed levels (Birch, Emanuel, James, & Nichols, 2016).

The contents of this report provide supplemental information in the following topic areas related to the irrigation of treated wastewater in forests and the effects of that type of application on the hydrologic budgets and soils of forest systems. Regional forest water reclamation facilities around Lake Coeur d'Alene and Lake Pend Oreille in North Idaho have been irrigating forests with secondary treated wastewater for varying amounts of time, with the longest application occurring for almost 45 years and the youngest occurring for about nine years. These water reclamation facilities set aside some of the treated wastewater and irrigate nearby forest plots with the water throughout the growing season. Previous studies conducted on the irrigation of wastewater on crops and forests supply the essential history and background of this land practice. I consider the processes of water uptake in conifers that are the driving factors of water movement from the soil and through a tree. When soil is has reached its water holding capacity, it drains below the rooting zone further into the soil profile. This water can be difficult to measure and I discuss the latest technologies in hydrologic models and devices where there are new opportunities to measure and estimate drainage. The Idaho Department of Environmental Quality regulations for the land application of wastewater provides guidelines for proper hydraulic loading rates of wastewater irrigation so that soil saturation does not occur. I evaluate that guidance with respect to the effects this land application has on soil properties and forest hydrologic budgets. In conjunction with collected data, I examine the use of hydrologic models in providing predictions on how this land application on forest systems is affecting soil-water drainage.

Wastewater Land Application

Many wastewater reclamation facilities are using a more cost-effective way to manage municipal wastewater without treating it to a drinking water level. The process of reclaiming wastewater to a drinking water level requires costly and time consuming processes and water quality tests. Before this water can be safely returned to surface water supply, it must go through the initial, secondary, and tertiary treatments at a water reclamation facility (EPA, 2012). After those processes are completed, quality control tests are conducted to determine whether the water is safe to return to surface water supply, where it can eventually be distributed to households and businesses. However, wastewater facilities can apply treated wastewater to delineated areas of land by just running the municipal sewage through primary and secondary water treatments. The wastewater facilities in northern Idaho treat the waste they receive with aeration and chlorination processes, which make up the main components of the primary and secondary water treatment procedures. When administered correctly, this application of treated wastewater provides vital nutrients and water to an ecosystem (IDEQ, 2007). Because this treated wastewater contains two limiting factors of plants (nutrients and water), this kind of land application is desirable in the domain of agriculture. Land managers are able to irrigate and fertilize their crops by applying treated wastewater to their fields, which has proven to be a very useful tactic for various crop types (J. Wang, Wang , & Wanyan, 2007).

Agricultural crop growth and water use are most frequently studied in response to wastewater treatment. A variety of ground crops have increased their yield with supplemental wastewater irrigation (Singh et al., 2012; J. Wang et al., 2007). Deciduous trees like poplars have also become recipients of treated wastewater irrigation (Isebrands & Richardson, 2014). In 1985, hybrid poplar plantation managers in British Columbia began applying treated wastewater to their fields. They suggested that by applying this irrigation to fast-growing trees there would be certain advantages compared to applying it to ground crops (Carlson, 1992). It was proposed that because hybrid poplar trees had deeper roots and a high leaf area index with a large above-ground surface area, these trees would improve percolation, reduce surface runoff, and have higher evapotranspiration rates (Isebrands & Richardson, 2014). Other benefits of irrigating trees include an extended growing season that would allow for more wastewater to be irrigated, and probable decrease in system operations and maintenance costs due to the tree plantations requiring less frequent irrigation cycles

(Kuhn, 2000). These advantages for irrigating trees in an agricultural setting can also be applied to natural stands of conifers, making forest systems a good fit for this land application.

Processes Involved with Water Uptake of Conifers

For applied reclaimed wastewater to have sufficient time to react with soil and avoid generating runoff and leaching, transpiration via plants must occur at an efficient rate. The driving force of transpiration is the gradient in water potential between leaves and the soil, which has a less negative water potential. This is created by evaporative loss occurring through the stomata. This gradient between the air and soil prompts water to flow from the roots to the crown of the tree (Taiz & Zeiger, 2002a). There is always a demand for water uptake in conifers due to the atmospheric exchange processes involved with transpiration (Waring, Running, Holbo, & Kline, 1979). Precipitation and irrigation replenish the soil's water content and restore the water potential gradient between the roots and soil.

The sapwood of trees allows transport of water used in the transpiration process. Sapwood is the portion of the vascular tissue that conducts water in conifers. The force needed to pull water up a tree through the sapwood is provided by the evaporation of water through the stomata. The sapwood in conifers is also a large reservoir for water storage, especially during dry summer months. The stem water storage in the sapwood has daily fluctuations, which can be progressively depleted during periods of drought when soil-water storage is not being replenished (Matheny et al., 2015). With the application of treated wastewater during dry periods, the sapwood in irrigated conifers would potentially be able to stay recharged, without excess drainage occurring below the root zone.

Measuring Drainage

The hydrologic cycle in a forest ecosystem can be summarized with a simple water balance equation totaling the inflow and outflow of water resulting in a change in soil water storage (ΔS) (see Equation 1). Processes like wastewater irrigation (I) and precipitation (P) are included in the inflow of water, and evapotranspiration (ET) of conifers, surface runoff (R), and soil drainage (D) constitute the outflow component (Waring, Rogers, & Swank, 1980). These processes can be measured through the use of various technologies, however, quantifying the outflow of water through soil drainage is difficult to measure so it is often determined using the water balance equation.

$$D = I + P - ET - R - \Delta S$$

Equation 1: Forest water balance equation calculation for drainage.

Instruments such as lysimeters can be installed to collect the drainage that occurs below the root zone. Measurements from lysimeters have been used to provide input data and compare drainage estimates with various hydrologic models (Ferro & Tammi, 2009; Van Der Heijden et al., 2013). One type of lysimeter is a passive-capillary wicking lysimeter. These lysimeters incorporate a passive wick comprised of inert material situated between the soil and collection chamber. Through capillary action, the passive wick creates a suction related to wick length, allowing for drainage collection in unsaturated soil conditions (Hall, 2018). Drain gauges are a type of passive-capillary wicking lysimeter used soil drainage needs to be measured. They are useful for collecting more accurate site-specific drainage compared to the water balance approach (Ferro & Tammi, 2009). These passive-capillary wicking lysimeters are assumed to quantify the volume of water that is draining from the root zone into groundwater. The drainage is able to be reliably recorded at a set timestep using a water level sensor and data logger (Gee, Zhang, Ward, & Keller, 2004). The ease of water collection with this device also allows for drainage to be sampled and analyzed for various constituents (METER, 2020).

IDEQ Regulations for the Land Application of Wastewater

The Idaho Department of Environmental Quality has laid out steps to calculate hydraulic loading rates for applying reclaimed wastewater. The hydraulic loading rate is the monthly volume of wastewater added to an area. As a basic rule, the IDEQ states that “water application rates should not exceed the soil infiltration [capacity]” which would prevent any excess runoff from occurring. IDEQ also implies that leaching past the rooting zone should not occur as a result of this land application. That general rule applies regardless of whether the facility is irrigating during the growing season or non-growing season. Regional forest water reclamation facilities only irrigate during the growing season, which is favored over irrigating during the non-growing season. The IDEQ requires permitted facilities to irrigate wastewater well below the estimated crop irrigation water requirement (IDEQ, 2007). The estimated irrigation water requirement is calculated using a historic average monthly crop evapotranspiration rate. Crop evapotranspiration rates are calculated using a crop coefficient and a reference crop evapotranspiration rate. Generally, alfalfa is used as the reference crop with a crop coefficient of 1. All other crops have a crop coefficient that relates the proportion of the reference crop’s evapotranspiration rate to obtain the other crop’s expected evapotranspiration rate (Docktor & Palmer, 1994). If a crop such as a conifer has an unknown evapotranspiration rate, the IDEQ recommends using a general crop coefficient of 0.7 with a reference evapotranspiration rate (IDEQ, 2007). Because these guidelines are based on cropland systems that typically receive reclaimed wastewater, it makes it difficult to accurately determine how much water is appropriate to load onto a forest system without exceeding its soil infiltration rate.

Regardless of how much total water is irrigated, the addition of wastewater to forest systems may be done through either an IDEQ approved high-rate or slow-rate system. According to the IDEQ handbook, a high-rate system of rapid infiltration is applied to permeable soils, which allows higher infiltration rates and larger volumes of treated wastewater to be applied over areas of land. This system relies on the chemical, physical, and biological processes in the soil profile to treat the wastewater as it percolates through the profile (IDEQ, 2007). While this method of hydraulic loading may be effective for coarser textured soils, it is not utilized in studies as commonly as the slow-rate system (Lee et al., 2020). The IDEQ recommends slow-rate systems be used specifically with forests because those systems tend to result in a more thorough and efficient treatment of wastewater irrigation (IDEQ, 2007). Slow-rate systems utilize sprinklers to spray the land surface with treated wastewater with the intent to support plant growth. Similar to the high-rate system, the slow-rate system employs chemical, physical, and biological processes occurring throughout the soil profile, as well as processes in the plant-soil matrix. The overall sustainability of the irrigated forest depends on the area's soil depth, minimum depth to ground water, soil permeability, slope, and the existing or planned land use (IDEQ, 2007). Slow-rate systems are especially effective for silt and clay soils because it allows these soils that have naturally slower infiltration rates to have the necessary time to allow for the wastewater to flow throughout the soil column. If too much wastewater is irrigated, the soil can become saturated with water and solutes, creating an anaerobic environment in the soil profile. Under this condition, the roots cannot respire and therefore transport less water (Drew & Lynch, 1980). This system also enables any soil microbial and chemical processes to have ample time to occur.

With the water reclamation facilities located in northern Idaho having irrigation sites near large freshwater lakes, there is a potential for the nutrients in the wastewater to leach into those systems. In order to maintain an ecosystem's integrity, constituent loading rates must be regulated to avoid nutrient leaching throughout the year. The two constituents that are mostly of focus when irrigating crops with wastewater are nitrogen and phosphorous because these are two nutrients that commonly limit plant growth and production (J. Wang et al., 2007). Excess nitrogen and phosphorus in water sources stimulate algae blooms, which deplete oxygen concentrations for aquatic life (NRC, 2012). Phosphorus is accumulated in the upper layers of soil as it is relatively immobile, while nitrogen can be present in the soil as forms of nitrite, nitrate, and ammonium. Multiple forms of nitrogen are subject to leaching, therefore it cannot, or is unable to be efficiently absorbed by plants (Brockway, Urie, Nguyen, & Hart, 1986). By utilizing slow-rate systems for irrigating wastewater, plants are able to have more time to absorb constituents like nitrogen and phosphorous from the water, and soil microbes are also able to process those nutrients (Dimitriou & Aronsson, 2011). Calculations for leaching losses during the growing season are provided to regulators and land managers in the IDEQ guidelines. There is also the danger of the soil's physical properties deteriorating when the soil particles can no longer conduct conventional chemical reactions when it is overloaded with salts (Bond, 1998). The IDEQ also states that "rest periods" are essential for facilitating soil-nutrient driven processes and preventing soil clogging. The IDEQ allows regulators and land managers to determine when and how often these rest periods take place at the irrigated locations. The combination of having calculated measures of leaching losses and runoff prevention measures and structures is the most beneficial way to prevent nutrient leaching with treated wastewater irrigation (IDEQ, 2007). Collected drainage can be measured and sampled for constituent concentrations and used to calculate nutrient flux data to determine the current constituent loading rate is appropriate.

Water Movement in Forest Soils

Water movement in forest soils is influenced by hydraulic conductivity, soil texture, macropores, and preferential flow paths. Hydraulic conductivity is a measure of the ability of a fluid to move through soil, making it a soil property involved with water flow. In forest soils, the hydraulic conductivity is governed by the soil texture and structure, which explains the mixed conclusions of how hydraulic conductivity is affected by treated wastewater irrigation (Leuther, Schlüter, Wallach, & Vogel, 2019; Vogeler, 2009). The proportion of clay, silt, and sand particles forms the soil's texture, which is practically unchangeable. Finer textured soils exposed to long-term reclaimed wastewater treatment tend to have a more reduced hydraulic conductivity as a result of soil pore clogging. However, for more sandy soils, treated wastewater irrigation has been shown to increase the connectivity of macropore networks, allowing for more leaching to occur through the soil (Leuther et al., 2019). Texture plays a large role in the hydraulic conductivity of a soil.

Macropore pathways in subsoil layers of forests are mainly due to the extensive underground root system of conifers. Living roots obstruct and alter vertical and downslope water flow, while decomposed root channels provide vertical porous zones in forest soils (Noguchi et al., 1997). The more mature roots of conifers contain hydrophobic materials, encouraging water to move alongside those channels (Taiz & Zeiger, 2002b). Belowground insect and organism channels also create soil macropore networks (Noguchi et al., 1997). The quantity of soil macropores is also related to the soil's hydraulic conductivity. Studies have found that regions in a soil column with high hydraulic conductivity indicate a higher amount of macropores in the area, whereas regions with low hydraulic conductivity indicate a higher amount of micropores in the area (Leuther et al., 2019; Noguchi et al., 1997; Vogeler, 2009).

The flow and transport of water and other substances are primarily influenced by the preferred paths in soils. Preferred pathways constitute preferential flow in soils, which results in uneven and rapid movements of water and solutes, typically in vertical and downslope directions (Hornberger, Germann, & Beven, 1991; Noguchi et al., 1997). Hydraulic conductivity provides a measured value of preferential flow in soils. While soil invertebrates are another common contributor of preferred pathways in soil, root channels are abundant throughout soil columns in forest ecosystems. Because conifers have broad root systems that promote preferential flow, the preferential flow model successfully explains the flow and transport of water and solutes in forest soil systems (Hornberger et al., 1991).

Effects of Wastewater on Soil Properties

Along with a soil's hydraulic conductivity, the soil water storage of a forest is heavily influenced by soil texture. As stated above, the hydraulic conductivity of a soil is determined by its particle composition, which determines the pore space available for water, air, and solutes to move throughout the soil profile. Patterns of soil water storage develop in response to precipitation patterns and growing seasons of plants. With most Pacific Northwest forests, there is a seasonal drought during the growing season. This lack of precipitation combined with the trees' seasonal water uptake creates a soil water potential gradient that controls soil water movement during that season. Deeper roots tend to have a larger contribution to conifer water uptake during seasonal droughts as the soil water potential in shallower soil layers becomes more negative (Warren, Meinzer, Brooks, & Domec, 2005). When treated wastewater is applied to a forest, the effect of the added nutrients, such as nitrogen, can decline with the soil's saturated hydraulic conductivity, and therefore alter the forest's soil water storage capability (Sparling et al., 2006).

To sustain an ecosystem's integrity, the hydraulic loading capacity of the area that will receive this irrigation must be analyzed. Saturating a soil with treated wastewater can lead to excess runoff, which can have large consequences to regions downslope (IDEQ, 2007). The salts and nitrogen concentration in treated wastewater also affect soils. A surplus of salt and nitrogen may saturate a soil's cation exchange capacity and risks leaching these constituents. There is also the danger of the soil's physical properties deteriorating when the soil particles can no longer conduct conventional chemical reactions when it is overloaded with salts (Bond, 1998). While the negative consequences of treated wastewater on a soil's physical properties can occur, it is difficult to predict how these properties will be affected due to the complicated relations between many soil factors and treated wastewater.

Soils that have been treated long-term with irrigated wastewater have different physical properties, some of which are positively impacted. A study conducted by Vogeler in 2009 assessed the effects of long-term wastewater irrigation on silt loam and sandy soils. The soils at the wastewater irrigation in northern Idaho sites are very similar to those that Vogeler analyzed – various loams and sands. Wastewater-irrigated soils displayed higher aggregate stability and higher internal soil strength, both of which are positive soil physical property alterations. The increases in aggregate stability and internal soil strength are a result of a shift to micropores in the soil, due to the larger pores being occupied by salt and other nutrients (Vogeler, 2009). These results provide promising outcomes for the overall sustainability of this kind of land management practice at wastewater irrigation sites.

The alteration of the physical properties of a soil plays a large role in the ability to hold water in a soil profile. Infiltration rates in soils irrigated with treated wastewater are observed to largely decrease, with the main conclusion that the soil pores are clogged due to an increase in microbial activity from the influx of nutrients in the water (Magesan, 2001). Decreases in the number macropores in a soil column can prompt decreases in infiltration rates, which can lead to ponding and potentially, runoff. All of these factors combined decrease the water storage capacity of a soil. The amount drainage will increase for a soil profile with a decrease in its water storage capacity, and with treated wastewater being irrigated on that soil, the risk of nutrients leaching with that increase drainage is elevated (Cook, Kelliher, & McMahon, 1994).

Wastewater Irrigation of Forests

Forests in the inland Northwest are largely limited by the nutrients and water they receive, which are crucial inputs for vegetation during the growing season (Gessel, Miller, & Cole, 1990). In response to irrigation and fertilizer applied together, annual growth of *Pinus radiata* stands increased (Benson, Myers, & Raison, 1992). By applying treated wastewater to forest systems, the productivity of forests may also be increased. Increased tree growth in coniferous forests has been documented in the years following the application of treated wastewater (Brockway et al., 1986; Gessel et al., 1990). Conifers, such as Douglas-firs, respond well especially to the nutrients in treated wastewater (Brockway et al., 1986; Gessel et al., 1990).

Studies on forests treated with municipal wastewater have been conducted with varying levels of irrigation and nitrogen concentration, however very few of these studies are able to look at a long time series of the effects of this action. There is a lack of studies in the literature that compares the drainage measurements at various forest wastewater irrigation sites over assorted lengths time. Previous studies have analyzed the application of treated wastewater over a limited time series in a forest system and the single irrigation of a forest with treated wastewater (Kim & Burger, 1997; Lee et al., 2020). While these studies provide supportive conclusions on wastewater irrigation, it is important to look at the effects from this long-term land practice may have. Another previous study was conducted on two New Zealand soil types over two different time series, however there was no assessment that focused on the differing length of application period (Vogeler, 2009). Evaluation of time-series data is crucial for regulators and water reclamation facility managers to assess the sustainability of this practice in a forest ecosystem.

At the individual tree level, the addition of water and nutrients allows for the affected trees to grow at faster rate. The ratio of a plant's growth to its evapotranspiration rate comprises that plant's water use efficiency. For poplars, the application of treated wastewater increased the trees' height and stemwood volumes, and was predicted to increase evapotranspiration rates (Carlson, 1992). With conifers, the effect of additional nutrients on water use efficiency is complicated. Douglas-fir stands in southwestern Oregon exposed to five years of reclaimed wastewater irrigation showed an increased volume growth of about 70% (Gessel et al., 1990). In another study of a one-time application of nitrogen fertilizer, Douglas-firs were found to have an increase in both growth and transpiration two years after the application. The increased availability of nitrogen was predicted to significantly increase water use efficiency as a potential result of plants being more controlled by the need for nutrients from the soil than by the drive to obtain carbon dioxide from the atmosphere (Lee et al., 2020). These outcomes may be more realistic for the conifers at our sites because treated wastewater is irrigated multiple times throughout the growing season, providing the trees with increased access to nutrients.

The key to making this land management practice successful is finding a balance in the water flux of a forest. A forest's water flux comprises of the overall water use efficiencies of its vegetation along with the soil's physical properties. In agreeance with the IDEQ guidelines, it is imperative that the water use efficiency of trees that are receiving treated wastewater be thoroughly understood in order to make this application sustainable. While forests in the inland Northwest are water limited, it's important to have accurate water outflow estimations to prevent over-irrigation and soil saturation. This can lead to unwanted consequences, such as nutrient leaching and subsurface runoff (Birch et al., 2016).

There is a potential risk of drainage and nutrient leaching during the wet season. As precipitation and snowmelt events occur, the soil moisture content increases throughout the profile. Elevated soil moisture content during the wet season results in the development of preferential flow pathways that greatly increase soil infiltration rates (Hardie et al., 2011). This risk of drainage is especially high during spring thaw events. When air temperature reaches above 0°C, snowmelt can rapidly infiltrate to all soil depths (Sutinen, Hänninen, & Venäläinen, 2008). The increased infiltration that occurs during the wet season may result in excess leaching of nutrients deposited through the reclaimed wastewater irrigation.

Hydrologic Models

Hydrologic models help define the complexities of hydraulic processes, which is important as it can be difficult to measure and quantify these processes. The type of models used for forests vary depending on what factors are being looked at. The Physiological Principles Predicting Growth (3-PG) model is a forest growth process model, and the BILJOU model is a forest water balance model. Both models have successfully modeled water fluxes, carbon sequestration, and nutrient leaching fluxes when applied to forest systems (Lee et al., 2020; Van Der Heijden et al., 2013). Although the 3-PG and BILJOU models are both designed specifically for forest system use, there are other non-ecosystem specific hydrologic models, such as Hydrus-1D and Watershed Erosion Prediction Project (WEPP), that can also be applied to forests. Hydrus-1D models one-dimensional movement of water and solutes through variously saturated soil media (Ramos et al., 2011; Van Der Heijden et al., 2013; Šimůnek, van Genuchten, & Šejna, 2008). WEPP is a complex hydrology and erosion simulation model that assessed land management impacts on various hydrological and environmental factors (Brooks, Dobre, Elliot, Wu, & Boll, 2016; Dun et al., 2009; Elliot, 2013; Srivastava, Wu, Elliot, & Brooks, 2015). WEPP is also able to assess potential impacts of future climates and changes of management practices on specified areas of land. Both of the Hydrus-1D and WEPP models were chosen to be utilized in this study because of their versatility in the fields of forestry and hydrology.

Hydrus-1D has exhibited exceptional capability to model a variety of hydrologic factors and processes in forest ecosystems. When compared to the results from a water tracer experiment conducted on a forest soil, Hydrus-1D accurately modelled preferential flow paths once the soil parameter values have been accurately calibrated to produce similar results to observed data. This model can also successfully compute nutrient leaching fluxes, especially when paired with in-field measurements. (Van Der Heijden et al., 2013). Hydrus-1D can analyze hydrologic processes that occur in soils at a more complex level compared to other simpler models. The success of this modeling complexity is dependent on the specific parameters it requires (Wongkaew, Saito, Fujimaki, & Šimůnek, 2018).

Hydrus-1D has been proven to be successful in simulating water and solute transport of irrigation waters containing different salinities and nitrogen concentrations (Ramos et al., 2011). The ability for users to enter multiple input parameters for a location allows for versatility in the use of this model. Hydrus-1D can simulate the movement of water and multiple solutes through the use of modified hydrologic equations and function, which allows for further calibration if needed (Šimůnek et al., 2008). The ability for calibration of parameters such as evapotranspiration rate, delineation of soil layers, and root water uptake is especially important when fine-tuning this model for forest systems.

While Hydrus-1D is a dependable tool for simulating water transport, the results of Hydrus-1D could be further refined by calibrating the input parameters. As with other models, Hydrus-1D model results can be improved with site-specific physical soil properties. Because there are numerous wastewater sites around Lake Coeur d'Alene and Lake Pend Oreille with a variety of soil textures, it is important for each site to be represented through multiple model runs in order to refine each site's soil input parameters. For Hydrus-1D to model the water flow at project-specific sites, the hydraulic parameters for the soil at each site must be entered into the Hydrus-1D input parameters. Aside from direct measurements of soil property parameters taken at each site for this study, there is still a need for site-specific soil hydraulic parameters.

The RETC model is designed to supplement Hydrus-1D by calculating site-specific hydraulic parameters based on soil textural properties. RETC allows users with limited access to the hydraulic property data of a soil to enter soil bulk density, texture, and water content information into the program and get predicted hydraulic conductivity data based on the fittings of analytical functions (Šimůnek et al., 2008). Combined with data from the USDA's Natural Resources Conservation Service's interactive Web Soil Survey application, users can gather the necessary soil properties, such as bulk density, texture, and water content needed to run a function in RETC. RETC will be used to gather the program-predicted calculations of hydraulic conductivity at the control and treated wastewater irrigation sites and input those into the Hydrus-1D model runs.

One of the most important calibrations needed for the input parameters of Hydrus-1D is the crop evapotranspiration rate within the study area. This can be calculated using a reference evapotranspiration rate and a crop coefficient (Docktor & Palmer, 1994). For most agricultural crops, there are calculated reference crop coefficients, which allow for the calculation of that specific crop's crop coefficient. However, there are not calculated crop coefficients for conifers in forests or the various species of trees (Petersen & Hill, 1985). And while there are some crop coefficients for deciduous trees, such as poplars and various fruit trees (Di et al., 2019; USBR, 2022), conifers in these forests may have a very different evapotranspiration rate than those types of trees due to differences in physiological structure, canopy conductance, and boundary layers in forest systems. An equation for calculating crop coefficients for small evergreens has been created, but it was done so on an agricultural scale at a Christmas tree farm (Petersen & Hill, 1985). Hydrus-1D provides a way to test the accuracy of various evapotranspiration rates when the drainage flux is also known. Being able to measure the hydraulic loading and drainage of conifers at specific sites will allow for the accurate calculation of a crop coefficient for conifers.

WEPP is another model that has previously been used in forest ecosystems. It has been used primarily for modeling soil erosion and sediment loading of watersheds. It is frequently utilized by forest managers to predict soil erosion and events that can facilitate soil erosion, such as wildfires (Elliot, 2013). The WEPP model's ability to simulate streamflow and sediment transport in forest watersheds is exceptional when specific input parameters regarding climate, pollutant concentrations, groundwater storage, and baseflow are provided (Brooks et al., 2016).

WEPP can model the hydrologic processes of forest ecosystems even though its original purpose was to model watershed erosion. WEPP has recently been modified to accurately model subsurface lateral flow and soil water percolation when modeling water balances of a watershed (Brooks et al., 2016; Dun et al., 2009). WEPP is able to differentiate between surface runoff, subsurface lateral flow, and baseflow, which are crucial components to the water balance of an area (Brooks et al., 2016). For the wastewater irrigation sites in northern Idaho that apply treated wastewater loaded with various solutes, WEPPcloud allows for some inclusion of solute concentrations in the model, which may be useful for analyzing the transport of these solutes in the watershed (Lew et al., 2022).

Part of the improvements made to WEPPcloud have been established with the creation of the WEPP-Water Quality (WEPP-WQ) model. WEPP-WQ is able to model deep soil percolation, which makes this a valuable tool for this type of land application. An evaluation of this model has concluded that WEPP-WQ is performing well when simulating nutrient and sediment losses for single storm events (L. Wang, Flanagan, & Cherkauer, 2017). The water drainage collected at wastewater application sites will provide the necessary data for WEPP-WQ to model the flow and transport of solute concentrations from the treated wastewater.

As with the Hydrus-1D model, crop coefficients for conifers are needed in order to better calibrate the WEPP model for water balance predictions. WEPP calculates actual evapotranspiration of a watershed through a reference evapotranspiration rate using the Penman-Monteith method. It is highly recommended that the evapotranspiration rates of stands included in the selected watershed be measured in order to provide accurate information for WEPP (Srivastava et al., 2015). For forests containing various coniferous species and ages, it's difficult to accurately predict an area's actual evapotranspiration rates (Pangle, Kavanagh, & Duursma, 2015), even with the Penman-Monteith method.

As seen in Lee et al., 2020, 3-PG model predictions for multiple factors in a nitrogen fertilized forest system agreed well with in-field measurements of those factors. The success of models like 3-PG predictions will encourage others to use it and similar forestry-based models for future research. Because there will be in-field measurements with this project, this is an ideal opportunity to evaluate the performance of the WEPP model for forest ecosystem drainage. A comparison of the Hydrus-1D and WEPP models to direct drainage measurements is especially important for future use of wastewater irrigation in forest systems – it will allow land managers interested in this type of wastewater application to assess the capability of an area to handle this practice.

Other studies have looked at the effects of treated wastewater irrigation on forest biomass production (Gessel et al., 1990), plant nutrient uptake (Brockway et al., 1986; Cromer, 1980), and soil physical properties (Cook et al., 1994; Leuther et al., 2019; Vogeler, 2009), but there is a lack of hydrologic studies on quantifying drainage in wastewater irrigated coniferous forests. It is important to assess the drainage flow of natural forests because of the potential large-scale environmental impacts that this type of land management can induce on the landscape. If the trees are truly efficient at consuming this wastewater, then this application would be a valuable way for other water reclamation facilities to dispose treated wastewater. By calibrating the Hydrus-1D and WEPP models for the northern Idaho forest ecosystems, a usable support tool will be available for land managers throughout the region to be able to assess which areas will be ideal locations for this kind of land management practice.

Description of Project

This project involves five regional water reclamation facilities in northern Idaho that are irrigating plots of forest with treated wastewater. Each facility has been irrigating plots of land around Lake Coeur d'Alene and Lake Pend Oreille for a various number of years ranging from seven to 45 years. Also, the loading rates of wastewater that each facility applies to their plots varies by facility, as well as the constituent concentrations. Multiple drain gauges were installed throughout the control and treatment sites to collect drainage data throughout the year. These measurements provide data for the input parameters needed to run the Hydrus-1D and WEPP models. The objectives for this project are to 1) measure the quantity and spatial variation of drainage at forest water reclamation facilities and 2) calibrate the Hydrus-1D and WEPP models to be used as support tools for drainage predictions.

Chapter 2: Measuring Drainage in North Idaho Water Reclamation Facilities

Introduction

As the growing human population produces more wastewater, it is imperative to develop sustainable and efficient ways of employing water reclamation. Water treatment facilities can effectively treat municipal wastewater without polluting nearby freshwater reservoirs through tertiary level treatment. Treating municipal wastewater to a secondary level results in the water containing plant growth-limiting nutrients, such as nitrogen and phosphorous. While these nutrients have beneficial values for terrestrial plants, if they elevate concentrations of freshwater bodies over a short time period, it may result in toxic algal blooms depleting oxygen for aquatic life (NRC, 2012). It is costly to remove these nutrients and safely dispose the treated water into freshwater sources, requiring a more affordable method of reuse. A cost-effective and resourceful management option for municipal wastewater reuse is irrigating secondary-treated wastewater onto designated areas of land (EPA, 2012).

Reclaimed wastewater irrigation is a cost-effective method to dispose secondary-treated wastewater, while simultaneously providing crops with supplemental irrigation during the growing season. Many conventional crops can benefit from the addition of reclaimed wastewater irrigation and show increased yields (Singh et al., 2012; J. Wang et al., 2007). Besides conventional crops, reclaimed wastewater irrigation has also been successfully used on some deciduous tree crops (Isebrands & Richardson, 2014). Along with poplars and willows, deciduous forests in the eastern United States have also been irrigated with reclaimed wastewater (Brister & Schultz, 1981; Kim & Burger, 1997). Because deciduous forests have been irrigated with reclaimed wastewater, it is believed that coniferous forests are also able to accommodate this land application. Coniferous forests in the Inland Northwest are water-limited due to annual seasonal droughts, making reclaimed wastewater irrigation a reasonable solution to replenish soil-water storage and provide trees with critical nutrients (Gessel et al., 1990; Schmidt, Mainwaring, & Maguire, 2020).

Irrigating crops with reclaimed wastewater requires irrigation scheduling guidelines. Methods used to outline irrigation schedules for a crop include plant stress measurements, soil water measurements, and soil water balance calculations (Jones, 2004). Soil water balance calculations can be used in computer models to produce crop-specific irrigation schedules (Al-Jamal et al., 2002). In Idaho, the IDEQ uses soil water balance calculations to determine monthly irrigation rates for crops receiving reclaimed wastewater. The Idaho Department of Environmental Quality (IDEQ) is the governing body that grants irrigation permits to these facilities. For permitted crop irrigation rates, an irrigation water requirement (IWR) is calculated for each month during the growing season. The IWR is a soil water balance calculation that estimates the amount of water required by a crop to efficiently sustain evapotranspiration and plant water requirements (IDEQ, 2007). For forest systems, the IWR is a function of the available water holding capacity of a soil and the evapotranspiration rates of vegetation. The data used to calculate IWRs are based on historic monthly evapotranspiration and precipitation rates and are fixed values in the permits. The permits also require that each month, the applied amount of wastewater irrigation must be "substantially less" than the monthly IWR (IDEQ, 2007). Two ways to maintain a level of irrigation substantially below the monthly IWR is through the use of crop coefficients and the incorporation of rest periods. A crop coefficient is a determined proportion that relates a reference crop evapotranspiration rate to another crop's estimated evapotranspiration rate (USBR, 2022). This estimated crop evapotranspiration rate is essential to prevent over-irrigation. Rest periods are a duration of time without irrigation, and are recommended by IDEQ to prevent soil saturation. Rest periods generally occur during weekends and after substantial precipitation events, however, the timing and duration of rest periods are determined by facility regulators and land managers (IDEQ, 2007). The inclusion of rest periods and irrigating well-below monthly IWRs are the main components in the irrigation schedule guidelines for forest water reclamation facilities in Idaho.

Deep soil drainage is a component of soil water balance calculations that is difficult to measure. Previous studies conducted on forests treated with reclaimed wastewater have not quantified deep soil drainage. These studies have primarily focused on the effects this application has on plant growth and production (Brockway et al., 1986; Gessel et al., 1990). Birch et al. (2016) evaluated the wastewater composition of streamflow, groundwater, and surface water in a coniferous forest irrigated with reclaimed wastewater, but did not assess the quantitative values of drainage. It is necessary to evaluate the magnitude of drainage in forests receiving this irrigation because of the potential large-scale environmental impacts this land practice can inflict on the surrounding landscape. A major environmental risk with reclaimed wastewater irrigation is nutrient leaching. While soils are drier during the seasonal drought, soil moisture increases during the wet season and with applied irrigation as water infiltrates into the soil profile. This increase in soil moisture content elevates the risk for nutrient leaching as water can rapidly percolate through soil pores and preferential flow pathways (Hardie et al., 2011; Lai, Liao, Feng, & Zhu, 2016). Measured soil drainage rates provide data to quantify the amount of nutrient leaching that is occurring in wastewater-irrigated forests.

Historically, soil drainage has been measured using pan lysimeters. A pan lysimeter is a reservoir buried under the soil surface exposed to the soil above. Pan lysimeters are not very efficient at collecting drainage, as their design encourages water to divert around the device. The significant drainage diversion reduces the efficiency of this device by almost 90% (Gee et al., 2004). Another device used to measure soil drainage is a passive-wick lysimeter. These lysimeters differ from pan lysimeters in that passive-wick lysimeters contain a wicking material that maintains a fixed tension on the bottom of the soil above the device. The tension produced by the wick pulls the water from the soil column above the lysimeter to the reservoir, keeping the soil in an unsaturated state (Gee et al., 2004). The inclusion of the wick in the design of the passive-wick lysimeter allows the device to capture more drainage than pan lysimeters, making these passive-wick lysimeters more accurate in quantifying deep soil drainage (Zhu, Fox, & Toth, 2002). When compared to other lysimeter types, studies show that passive-wick lysimeters tend to over-estimate deep soil drainage during times of increased precipitation (Meissner, Rupp, Seeger, Ollesch, & Gee, 2010).

In this study we used multiple drain gauges to measure drainage, parameterized hydrologic models, and predicted potential drainage occurring at five north Idaho forest water reclamation facilities. These facilities have been irrigating areas of forest with secondary-treated wastewater for various time periods, with the earliest facility established in 1978 and the newest facility established in 2013. The main objectives of this study are 1) measure the rate and spatial variability of drainage within and across sites irrigating forests with reclaimed wastewater during the non-growing and growing season and 2) assess potential hydrologic models (Hydrus-1D and WEPP) to be used as a support tool to predict potential drainage in locations receiving irrigation. We hypothesize that drainage measured from drain gauges will not be significantly different between irrigated and non-irrigated plots within facilities. We also hypothesize that using the crop coefficient recommended by the IDEQ handbook, forests can assimilate permitted irrigation rates during the growing season. If we can validate that forests are efficient at consuming reclaimed wastewater, then this application would be an effective way for water reclamation facilities to discard treated wastewater.

Materials/Methods

Study Area

The forest water reclamation facilities involved in this study are located around lakes Coeur d'Alene and Pend Oreille in northern Idaho (Figure 1, Table 1). The mean annual temperature for all five sites are very similar, with the mean minimum temperature at all sites ranging within -5 and -6°C. The sites around Lake Coeur d'Alene – Heyburn State Park and Cave Bay – are dominated by *Pinus ponderosa* and *Pseudotsuga menziesii*, while the sites around Lake Pend Oreille – Bottle Bay, Garfield Bay, and Ellisport Bay – are dominated by *Thuja plicata* (Table 2). The soils across all five sites contain loess and most contain volcanic ash. The sites around Lake Pend Oreille have nearly identical soils.

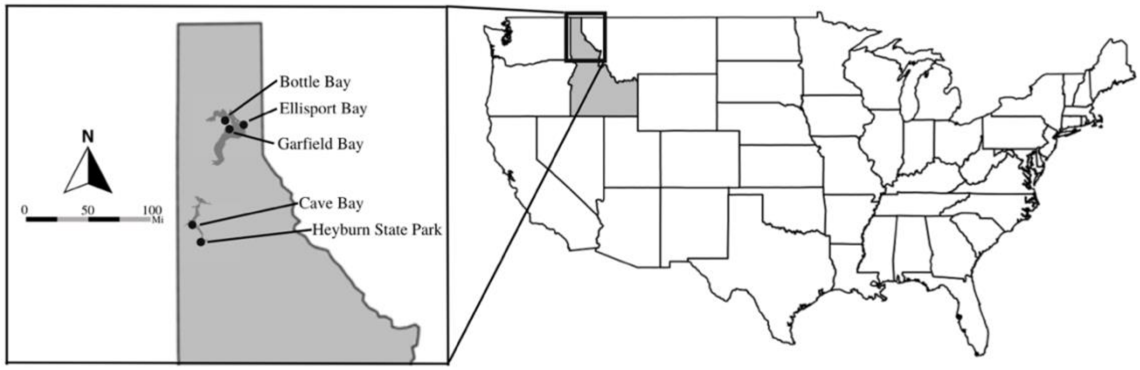

Figure 1: Map of five wastewater facilities involved in study.

Table 1: Climate information for all five facilities.

Facility	Location	Establishment Date	Mean Annual Precipitation (cm)	Mean Annual Temperature (°C)	Mean Maximum Temperature (°C)	Mean Minimum Temperature (°C)
Cave Bay	Worley, ID	2013	53.4	8.4	19.6	-5.1
Heyburn State Park	Plummer, ID	2010	66.3	8.2	19.4	-5.2
Ellisport Bay	Hope, ID	2000	63.3	7.7	18.8	-5.6
Bottle Bay	Sagle, ID	1989	75.2	7.4	27.4	-5.7
Garfield Bay	Sagle, ID	1978	70.9	7.4	27.4	-5.8

Table 2: Soil descriptions and overstory and understory compositions for all five facilities. Joshi and Coleman unpublished data.

Facility	Soil Description	Overstory Composition	Understory Composition
Cave Bay	Loess and/or colluvium oven bedrock derived from basalt	Pinus ponderosa, Pseudotsuga menziesii	Physcocarpus opulifolius, Symphoricarpos albus, Holodiscus discolor
Heyburn State Park	Volcanic ash over loess	Pinus ponderosa, Pseudotsuga menziesii	Physcocarpus opulifolius, Symphoricarpos albus, Holodiscus discolor
Ellisport Bay	Volcanic ash and/or loess over till derived from granite and/or metamorphic rock	Thuja plicata, Pseudotsuga menziesii, Tsuga heterophylla, Abies grandis, Larix occidentalis, Betula papyrifera	Mahonia repens, Polystichum munitum, Rubus idaeus
Bottle Bay	Volcanic ash and/or loess over till derived from granite and/or metamorphic rock	Thuja plicata, Pseudotsuga menziesii, Abies grandis, Larix occidentalis, Betula papyrifera, Acer glabrum	Physcocarpus opulifolius, Symphoricarpos albus, Holodiscus discolor
Garfield Bay	Volcanic ash and/or loess over till derived from granite and/or metamorphic rock	Thuja plicata, Pseudotsuga menziesii, Tsuga heterophylla, Abies grandis, Larix occidentalis, Betula papyrifera	Mahonia repens, Holodiscus discolor

A total of ten plots (0.1 ac diameter) were established at each of the five sites – five plots located within the forest wastewater management units and five plots located outside of those zones on non-irrigated forested land either upslope from irrigate plots or otherwise isolated hydraulically. Each plot in a wastewater irrigation (effluent) area was matched up to a plot in a non-irrigated (control) area by cruising the non-irrigated areas for stands with similar tree species and stand structure to the irrigated plots.

Data Collection

Soil bulk density, leaf area index (LAI), and irrigation distribution measurements were taken at each plot. Soil samples to measure bulk density were collected with a 4.91 cm diameter bulk density soil sampler (AMS Inc., American Falls, ID, U.S.A.) at two locations in each plot at three depths: 0-15 cm, 15-45 cm, and 45-75 cm (Appendix A). Soil bulk densities of the three depths were calculated by dividing the dry weight by the known volume of the sample. LAI measurements collected for each plot were used to estimate plot-specific throughfall percentages. LAI was measured at each plot using the LAI-2200C Plant Canopy Analyzer (LI-COR, Lincoln, NE, U.S.A.) and following the protocol associated with the device. Light level measurements for LAI values were collected during a session either within one hour after sunrise or one hour before sunset. Because light levels were measured under indirect sunlight conditions, a light correction factor did not need to be included in the measurements. All ten plots at a facility were measured during a single session. An above canopy sensor was set up on a tripod in an open area outside of the forest canopy and at least two tree heights from the nearest canopy to measure incident light above the canopy. A below canopy sensor was attached to the console held by the researcher collecting transmitted light at each plot. Both sensors were fitted with 270° lens caps to appropriately capture light levels under the indirect sunlight conditions. The above canopy sensor was also programmed to auto-log light level measurements, which ensured above and below canopy light levels were measured at the same time. Light levels were measured in 20 random locations at each plot. Plot LAI measurements were calculated using the LAI-2200C software.

To collect irrigation distribution data and analyze irrigation uniformity, rain gauges were installed in irrigated plots during the growing season. Ten 5-inch capacity rain gauges (Forestry Suppliers Inc., Jackson, MS, U.S.A.) were arranged in a plot sampling grid. Each rain gauge was mounted 1.2 m above the ground. Rain gauges were partially filled with mineral oil to prevent evaporation during the collection period. The rain gauges were installed at a facility for two weeks after which the collected irrigation was manually recorded.

Daily irrigation logs were obtained through annual reports submitted to IDEQ by each facility following the 2021 growing season. At the time of writing, only four annual reports were available, resulting in missing data from Cave Bay. At all facilities, irrigation was distributed using solid set lateral sprinklers with an irrigation application efficiency ranging from 65-85% (IDEQ, 2007). The sprinklers were set up along multiple transects in the management zones designated for irrigation. Along transects, the spacing between sprinkler heads was consistent, but the distance between sprinkler heads and irrigation lines varied by facility. The distance between sprinkler heads ranged from 12 to 24 m at any facility. The height of the sprinkler nozzle was consistent throughout each facility, and varied between about 0.75 and 4.5 m above the ground surface, depending on facility. The angle of the nozzle also varied between locations and ranged from 90° to 150°, which created a coverage area for each sprinkler of between about 6 to 12 m. Daily reference crop evapotranspiration rates were collected from nearby AgriMet stations (USBR, 2022). Daily precipitation data for Hydrus-1D model runs were collected for georeferenced facility locations from PRISM Climate Group (PRISM, 2022; USBR, 2022). Daily precipitation data for WEPP model runs were gathered for georeferenced facility locations from WEPPcloud (WEPPcloud, 2022). The closest AgriMet station to the sites around Lake Coeur d'Alene was Liberty Lake, Washington Weather Station and the closest station to the sites around Lake Pend Oreille was Silverwood WWTP Athol, Idaho

Weather Station (Figure 2). Liberty Lake Weather Station is within 27 and 42 km and within 369 and 418 m elevation of the Lake Coeur d'Alene sites. Silverwood WWTP Athol Weather Station is within 39.5 and 47 km and within 489 and 511 m elevation of the Lake Pend Oreille sites.

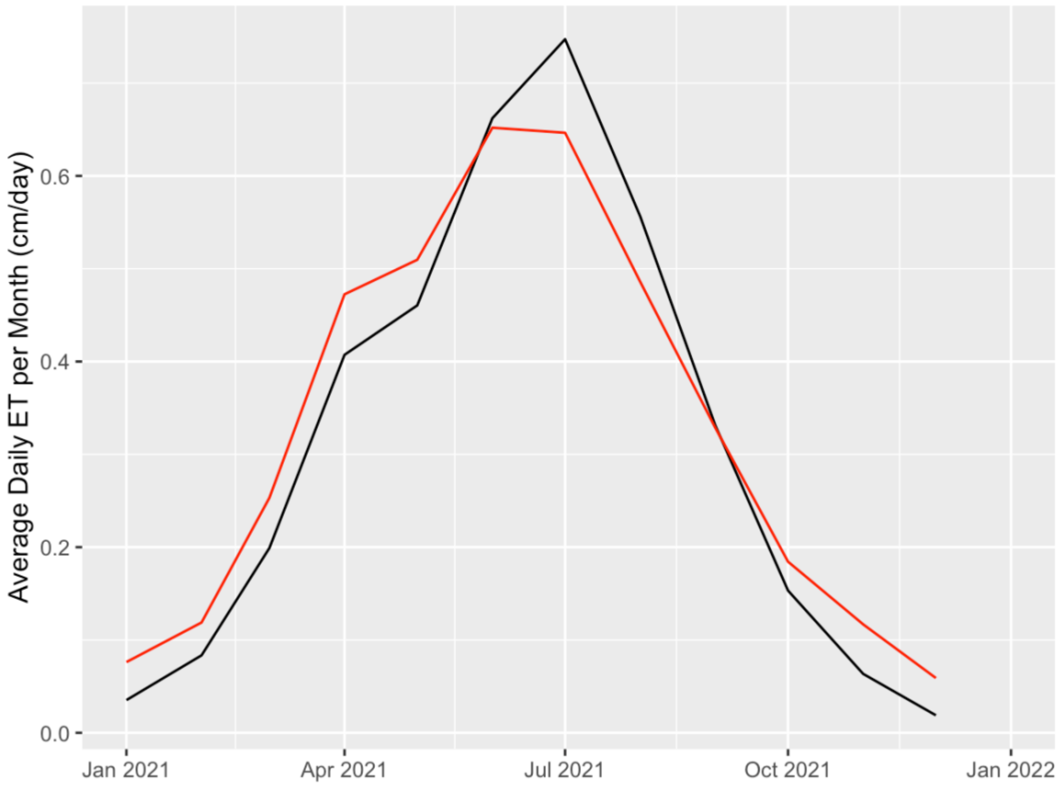

Figure 2: Average daily evapotranspiration (ET) rate of reference crop (alfalfa) per month in 2021. The red line refers to evapotranspiration rates for Cave Bay and Heyburn State Park, and the black line refers to evapotranspiration rates for Ellisport Bay, Bottle Bay, and Garfield Bay.

Passive-wick drain gauges (Gee et al., 2004) were used to measure the amount of drainage occurring below the tree rooting zone at the five sites. These devices were made up of three main components: a diversion tube, a wick, and a reservoir (Figure 3). The diversion tube provided an intact and representative soil monolith for water and nutrients to naturally pass through. From there, the applied tension from the wick guided the water into the reservoir where it was stored until the reservoir was emptied. The water level in the reservoir was measured to record drainage every hour.

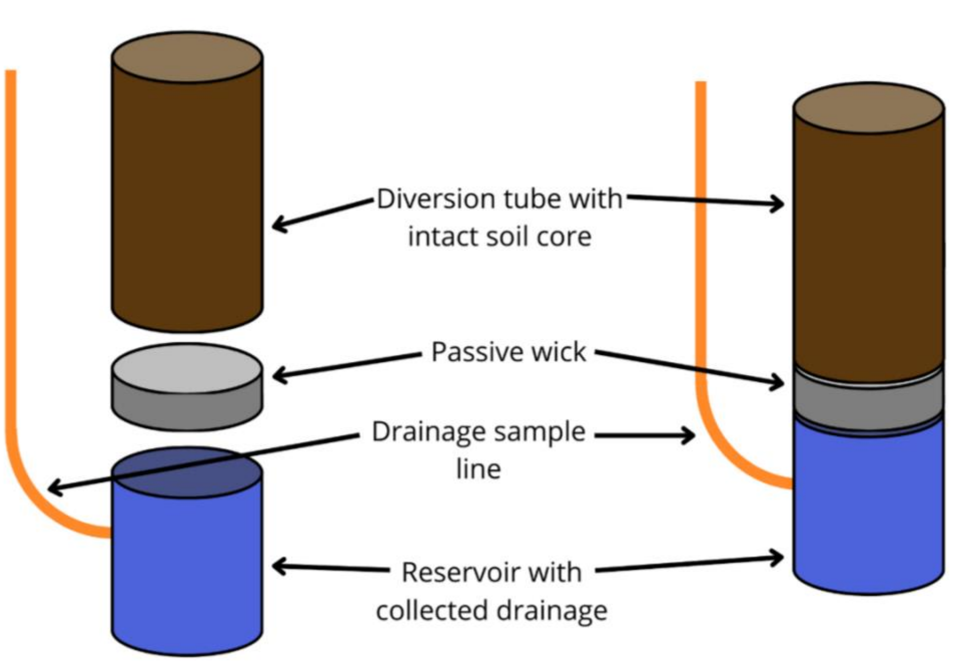

Figure 3: Diagram of a passive-wick drain gauge and its components.

Three of ten plots at each site were equipped with drain gauges with two drain gauges installed in irrigated plots and one installed in a non-irrigated plot. Two types of passive-wick drain gauges were installed: one was commercially-built (G3 drain gauge, METER Group, Pullman, WA, U.S.A.) and one was constructed based on the protocol from Hall, 2018 (“handmade” drain gauge). The G3 drain gauge had a reservoir water depth capacity of 100 mm and the handmade drain gauge had a reservoir water depth capacity of 234 mm. The G3 drain gauges were furnished with a steel diversion tube and a reservoir with a self-contained wick. The protocol followed for constructing a handmade drain gauge included a steel diversion tube that was fabricated from rolled 11 gauge steel pipe, 25 cm (10 in) in diameter and 63.5 cm (25 in) long (Appendix B). The handmade diversion tube size was based on the G3 dimensions, thus both types had identically sized diversion tubes.

The G3 and handmade drain gauges were both installed in similar manners. Within the boundaries of each drain gauge plot, a 71 cm diameter circle was selected for the installation of the drain gauge. The surface forest litter and the first 20 cm of soil were separately removed from the designated circle and set aside. A skid steer with a 71 cm (24 in) diameter auger was used to drill down 1.8 m deep for the G3 drain gauges and 1.2 m deep for the handmade drain gauges. Throughout the drilling process, dirt was removed from the auger and placed in piles by soil layers. The bottom of the hole was tamped down to approximate the original bulk density and made level. For the G3 drain gauges, the diversion tube was attached to the main G3 drain gauge reservoir with a 3.8 cm (1.5 in) layer of silica flour in between the wick and the diversion tube. The G3 drain gauge was then lowered into the 1.8 m deep hole by strapping it to the skid steer. For the handmade drain gauges, the drain gauge reservoir was first placed and packed into place with soil, a 3.8 cm layer of silica flour was placed on top of it, and the diversion tube was placed on top of the reservoir using the skid steer.

Once a drain gauge was lowered into its respective hole, it was held steady resting on the bottom of the hole while the appropriate soil layers were shoveled and tamped back into the hole to approximate the original bulk density. The handmade drain gauges required an extra step of pouring a thick layer of bentonite around the seam where the reservoir met the soil core atop the plastic funnel to seal and only allow water to enter the bucket through the diversion tube. When the soil surrounding the drain gauge was mostly packed, the plastic covering over the core was removed, and as the packed soil reached the original soil surface, the top 20 cm of forest soil was replaced. The original litter was replaced over the top of the packed soil surface.

A Hydros 21 water level sensor (METER Group, Pullman, WA, U.S.A.) was placed at the base of the drain gauge reservoir. At each drain gauge plot, two Terros 21/MPS-2 soil water potential sensors (METER Group, Pullman, WA, U.S.A.) were installed, a Terros 21 sensor was placed at 10 cm below the soil surface and a MPS-2 sensor was buried below the first one at 50 cm below the soil surface (Appendix C). Hourly drainage data was recorded with the water level sensor and an EM50 data logger (METER Group, Pullman, WA, U.S.A.), which was compiled to obtain daily drainage rates that were summed for monthly drainage rates. The soil water potential and temperature sensors transmitted hourly soil water potential and temperature data to the data logger, which illustrated the daily and seasonal soil water potential and temperature patterns. All sensor data were downloaded from data loggers once a month. Drain gauge reservoirs were also emptied at the same time (Appendix D).

Modeling Drainage

Modeling drainage consisted of model calibration runs and model simulation runs. Model calibration involved conditioning soil input parameters, gathering facility-specific input data, and modifying facility-specific input data ratios to optimize model drainage predictions. Calibration model runs using drain gauge plots were necessary to calibrate the models for the plots where drainage was not measured. Simulation model runs were conducted on all 50 plots to predict drainage based on the calibration model runs. Input soil input parameters for simulation model runs were extracted from calibration model runs. Facility-specific input data was the same across calibration and simulation model runs. Vegetation-related processes were excluded from calibration model runs and included in simulation model runs.

All soil data used to produce soil input parameters, except for soil bulk density, were gathered using Web Soil Survey. Gathered soil input parameters included field capacity, wilting point, and texture at three soil depths: 0-15 cm, 15-45 cm, and 45-80 cm (NRCS, 2022). All listed soil input parameters were used for Hydrus-1D and WEPP model runs, however Hydrus-1D required an additional step for the soil input parameters.

The RETC program processed the soil input parameters for Hydrus-1D model runs. Using the soil input parameters, RETC produced soil water retention function variables for the three soil depths (Clark, 2020c). The soil water retention variables were residual water content (*Qr*), saturated soil water content (*Qs*), α parameter in the soil water retention function (*Alpha*), *n* parameter in the soil water retention function (*n)*, saturated hydraulic conductivity (*Ks*), and tortuosity parameter in the conductivity function (*I*). These soil water retention variables were utilized as soil input parameters in the soil hydraulic property model.

Hydrus-1D also provided a selection of soil hydraulic property models to use for model runs. The options for soil hydraulic property models included single porosity, dual-porosity, and dual-permeability models. The soil hydraulic property model managed the soil water retention curve calculation for a model run. The dual-porosity model better reflected the timing and quantity of observed daily drainage data, and therefore was used for all Hydrus-1D calibration and simulation runs.

Vegetation-related processes involved in the simulated model runs included root water uptake, root distribution, land management selection, and crop coefficients. Hydrus-1D simulated runs incorporated root water uptake, root distribution, and a crop coefficient, and WEPP simulated runs incorporated land management selection and a crop coefficient. A crop coefficient of 0.7 was recommended by the IDEQ guidelines to represent the evapotranspiration rate in a forest (IDEQ, 2007). For Hydrus-1D, the selected root water uptake model was the Feddes model (Feddes, Kowalik, & Zaradny, 1978). The Feddes root water uptake model computes root water extraction at specified depths taking into account potential transpiration rate, plant root depth, and soil water pressure head of the surrounding soil (Hoogland, Feddes, & Belmans, 1981). The root water uptake model involved the root distribution in soil layers. The root distribution in each soil layer was determined from a meta-analysis of root distribution studies (Jackson et al., 1996). Root distribution data from the temperate coniferous forest biome (i.e., $Y = 1 - \beta^d$, $\beta = 0.976$) was used for all plots in this study. The evapotranspiration rates for Hydrus-1D runs were calculated by multiplying the crop coefficient of 0.7 by the AgriMet daily alfalfa reference crop evapotranspiration rates. For simulated WEPP runs, the land management of a 20-year-old forest with a 0.7 crop coefficient was selected.

Hydrus-1D and WEPP models ran on a daily timestep, but started and ended on different days. WEPP model runs began on January 1, 2019 to initialize the model and ran through December 31, 2021. WEPP predicted drainage for the entirety of 2021 (January 1 – December 31). Hydrus-1D model runs began on March 17, 2021 and ran through October 31, 2021. Hydrus-1D predicted drainage during the 2021 growing season (April 1 – October 31). Although Hydrus-1D was able to model snow hydrology, the model was not capable to account for the daily freeze-thaw fluctuations that frequently occurred during the wet season, limiting the modeling timeframe to the frost-free irrigation period.

The initial soil water potential conditions were specified for the first day of calibrated and simulated Hydrus-1D model runs. Because drain gauge plots contained in-plot soil water potential sensors, the soil water potential measurements taken within those plots on April 1, 2021 were used for model runs of those plots. The initial 0 and 80 cm soil water potential conditions used in Hydrus-1D were extrapolated from the 10 cm and 50 cm soil water potential sensor measurements. For effluent plots that did not contain drain gauges, the April 1, 2021 soil water potential measurements from the two effluent drain gauge plots at the same facility were averaged to produce 10 cm and 50 cm soil water potential values. For control plots that did not contain drain gauges, the April 1, 2021 soil water potential measurements collected at the control drain gauge plot at the same facility were supplied as 10 cm and 50 cm soil water potential values. The soil water potential measurements were extrapolated to produce initial 0 and 80 cm soil water potential conditions in the same manner as the drain gauge plots.

The daily output data produced by the models differed between Hydrus-1D and WEPP. Hydrus-1D model runs produced outputs of actual surface flux, actual bottom flux, mean pressure head, inflow through soil profile, and volume of water in the entire profile. WEPP model runs produced many soil-water outputs, which included daily runoff, plant transpiration, soil evaporation, deep percolation, and total soil water. The outputs for daily predicted drainage were “bottom flux” for Hydrus-1D and “deep percolation” for WEPP.

Hydrus-1D and WEPP model runs were calibrated for plots that contained drain gauges during the growing season. The calibration model runs excluded vegetation-related processes, as the drain gauge diversion tubes were assumed to not contain any live roots or vegetation during the time of data collection. Hydrus-1D calibration runs excluded a root water uptake model, root distribution, and daily evapotranspiration rates. WEPP calibration runs eliminated vegetation-related processes by selecting the land management of fallow. Calibration model runs included soil input parameters and facility-specific input data. Facility-specific input data were input to parameterize the models.

Facility-specific input data were comprised of daily precipitation and plot-specific irrigation rates. For drain gauges that received drainage during the growing season, the precipitation and irrigation ratios were adjusted to predict monthly drainage that best matched the observed monthly drainage collected at a plot. For drain gauges that did not observe drainage during the growing season, the precipitation and irrigation ratios were parameterized to the point just before drainage was observed in the models. This was conducted in such a way to provide conservative estimates of the amount of precipitation and irrigation potentially received by the drain gauges. About 15 to 45 calibration runs were conducted for each drain gauge plot, with the optimized precipitation and irrigation ratios producing high NSE and R^2 values and a low RMSE value.

The model setup to calibrate drainage for WEPP during the non-growing season was similar to the set up for the growing season. The non-growing season simulated runs included soil input parameters, facility-specific input data, and vegetation-related processes. However, the precipitation ratio for all plots simulated during the non-growing season was 100% of the daily precipitation rates. Also, the selected land management was that of a 20-year-old forest because the fallow selection used during the growing season model calibrations allowed for minimal deep soil percolation to occur.

Hydrus-1D and WEPP simulated drainage for each of the 50 experimental plots. Simulated runs included soil input parameters, facility-specific input data, and vegetation-related processes. It was necessary to include vegetation-related processes to represent the natural processes affecting drainage in areas outside of the diversion tubes. The same facility-specific input data estimates were used by both models to simulate drainage.

The precipitation and irrigation ratios were estimated at all plots for simulating model runs. The precipitation ratio for simulated Hydrus model runs involved a relationship between LAI and canopy throughfall (Molina & del Campo, 2012), Using data on stemflow in pine forests from previous studies, estimated proportions of stemflow to bulk precipitation measurements were about 1% of the bulk precipitation, which did not significantly affect drainage predictions as it was small in comparison to other fluxes (Fan, Oestergaard, Guyot, Jensen, & Lockington, 2015; Molina & del Campo, 2012). For WEPP simulated model runs, the precipitation ratio remained at 100% due to LAI already being factored into the forest management selection. Irrigation was one of the larger water fluxes at each effluent plot. Although irrigation applications were not uniform within each plot, irrigation was assumed to be uniform in simulated runs to provide an average estimate of drainage. This uniformity assumption accounted for the in-plot hot and cold spots of irrigation. Precipitation and irrigation ratio estimates allowed the simulated runs to represent predicted drainage throughout entire plots instead of a single location within a plot.

Data Analysis

We used several techniques to evaluate the performance of a model. A common model evaluation technique for hydrological models is the Nash-Sutcliffe efficiency (NSE) (Moriasi et al., 2007). It determines the amount of residual variance compared to the observed data variance. NSE was calculated using equation 2:

$$NSE = 1 - \left[\frac{\sum_{t=1}^{n}\left(Y_t^{obs} - Y_t^{pred}\right)^2}{\sum_{t=1}^{n}\left(Y_t^{obs} - \bar{Y}_t^{obs}\right)^2}\right]$$

Equation 2: Nash-Sutcliffe efficiency equation.

where Y_t^{obs} is the observed drainage at month *t*, Y_t^{pred} is the modeled-predicated drainage at month *t*, $\bar{Y}_t^{obs}$ is the mean observed monthly drainage, and *n* is the total number of monthly drainage observations. Pearson's coefficient of determination (R^2) is another technique to evaluate the collinearity between observed and predicted drainage data. R^2 values range from zero to one, with one a perfect linear relationship between the observed and predicted data. Another supporting measurement of residual variance is root mean square error (RMSE). The closer the RMSE value was to zero, the more accurate the predicted monthly drainage was to the observed monthly drainage data. RMSE does not reflect the predictive skill of a model as NSE and R^2 do, instead, RMSE measures the spread of residuals for predicted values compared to observed values.

The best fitting model run for each plot was determined based on the highest NSE value and was supported by the associated R^2 and RMSE values. Model runs containing observed drainage data greater than zero were calibrated to achieve NSE and R^2 values as close to one and RMSE values as close to zero as possible. For model runs with observed data exhibiting no drainage throughout the growing season, an RMSE value of zero was used to determine model parameter optimization as NSE and R^2 are unable to account for datasets containing all zeros.

Multiple analyses of variance (ANOVA) were conducted on the results of this study. A one-way ANOVA test was conducted to compare the effect of facility location on irrigation distribution. A two-ANOVA test was conducted to compare the effects of treatment and facility location on LAI and throughfall. A three-way ANOVA test was conducted to compare the effects of facility location, treatment type, and month on observed monthly drainage. A regression analysis was conducted to test if there was a significant difference between the predicted drainage from the calibrated runs and the observed drainage for each model during the growing season. A three-way ANOVA test was conducted to compare the effects of treatment type, soil depth, and facility location on soil bulk density. A regression analysis was conducted to test if there was a significant difference between observed and WEPP-predicted monthly drainage for the non-growing season. A one-way ANOVA test was conducted to compare the effect of facility on observed and WEPP-predicted monthly drainage for the non-growing season. A four-way ANOVA was conducted to compare the effects of model (Hydrus-1D vs. WEPP), facility, month, and treatment on monthly drainage predictions. Finally, a three-way ANOVA was conducted to compare the effects of facility, month, and treatment on simulation model run monthly drainage predictions.

Results

Plot-Specific Data

LAI and calculated throughfall varied between sites and treatment groups. Individual LAI plot values ranged from 1.53 to 5.84 (Figure 4). Individual throughfall plot values ranged from 16% to 69% of total precipitation (data not shown). Garfield Bay had the highest average LAI and lowest throughfall values for irrigated plots. The highest average LAI for non-irrigated plots was also recorded at Garfield Bay. Bottle Bay had the lowest throughfall values for non-irrigated plots. Heyburn State Park had the lowest average LAI and highest average throughfall values for irrigated and non-irrigated plots. LAI and throughfall values were both significantly different between sites and between control and effluent plots, yet there was a significant interaction indicating the magnitude of the treatment effect depended on facility.

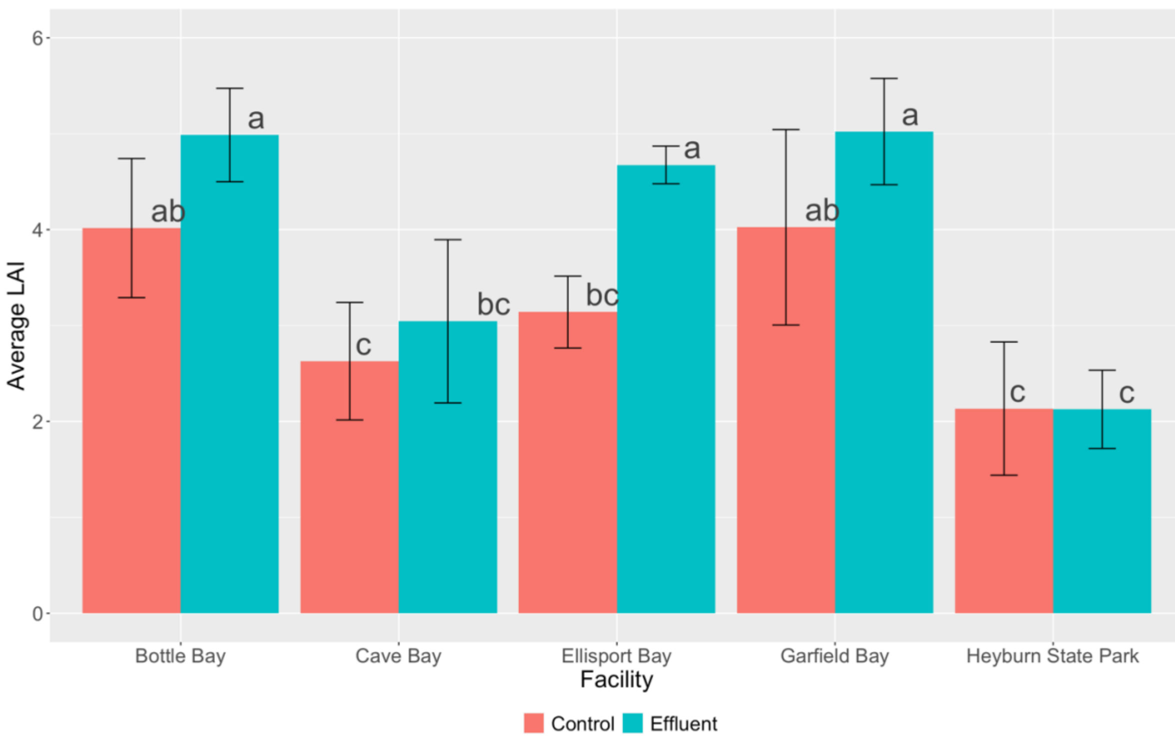

Figure 4: Average measured LAI for control (C) and effluent-irrigated (E) plots at each facility. Two-way ANOVA test showed a significant interaction of facility and treatment type on LAI.

Soil water potential and temperature fluctuated at 10 cm and 50 cm depths throughout the year (Table 3, Appendix E). The soil at both depths stayed relatively wet from the beginning of the year and into the start of the seasonal drought. For most plots, the soil began drying out at 10 cm slightly before it began drying out at 50 cm. Deeper soil was able to contain more moisture than shallower soil depths at the peak of the seasonal drought before the shallower depths were replenished with precipitation and irrigation heading into the wet season. The soil temperature at both depths followed a similar pattern of warming from March into April, until July through August where the warmest soil temperatures were recorded, and then steadily cooling through the end of the year. The 50 cm depth did not reach temperatures as warm as those recorded at the 10 cm depth during the peak of the seasonal drought, and it did not have large daily temperature fluctuations as the 10 cm depth sensor recorded during that time. All plots containing drain gauges showed similar seasonal patterns in soil water potential and temperature.

Table 3: Descriptive statistics for 10 cm and 50 cm depths at control and effluent drain gauge plots. Hourly soil temperature and soil water potential data for all drain gauge plots are found in Appendix E. Some soil water potential measurements exceeded the device's range of accuracy. Accurate soil water potential measurements for Terros 21 sensors ranged from -9 kPa to -100 kPa, and for MPS-2 sensors ranged from -10 kPa to -100 kPa.

Soil Temperature (°C)				
	Control		**Effluent**	
	10 cm	**50 cm**	**10 cm**	**50 cm**
Annual Maximum	23.2 ± 2.5	18.1 ± 1.9	20.8 ± 1.2	16.5 ± 1.1
Annual Minimum	0.0 ± 0.3	1.8 ± 0.4	0.3 ± 0.3	1.5 ± 0.6
Annual Average	8.4 ± 7.0	8.4 ± 6.9	7.8 ± 6.7	7.7 ± 6.9
Growing Season Average	12.6 ± 10.4	11.3 ± 9.2	11.5 ± 9.9	10.2 ± 9.4
Non-Growing Season Average	3.0 ± 2.6	4.5 ± 4.0	3.1 ± 1.7	4.6 ± 3.2
Soil Water Potential (kPa)				
	Control		**Effluent**	
	10 cm	**50 cm**	**10 cm**	**50 cm**
Annual Maximum	-9.0 ± 0.4	-9.0 ± 0.4	-9.0 ± 1.6	-9.0 ± 0.3
Annual Minimum	-100.0 ± 0.0	-100.0 ± 0.0	-100.0 ± 0.0	-100.0 ± 0.0
Annual Average	-42.7 ± 17.9	-46.4 ± 19.4	-39.5 ± 20.6	-36.8 ± 10.4
Growing Season Average	-56.7 ± 21.7	-58.8 ± 14.7	-53.2 ± 20.4	-48.6 ± 14.9
Non-Growing Season Average	-22.8 ± 14.9	-28.9 ± 26.3	-20.0 ± 27.1	-20.0 ± 12.0

Irrigation distribution greatly varied within plots and between plots located at the same facility. The amount of irrigation received in the rain gauges ranged from 0 cm to almost 17 cm (Figure 5). The irrigation distribution at Ellisport Bay was similar between plots in that facility. Multiple rain gauges within plots at Bottle Bay did not receive any irrigation, resulting in the average amount of irrigation collected a rain gauge to be 0.76 cm. Three plots at Garfield Bay had the highest in-plot variability of irrigation distribution across all facilities. Variation of in-plot irrigation distribution was illustrated with heatmaps (Figure 6, Appendix F). Although in-plot irrigation distribution greatly varied, the average distribution of irrigation was significantly different between facilities.

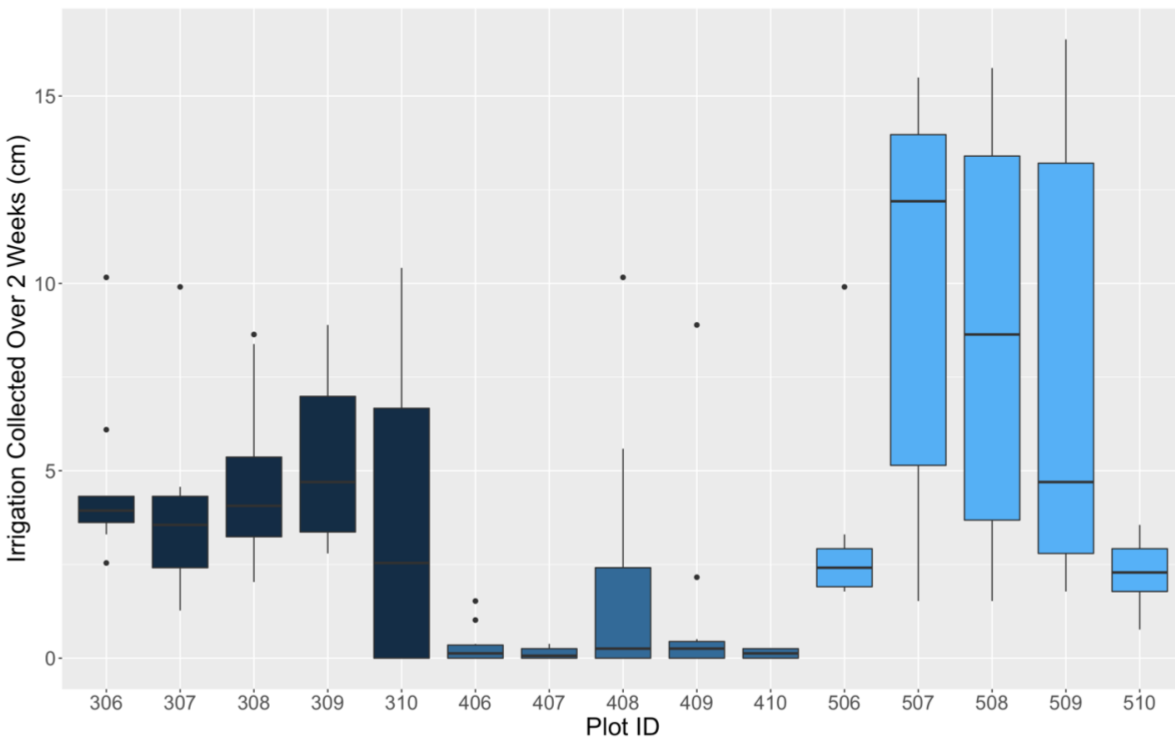

Figure 5: Irrigation distribution per irrigated plot over two week periods. Plot numbers in the 300's were located at Ellisport Bay, 400's were located at Bottle Bay, and 500's were located at Garfield Bay. Plots at Heyburn State Park were not irrigated at the time of measurement and measurements at Cave Bay were not able to be analyzed as the irrigation logs were not provided by the time of data analysis. The standard error for across all plots was +/- 0.35 cm. One-way ANOVA test produced a p-value <0.05 for the effect of site on plot irrigation distribution.

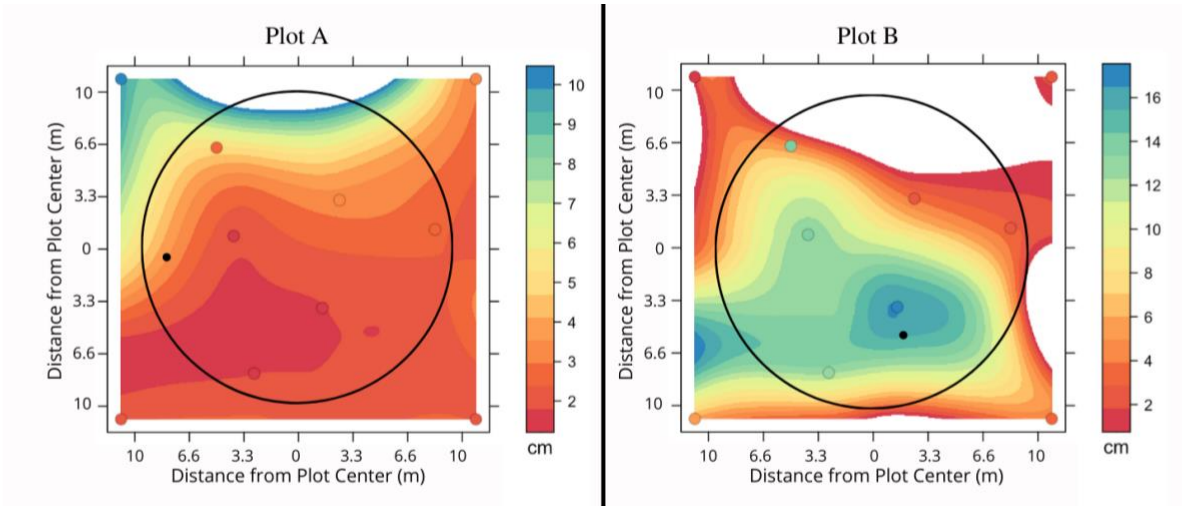

Figure 6: Irrigation distribution heat maps for two irrigated plots containing drain gauges at Garfield Bay. Black circles delineate the plot area, colored dots show locations of rain gauges, and black dots show locations of drain gauges. Irrigation distribution heat maps for all irrigated plots found in Appendix F.

Observed Drainage

In 2021, observed drainage varied between sites, but followed a general pattern throughout the year. Most drainage was observed during the first four and last two months of the year where rain and snow events occurred and affected local snowpack and snowmelt (Table 4). January and December recorded the highest amount of drainage during the year. Many of the monthly totals during the spring thaw (March through April) underestimated drainage because drain gauge reservoirs exceeded capacity hours after being emptied. Because reservoir capacities differed between the handmade and G3 drain gauges, G3 drain gauges with the smaller reservoir volume exceeded capacity quicker than the handmade drain gauges. During the growing season, the highest recorded values of observed drainage emerged during September, when irrigation was being applied and precipitation events became more frequent. A third of the plots did not collect drainage during the 2021 growing season. Of the five plots that did not receive drainage during the growing season, four of them were control plots. The one control plot drain gauge that received drainage was at Ellisport Bay. The Ellisport Bay control plot was an anomaly for collected monthly drainage measurements as it was involved in a timber harvest, which resulted in many of the trees surrounding the drain gauge removed as part of the operation. Regardless of treatment group, the annual drainage pattern observed across all five locations revealed that the majority of drainage occurring during the non-growing season.

Table 4: Monthly drainage totals (cm) collected in drain gauges during 2021. Values of “N/A” were missing data as a result of faulty water level sensors and/or dead batteries in data loggers that occurred during the entire month. Values containing “>” represent drainage that exceeded the capacity of the drain gauge, faulty water level sensors, and/or dead batteries in data loggers at some point during the month. “C” represents “control” non-irrigated plots and “E” represents “effluent” irrigated plots. The “C” plots contained handmade drain gauges. The first column under each “E” was an irrigated plot that contained a G3 drain gauge and the second column was an irrigated plot that contained a handmade drain gauge. A three-way ANOVA test revealed there was a statistically significant interaction between the effects of facility and treatment type on observed monthly drainage ($p = 0.01$), and a statistically significant effect of month on observed monthly drainage ($p < 0.05$).

	Cave Bay			**Heyburn State Park**			**Ellisport Bay**			**Bottle Bay**			**Garfield Bay**		
	C	E		C	E		C	E		C	E		C	E	
Jan	0	>46.1	0.2	>5.3	5.4	>32.3	N/A	9.6	N/A	18.2	>2.7	N/A	>23.4	>13.0	>5.2
Feb	0	>1.4	0.1	5.8	1.3	N/A	16.0	2.8	>0.4	0	>8.7	N/A	>1.1	2.8	2.5
Mar	0	>16.2	5.4	>35.7	7.0	>23.4	4.4	0.2	N/A	0	>13.8	>23.4	N/A	2.7	2.6
Apr	0	>1.5	0.9	>0	1.1	>0	1.8	0	N/A	0	>0.1	>23.4	>0	0.2	0.1
May	0	0	0.1	0	0.2	0	7.4	0	N/A	0	0	>0	0	0	0
Jun	0	0	0	0	0.1	0	7.1	0	0	0	0	0.2	0	0	0.1
Jul	0	0	0	0	0	0	0	0	0	0	0	0	0	0	0
Aug	0	0	0	0	0	0	0	0	0	0	0	0	0	0	0
Sept	0	0	0	0	0	0	14	0	0	0	0	0	0	5.9	17.6
Oct	0	>0.1	0	0	N/A	0	10.2	0	N/A	>0	0.9	0	0	0.1	>3.8
Nov	0	N/A	0	7.3	N/A	7.9	19.8	0	N/A	>0.3	11.4	0	1.6	10.5	>8.8
Dec	0	>29.9	>4.4	29.5	N/A	22.3	10.1	9.6	N/A	0.6	7.4	>23.2	12.3	5.7	8.9
Annual Total	0	>94.7	>11.1	>83.6	>15.1	>85.9	>90.8	22.2	>0.4	>19.1	>45.0	>70.2	>38.4	>40.9	>49.6
Growing Season Total	0	>1.6	1.0	>0	>1.4	>0	40.5	0	>0	>0	>1.0	>23.6	>0	6.2	>21.6
Non-Growing Season Total	0	>93.6	>10.1	>83.6	>13.7	>85.9	>50.3	22.2	>0.4	>19.1	>44.0	>46.6	>38.4	>34.7	>28.0

Calibrate Model Runs

Both single-porosity and dual-porosity soil hydraulic models were run in Hydrus-1D for each plot. Neither model was able to accurately estimate the quantity of drainage that was measured on a daily timestep for all sites, even when root water uptake and evapotranspiration were excluded from model predictions (Figure 7). However, the dual-porosity model was able to capture a similar pattern of the timing of drainage, thus making it more successful at predicting drainage quantities on a monthly scale than the single-porosity model. With a fitted linear regression R^2 of 0.99 and a NSE value of 0.96, the dual-porosity model was more skilled in predicting monthly drainage than the single porosity model with an R^2 of 0.26 and a NSE value of -41.2. The values of porosity that were used in the calibrated and simulated dual-porosity model runs for all plots ranged from 2 to 4.4.

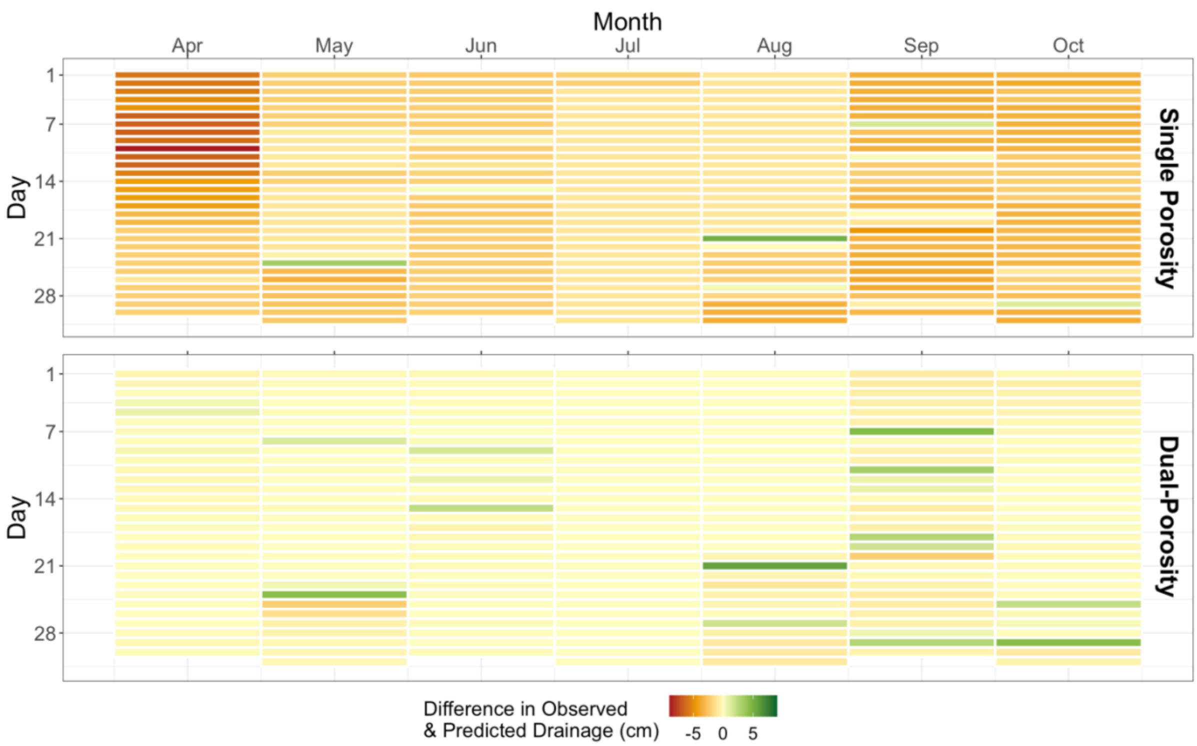

Figure 7: The total daily difference in observed and predicted drainage during the growing season for all drain gauge plots using Hydrus-1D. The top heatmap compared the single-porosity van Genuchten-Mualem model drainage with observed daily drainage, and the bottom heatmap compared the Durner dual-porosity model drainage with observed daily drainage. Root water uptake and evapotranspiration were excluded from model predictions.

Overall, Hydrus-1D had a higher predictive skill than WEPP when predicting monthly drainage. A fitted linear regression of the observed and calibrated monthly drainage values for all plots during the growing season produced an R^2 value of 0.92 and a NSE value of 0.91 for Hydrus-1D and an R^2 value of 0.85 and a NSE value of 0.84 for WEPP (Figure 8). Both lines of best fit were located below the 1:1 line, indicating that both models underpredicted drainage even when root water uptake and evapotranspiration were excluded from model predictions. The lines of best fit for

Hydrus-1D and WEPP are not significantly different. Both models were most successful at predicting drainage at Garfield Bay, however the models struggled with predicting drainage for individual plots at Ellisport Bay and Heyburn State Park (Appendix G).

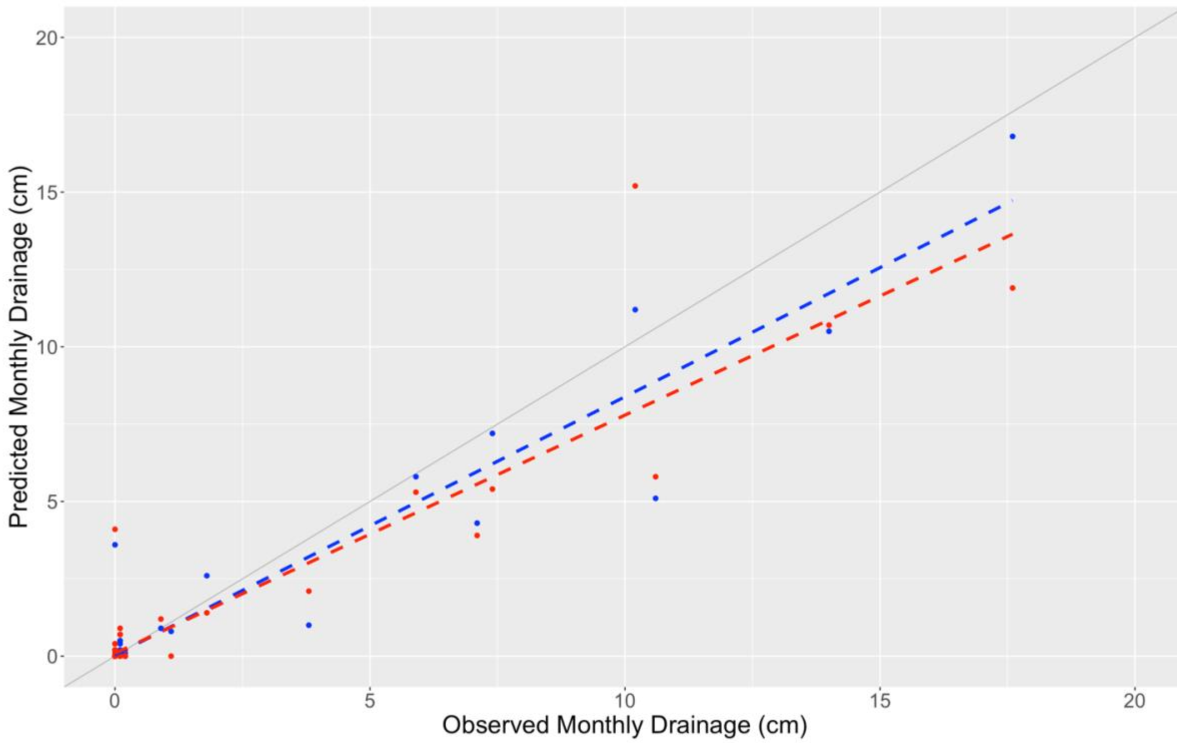

Figure 8: Observed and predicted values of monthly drainage during the growing season at all drain gauge plots except for two effluent irrigated drain gauge plots at Cave Bay due to lack of daily irrigation logs. Root water uptake and evapotranspiration were excluded from calibrated model predictions. Blue points are Hydrus-1D-predicted drainage and red points are WEPP-predicted drainage. The blue dotted line is best fit for the Hydrus-1D and the red dotted line is best fit for WEPP. Solid gray line is 1:1 line. A regression analysis revealed that there was not a statistically significant difference in monthly drainage values between the collected data and predicted values for each model.

Simulated Model Runs

Although both models were able to model potential drainage during the growing season, only WEPP could perform models runs for our study sites over the entire year. For simulated runs that included root water uptake and evapotranspiration, WEPP was able to predict monthly drainage within the range of the observed monthly drainage values during the non-growing season. However, a two-way ANOVA test showed that the mean observed monthly drainage was significantly different to the mean WEPP-predicted monthly drainage during the non-growing season (Figure 9). The two-way ANOVA test also showed that there was not a significant difference in the observed and WEPP-predicted monthly drainage between the facilities. The median of the predicted non-growing season monthly drainage values agreed well with the median of the observed monthly drainage values for Ellisport Bay, Bottle Bay, and Garfield Bay. The range of predicted non-growing season monthly drainage for Heyburn State Park was on the lower end of the range of observed non-growing season monthly drainage.

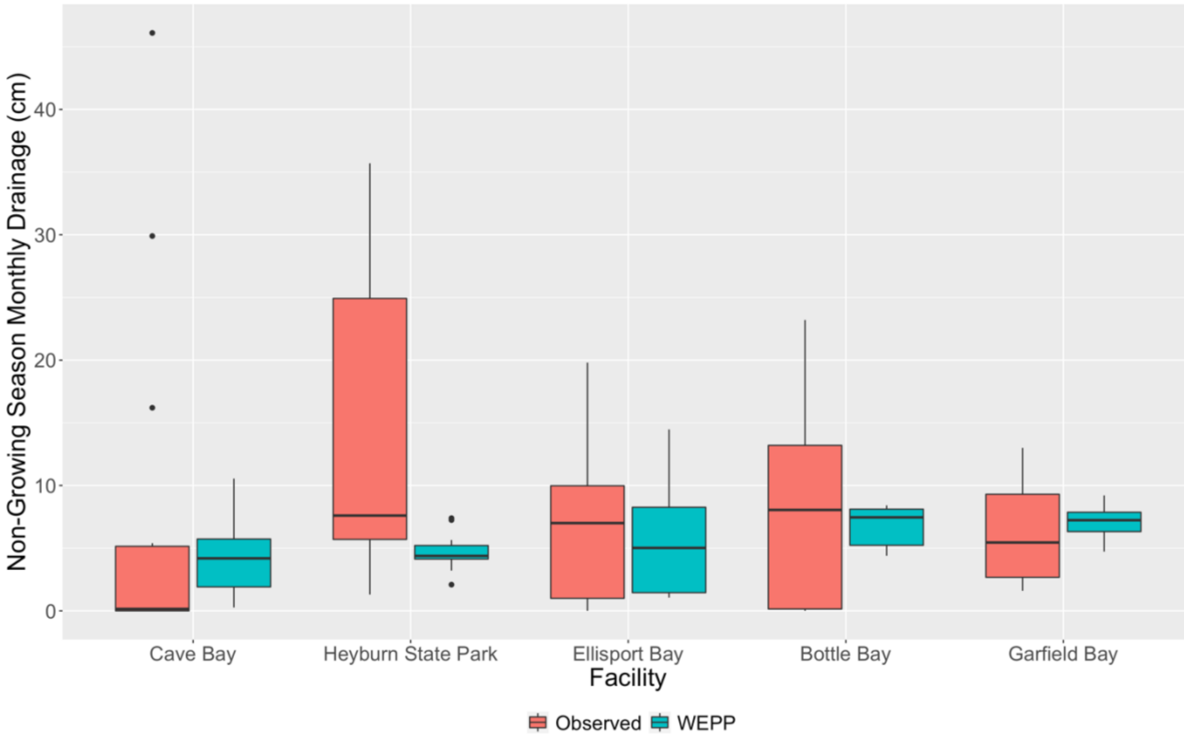

Figure 9: Box-and-whiskers plot comparing all drain gauge observed monthly drainage (cm) and WEPP-predicted monthly drainage (cm) during the non-growing season months for all facilities. Monthly drainage data for January, February, March, November, and December. Root water uptake and evapotranspiration were included in simulated model predictions. A regression analysis showed that there was a statistically significant difference in non-growing season monthly drainage values between the collected data and WEPP-predicted drainage values. A one-way ANOVA revealed that there was not a significant different in observed and WEPP-predicted monthly drainage values between facilities ($p = 0.353$).

Hydrus-1D and WEPP produced different values of predicted monthly drainage for simulation model runs that included root water uptake and evapotranspiration. A four-way ANOVA test showed that there was a significant interaction of model (Hydrus-1D vs. WEPP), facility, month, and treatment on monthly drainage predictions during the growing season. The ANOVA test also showed a significant difference in the mean predicted monthly drainage values for Hydrus-1D and WEPP models. The greatest difference in mean predicted monthly drainage for the models was 6.76 cm between the mean Hydrus-1D-predicted drainage for October and the mean WEPP-predicted drainage for May and June. WEPP only predicted drainage to occur during April, August, September, and October at some facilities. For the Hydrus-1D simulated runs, the model predicted drainage to occur throughout the growing season (Figure 10). The highest average predicted monthly drainage for the Hydrus-1D simulations was 1.2 cm in April for the control plots at Heyburn State Park. The lowest average predicted monthly drainage for the Hydrus-1D simulations was 0.007 cm in October for the control plots at Bottle Bay. Although Hydrus-1D and WEPP predicted significantly different monthly drainage values, both models agreed that drainage was predicted to occur during the month of April.

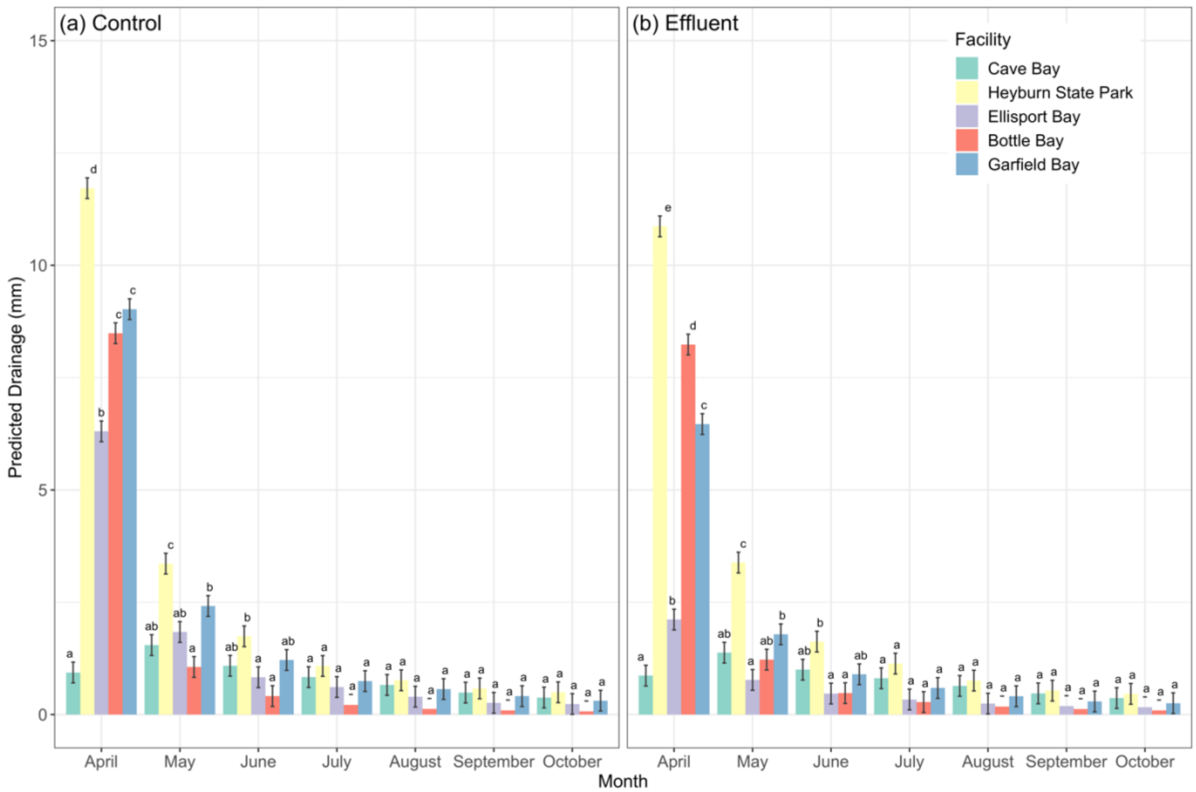

Figure 10: Predicted monthly drainage (mm) from Hydrus-1D simulated runs. Root water uptake and evapotranspiration were included in simulated model predictions. A three-way ANOVA showed a significant interaction effect of facility location, treatment type, and month of growing season on predicted monthly drainage ($p < 0.05$).

Discussion

Observed Drainage

During the growing season, drainage in drain gauges occurred in 70% of the irrigated plots and 20% of the non-irrigated plots (Table 4). During the peak months of drought (July and August), the drain gauges in the treatment plots did not receive any drainage as the soil remained relatively dry throughout the profile. This soil moisture pattern is commonly found in Pacific Northwest forests (Schmidt et al., 2020). This drainage pattern observed in drain gauges in this study agrees with that from Gee et al. (2004), which was conducted in similar semi-arid climates with wet winters and dry summers. In that study with passive-wick drain gauges in soil without vegetation, little to no drainage occurred during the peak summer months and then occurred during the wet season (Gee et al., 2004). When analyzing our daily irrigation logs and precipitation records, the drainage that occurred during the end of the seasonal drought (September and October) appeared to be the result of a combination of reclaimed wastewater being irrigated and the occurrence of precipitation events. As shown in another study involving soils irrigated with reclaimed wastewater, the soil water storage capacity can be decreased by this land practice through the clogging of soil pores with nutrients in the wastewater, therefore increasing drainage (Cook et al., 1994). Another likely confounding factor in the increased drainage is the elevated soil moisture content, accelerating the rate of soil water movement (Lai et al., 2016). Potential drainage from irrigation can be further increased with the addition of water from a precipitation event, making the soil sensitive to irrigation during the end of the seasonal drought. In accordance with the drain gauge results, irrigation season should be primarily applied from June through August with adjustments made to the IWR calculations during the shoulder months of the growing season, being mindful of the timing and duration of any precipitation events.

The non-uniformity of irrigation within plots has larger implications for spatial drainage patterns in irrigation management units. The trees located in the management units impede direct paths of irrigation from the sprinklers, and sprinkler spacing may cause gaps in irrigation distribution. Vegetation blockage and irregular irrigation distribution resulted in variation of irrigation throughout the plots (Appendix H). Low spots of irrigation may have little to no drainage while high spots of irrigation may have large amount of preferential flow. While water can spread somewhat laterally in soil layers, there still may be variation in soil moisture between wet and dry spots of irrigation, magnifying the variation in spatial drainage. Areas receiving more irrigation are targets for higher risks of nutrient leaching as more drainage occurs in those areas compared to other locations.

Most of the observed drainage occurred during the non-growing season months, when soil water potential is high (Table 3, Appendix E). As shown in previous studies, high antecedent soil moisture resulting from a precipitation event increases the infiltration rate of the soil (Hardie et al., 2011; Sutinen et al., 2008). Antecedent soil moisture also heavily influences deep soil drainage in forest systems (Lai et al., 2016). The recorded soil water potential values from this study follow a seasonal pattern of higher soil water potential during the non-growing season months. The average soil water potential at the 10 cm depth was -21.0 kPa and the 50 cm depth was -23.0 kPa during the non-growing season (Table 3). This pattern of soil water potential combined with the observed drainage during the non-growing season months highlight the major effect of preferential flow pathways on soil drainage rates. Preferential flow pathways throughout the soil profile are also further initiated with increased soil moisture (Hardie et al., 2011). The increase in preferential flow in the drain gauge diversion tubes may have been another cause for the large magnitude of drainage during the non-growing season months. A large portion of the precipitation that the facilities received during the non-growing season was in the form of snow. Sutinen et al., 2008 found that when the air temperature was above 0°C, snowmelt quickly infiltrated into forest soils, significantly raising the soil water content in all soil depths and allowing the water to percolate throughout the soil profile. The daily temperature fluctuations and snow events experienced at our study sites throughout the non-growing season may have been another cause for the large observed drainage values. Elevated antecedent soil moisture coupled with snowmelt appears to be the cause for the large magnitude of drainage occurring during the non-growing season months.

The drainage data that was observed in the drain gauges may have been an overestimation of drainage that occurred outside of the diversion tube. This overestimation is due to the design of the drain gauges, as there was no vegetation on the soil above the diversion tube. When the intact soil cores in the diversion tubes were collected, the top 20 cm of soil was removed along with any vegetation that had previously been there. This limits the direct effect of evapotranspiration on the diversion tube connected to the drain gauge as the processes that occurred outside of the drain gauge included evapotranspiration of the surrounding vegetation. However, acquiring an intact soil core preserves any macropore networks or preferential flow pathways as well as the soil profile's structure. The drain gauges could also be installed with perennial vegetation planted on the soil above the diversion tube and drainage not measured immediately to allow the site to heal after the installation disturbance, which may provide a more accurate measurement of drainage.

The effect of a timber harvest on drainage could be analyzed at a non-irrigated plot. The winter after the drain gauge was installed at an Ellisport Bay control plot, half of the plot was inadvertently included in a timber harvest operation. Over half the trees in the plot were harvested and trees on one side of the drain gauge were removed, thus eliminating some canopy interception that may affect the interception throughfall that reached the drain gauge. The drain gauge in this control plot recorded the second-greatest amount of drainage throughout the growing and non-growing seasons. The amount of drainage the occurred with the removal of trees emphasizes the magnitude that canopy cover has on drainage without the direct involvement of evapotranspiration and root water uptake. Eliminating trees from an area receiving additional water in the form of irrigation also removes evapotranspiration and root water uptake fluxes, potentially resulting in more drainage to occur. If a facility wanted to harvest trees within the irrigation management units, it should be done in a conservative manner, to avoid significantly decreasing canopy cover and the rate of water uptake processes.

Parameterization and Assessment of Models

Hydrus-1D and WEPP calibration runs were parameterized using the same gathered soil input parameters and daily precipitation, irrigation, and evapotranspiration data. For Hydrus-1D and WEPP calibration runs, plot uniformity data was useful in providing a starting point for the proportion of irrigation a drain gauge might receive, however it was ultimately through numerous assessments of altered precipitation and irrigation ratios that agreeable proportions were identified. The optimal proportions were selected by assessing the highest NSE value when altering the precipitation and irrigation ratios. To improve both Hydrus-1D and WEPP's parameterization, the estimated crop coefficient should be validated to provide the models with more accurate estimations of daily evapotranspiration rate for the forests in this study. The soil input parameters provided to the models were processed in different ways, which may be the source of some of the variation in predicted drainage between the models. The dual-porosity hydraulic model used in Hydrus-1D model runs well captured presence of macropore flow, and produced agreeable results in the timing of drainage (Figure 7). In a previous study comparing observed and predicted soil water content in an irrigated soil system containing a large macropore flow effect, Hydrus-1D was successful in modeling soil water dynamics using the dual-porosity hydraulic model (Wongkaew et al., 2018). Regardless of the adjusted input parameters, the models were able to capture the magnitude and timing of drainage well during the growing season (Figure 8).

The model prediction results confirmed that regardless of the inherent differences in the purposes of each model, Hydrus-1D and WEPP have potential to be used a support tool for land managers and regulators involved in this land application. WEPP was designed to be a hillslope erosion prediction model used at a watershed level, whereas Hydrus-1D was designed as a one-dimension, small-scale soil-water and solute movement prediction model. Hydrus-1D and WEPP predicted monthly drainage during the growing season successfully (Figure 8). WEPP was also able to predict monthly drainage values within the range of the observed monthly drainage values during the non-growing season, making WEPP a useful model to obtain drainage estimates throughout the year (Figure 9). Another model that may be useful for facility managers and regulators to evaluate current plant available water conditions is an irrigation schedule model, such as Irrigation Scheduler Mobile (Peters & Hill). Overall, both Hydrus-1D and WEPP models are adequate tools to support reclaimed wastewater irrigation decisions.

Another potential cause of the difficulty to parameterize the models in plots irrigated with reclaimed wastewater is the alteration of soil physical properties. Previous studies have shown that soils irrigated with treated wastewater have decreased water storage capacity and soil hydraulic conductivity (Cook et al., 1994; Leuther et al., 2019). Decreased water storage capacity elevates the risk for drainage, as the soil cannot hold as much water prior to the application of reclaimed wastewater (Cook et al., 1994). Finer textured soils exposed to long-term reclaimed wastewater exhibit reduced hydraulic conductivity allowing for more pore space, which facilitating drainage throughout a soil column and decreased the soil's water storage capacity. The database used to gather soil properties like hydraulic conductivity may have values of soil physical properties that are quite different to the actual values if these properties have been altered by the reclaimed wastewater irrigation. Therefore, some of the soil input parameters used by the models may not have been accurate, resulting in the underestimation of drainage. This potentially inaccurate soil data confirms the need for site-specific soil hydraulic properties measurements.

Predicted Drainage

A four-way ANOVA test revealed the significance of the model selected, facility location, month of growing season, and treatment type on predicted monthly drainage. The difference in model predictions of monthly drainage were primarily highlighted in the months of April, September, and October. Hydrus-1D predicted the majority of growing season drainage to occur during April (Figure 10). This predicted drainage pattern appears to reflect the relatively wet soil conditions calibrated 15 days prior to the model run time. From May to the end of October, the average monthly drainage predicted by Hydrus-1D for both treatment areas at all facilities was less than 0.3 cm. Unlike the observed data and the WEPP-predicted drainage data, Hydrus-1D did not predict an increase in drainage during the last two months of the growing season (Figure 10). It appears that with the inclusion of root water uptake and evapotranspiration, the vegetation-related processes in Hydrus-1D removed a large amount of the water being applied throughout the growing season. WEPP predicted the majority of growing season drainage to occur in September and October. The largest average amount of monthly drainage was 3.6 cm, and was predicted to occur at Ellisport Bay in October. The only predicted drainage to occur in April was for both treatment areas at Heyburn State Park. The lack of predicted drainage in April for four of the five facilities may be a result of the forest management selection in WEPP simulation runs. This selection may have the associated vegetation-related processes beginning earlier in the model timescale, effectively reducing the soil water storage by the start of the growing season. Although there were differences between model predictions of monthly drainage, there were similar monthly and locational patterns predicted within the growing season for each model.

The combined predicted monthly drainage values produced by Hydrus-1D and WEPP illustrated a significant interaction involving facility location, treatment type, and month of growing season. A three-way ANOVA test showed that similar to the observed drainage data, there was a significant interaction effect of facility location, treatment type, and month of growing season on predicted monthly drainage. The differences between models occurred across all facilities and treatment types primarily in the months of April, September, and October. The effects of facility on drainage depends on the month, which reflects the temporal pattern of observed monthly drainage during the growing season (Table 4). The interaction effect of facility location, month of growing season, and treatment type emphasizes the importance of each facility creating an irrigation plan that is conducive to that location's soil hydrology and climate in order to prevent excess drainage from occurring in irrigated areas.

Conclusion

Forests irrigated with reclaimed wastewater experienced minimal drainage during the growing season, with an average of 1.1 cm of drainage per month. The majority of growing season drainage primarily occurred in late spring and early fall. During the non-growing season, the monthly drainage was as high as 23.4 cm. Large amounts of observed drainage occurring during the non-growing season and the shoulder months of the growing season suggests a risk of leaching nutrients to groundwater sources if they are not absorbed by the surrounding vegetation. The high spatial variability of irrigation distribution suggests localized leaching may be occurring throughout the irrigation management units. Hydrologic models were able to successfully simulate drainage, and can be useful support tools at forest water reclamation facilities to evaluate the leaching risk of this land application for various soil types and climates.

Chapter 3: Conclusion

As communities continue to grow, so does the demand for sustainable and cost-efficient options to manage municipal wastewater. A popular option to handle this wastewater is to treat the wastewater at a water reclamation facility. Treating this wastewater to a secondary-treatment level, allows facility managers acquire permits to irrigate areas of land with this reclaimed wastewater. The reclaimed wastewater contains plant growth-limiting nutrients. Forests in the northern Idaho experience a seasonal drought, therefore irrigating these forests with reclaimed wastewater provides supplemental water and nutrients during a water-stressed period. If over-irrigation occurs, there is a risk that drainage containing elevated levels of these nutrients may leach into the baseflow and into the surrounding lakes, potentially causing algal blooms (NRC, 2012).

With many water reclamation facilities applying reclaimed wastewater to areas of land, studies have investigated the effects of this irrigated reclaimed wastewater on vegetation and soil. Numerous ground crops have increased yields through reclaimed wastewater irrigation (Singh et al., 2012; J. Wang et al., 2007), and fast-growing deciduous trees have also positively responded to this application (Isebrands & Richardson, 2014). There is a lack of knowledge in the movements of water and drainage after the application of reclaimed wastewater irrigation. Previous studies have analyzed the effects of reclaimed wastewater irrigation on forest biomass production (Gessel et al., 1990), plant nutrient uptake (Brockway et al., 1986; Cromer, 1980), and soil physical properties (Cook et al., 1994; Leuther et al., 2019; Vogeler, 2009). There is an absence of studies conducted on the hydrologic studies on the quantification and patterns of deep soil drainage in coniferous forests irrigated with reclaimed wastewater, however, this study addresses this gap in the literature.

In this study, soil-water drainage was measured at forest water reclamation facilities and two hydrologic models were parameterized to predict potential drainage at plots located in the facilities. Little to no drainage occurred in most of the drain gauges during the seasonal drought. However, a large magnitude of drainage occurred at all drain gauge plots during the shoulder months of the non-growing season. We now have data on the timing and amount of drainage that occurs during the entire year at forest water reclamation facilities. Based on the data collected in this study, irrigation rates in conjunction with precipitation events should be closely monitored in April, September, and October in order to avoid drainage enhanced by irrigation. Drainage during the non-growing season should be tested for leachate concentrations, as that is when most of the drainage is occurring at these facilities, creating a potentially high environmental risk to water quality. This information is useful for facility managers and regulators when making decisions regarding irrigation schedules to avoid drainage, particularly during the beginning and ending of the wet season. These results help fill in identified gaps in the literature.

Hydrologic models other than Hydrus-1D and WEPP have been successfully used to model irrigation schedules for reclaimed wastewater application on crops with the goal of predicting crop growth and increasing crop yield (Al-Jamal et al., 2002; Dragonetti et al., 2020). However, there is a deficiency in the use of models for predicting soil-water drainage for forest systems irrigated with reclaimed wastewater. The results of this study show that Hydrus-1D and WEPP are able to predict potential drainage in forest water reclamation facilities although both models slightly underpredicted monthly drainage during the growing season. Along with the ability to select the type of soil hydraulic model, generated parameters used in the soil hydraulic model for Hydrus-1D may be the source to the slightly higher predictive skill of Hydrus-1D. WEPP is also more user-friendly and simpler to learn than Hydrus-1D, making it easier for facility managers and regulators to learn and utilize. Although there is no significant difference in their predictive capability during the growing season, WEPP would most likely be the best fitting program to use a support tool for facility manager and regulators because of its ability to model drainage year-round.

The supplied crop coefficient from the IDEQ guidelines provided the models with the necessary evapotranspiration rate parameter. There are crop coefficients for deciduous trees, including poplars and fruit trees, but not for mixed coniferous forests (Di et al., 2019; USBR, 2022). While the provided crop coefficient is useful in providing estimations of potential drainage, it would be advantageous to have a crop coefficient estimate of these forests to validate the crop coefficient provided by IDEQ as it is difficult to accurately predict the evapotranspiration rate of a mixed-species and age coniferous forest (Pangle et al., 2015). Some methods include individual tree sapflow measurements, eddy covariance systems, and catchment water balance calculations. It is difficult measuring evapotranspiration rates of coniferous forests as many methods require measurements over specified spatial and temporal scale that may be unattainable depending on location (Tie, Hu, Tian, & Holbrook, 2018). In order to provide the models with more accurate estimations of evapotranspiration rates, it would be beneficial to directly measure the evapotranspiration rates of the forests receiving reclaimed wastewater irrigation. Through the use of hydrologic models like Hydrus-1D and WEPP, facility managers and regulators are able to predict potential drainage, providing data that they can use to continue to sustainably manage this land practice.

Reflecting on the research outcomes, there are opportunities to improve the approaches of this study. One of the limitations to the drain gauges was the restricted reservoir capacity, especially for the G3 drain gauges. Especially during the wet season, it would be advantageous to check on the drain gauges and empty them out more than once a month. A larger reservoir for the drain gauges would also reduce the amount of missing data caused by the exceeded capacity of the drain gauges, especially during the wet season. Another solution to the problem of exceeded reservoir capacities is to install a pump that would automatically pump out the reservoir when the water reached a set level. This may run into problems during the frost-periods with water freezing in the water sample line. In this study, evapotranspiration was one of the primary variables in the hydrologic cycle that was not able to be compared to in-field collected data. It's necessary to measure the evapotranspiration rates of the forests in this study to obtain a more exact estimation of the crop coefficient used in the models. This data would also illustrate any seasonal patterns of evapotranspiration, and would highlight any differences between the rates at facilities and treatment groups. Another variable in the hydrologic cycle that could be more accurately measured is precipitation. While some facilities have precipitation gauges on-site, it is not required that the facilities include the daily precipitation data in the annual reports, eliminating the availability of that data for model setup. Those facilities that do include precipitation data, include data for the irrigating months. A precipitation gauge installed at each site would provide more accurate daily precipitation information for the entire year. Furthermore, throughfall measurements, instead of predictions based on LAI, would also be able to be collected in each plot with the use of established rain gauges. As for the soil physical properties, only bulk density was measured at three depths in each plot, all other properties were extrapolated from Web Soil Survey. While this database is extremely useful in obtaining soil properties that are difficult to measure, these data may not be well-representative of the properties of forest soils irrigated with reclaimed wastewater. It would be most beneficial to conduct laboratory analyses of soil physical properties at various layers to validate those values provided by Web Soil Survey. Making the suggested improvements would help provide more accurate drainage measurements and model predictions for future forest water reclamation studies.

Appendix A: Average Soil Bulk Density Measurements & Three-Way ANOVA Test

A bar chart with the average soil bulk density measurements for all plots in each facility at three soil depths. A table with the three-way ANOVA test analyzing the effects of treatment, facility location, and soil depth layer on soil bulk density.

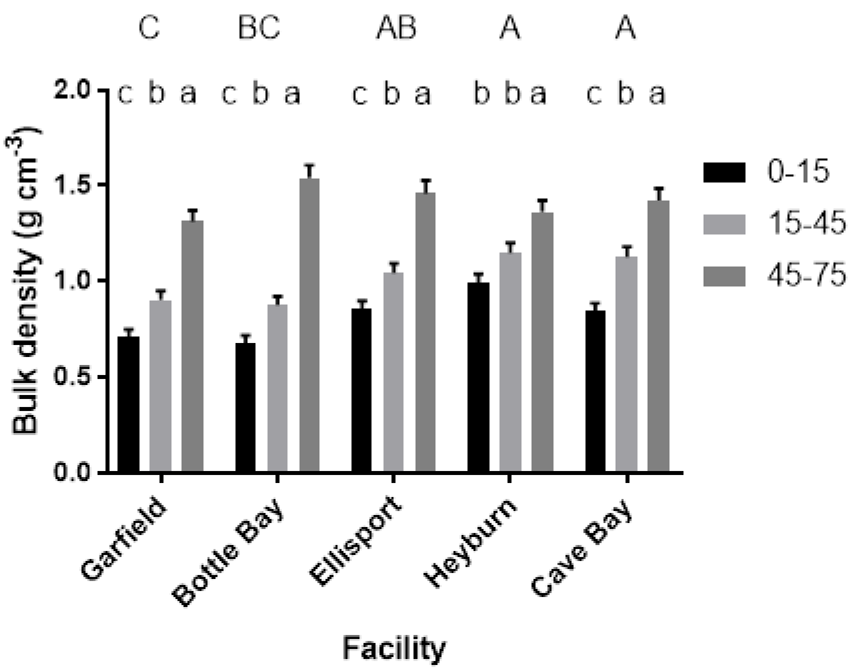

Type 3 Tests of Fixed Effects				
Effect	Num DF	Den DF	F Value	P Value
Treatment	1	40	1	0.3244
Facility	4	40	6.56	0.0004
Treatment*Facility	4	40	0.57	0.6833
Soil Depth Layer	2	79	182.17	<0.0001
Treatment*Soil Depth Layer	2	79	0.67	0.5156
Facility*Soil Depth Layer	8	79	4.93	<0.0001
Treatment*Facility*Soil Depth Layer	8	79	0.9	0.5224

Appendix B: Handmade Drain Gauge Construction

A 19 liter (5 gal) bucket with a lid was used as the foundational structure for the handmade drain gauge design (following the instructions of Hall, 2018). Some of Hall's design were modified, of which included using a 19 L bucket instead of a 22.7 L bucket, a rubber toilet gasket instead of metal and rubber washers, the sample line not housed in the PVC pipe instead of being housed inside of the pipe, and the water level sensor access pipe directed up along the side of drain gauge straight up to the surface instead of extending from the bucket angled gradually towards the surface. The air line was eliminated from our design as the PVC pipe that directed a water level sensor to the reservoir provided a path for air to reach the reservoir.

The metal bucket handle was removed and a 5.1 (2 in) centimeter diameter hole was drilled on the side of the bucket, directly below the lip of the bucket opening. A female 5.1 cm (2 in) diameter PVC slip joint was sawed in half so that the slip joint consisted solely of threads. The female slip joint was threaded onto the male 5.1 (2 in) cm diameter PVC slip joint in order to file down the cut edge of the female slip joint. The slip joints were then unthreaded, and a rubber toilet gasket was placed on the threads of the male PVC slip joint with the larger outside diameter of the gasket pressed up against the non-threaded part of the slip joint. The male PVC slip joint was set in the drilled hole in the side of the bucket so that the gasket was pressed against the outside of the bucket and the rest of the threads were inside the bucket. The toilet gasket washer was placed around the slip joint threads inside the bucket and the female PVC slip joint was screwed on from inside of the bucket. A 0.6 cm (0.25 in) diameter hole was drilled into the side of the bucket, about 5 cm to the left of the PVC slip joints. From the outside of the bucket, a 0.6 cm (0.25 in) plastic irrigation barbed elbow was placed into the 0.6 cm drilled hole and secured with marine sealant. A 61 cm (24 in) long piece of 0.6 cm (0.25 in) diameter rubber irrigation tubing was cut with one end cut at a 45° angle and the other end cut at a 90° angle. The 90° angle end was gently heated with a lighter and attached to the plastic barbed elbow located inside of the bucket. About 15 cm (6 in) from the 45° angle end of the rubber irrigation tubing piece, as well as the edge of the bottom of the bucket where the tubing was going to be glued down to, was scuffed using 80-grit sandpaper. A generous amount of marine sealant was placed on the scuffed part of the bucket, and then the scuffed tubing was pressed onto the marine sealant until the sealant dried. The center of the bucket lid was drilled out using a 3 cm diameter drill bit, and ten 0.6 cm (0.25 in) diameter holes were drilled at random around the center hole. The lip of the bucket lid was cut off and discarded, leaving a circular piece of the plastic roughly 25.4 cm (10 in) in diameter. Two PVC pipe pieces, one 7.6 cm (3 in) long and the other 8.3 cm (3.25 in) long, were cut from a 3 meter long (12 in) 5.1 cm (2 in) diameter PVC pipe. The 8.3 cm (3.25 in) long PVC pipe was attached to male PVC slip joint at one end, and the other end was attached to a 45° angle PVC elbow. The 7.6 cm (3 in) long PVC pipe was joined at one end to the 45° angle PVC elbow attached to the other PVC pipe piece, and the other end was attached to another 45° angle PVC elbow. The PVC elbows were aligned so that the shape of the attachments resembled a wide "U". The bottom 25 cm of a 30.5 cm (12 in) diameter plastic funnel was cut off and discarded, and the funnel was placed on top of the bucket. The location where the plastic funnel hits the female PVC slip joint inside of the bucket was cut out so that the funnel sits flat on top of the bucket.

To create a filtration system for the soil drainage, landscape fabric was cut into two 25.4 cm (10 in) diameter circular pieces. A 2.5 cm (1 in) diameter circle was cut out of the middle of the landscape fabric pieces and ten 0.5 cm (0.25 in) diameter holes were cut into the fabric pieces randomly placed around the larger center hole. Another two 25.4 cm (10 in) diameter circular pieces were cut out of the landscape fabric – no extra holes were cut into these. A 2.4 m (8 ft) strip of rubber irrigation tubing was cut and the end of it was heated with a lighter and secured to the plastic barbed elbow sticking out of the side of the 19 L (5 gal) bucket. To create the wick used to distribute the drainage into the bucket, 30.5 cm (12 in) of 1.9 cm thick braided fiberglass rope was submerged in a solution of water and laundry detergent (2:1 mixture) and left to soak for 20 minutes. After the 20 minutes had expired, the rope was rinsed with water, placed on a pan, and set in the oven at 400° Fahrenheit (204.4° Celsius) for about two hours or when the rope begins to turn a light tan color. Once cooled, half of the rope was unbraided and the rope was strung through the center hole in the bucket lid so that the unbraided and braided sections met in the hole opening. Marine sealant was placed on the edge of the center hole to secure the rope to the bucket lid. When the marine sealant was dry, the unbraided section of the rope was unraveled and separated into two sections. The two sections were then threaded through the center hole of one of the landscape fabric pieces with multiple holes cut into it. One of the sections of the rope was set aside while the other was spread apart and laid on top of the landscape fabric piece. The other section of rope was separated and threaded through the multiple holes cut into the second landscape fabric piece. The extra length of the rope pieces were then laid on top of the landscape fabric piece similarly to the first rope section. To finish the assembly, the plastic funnel was set on top of the bucket with the bucket lid, landscape fabric, and rope assembly set inside of the funnel.

How to Build a Homemade Drain Gauge (part 1) (Clark, 2020a)

How to Build a Homemade Drain Gauge (part 2) (Clark, 2020b)

Appendix C: Install Data Loggers, Water Level Sensors, and Soil Water Potential Sensors

One EM50 data logger was installed at each drain gauge plot after the drain gauges were set up. A 5.1 cm (2 in) diameter auger was utilized to dig a hole about 30.4 cm (12 in) deep for the PVC pipe used to mount the data logger. A 61 cm (24 in) long, one and a 1.3 cm (0.5 in) diameter PVC pipe was placed in the auger hole and then packed down with dirt until the pipe was stable. Five AA batteries were placed in the data logger and the data logger was turned on. Using the USB to stereo jack cord, the data logger was connected to the laptop to ensure it was working properly. After the data logger was disconnected, it was screwed into the PVC pipe using two screws and a screwdriver.

Along with the data loggers, two soil water potential sensors and one water level sensor were also installed at each drain gauge plot. The water level sensor, Hydros 21, was installed at both the G3 and handmade drain gauge plots. For the G3 plots, the translucent blue tubing that came with the G3 drain gauge was attached about one cm above the bottom of the black base of the water level sensor using duct tape. The blue tubing was held up along the cord of the water level sensor towards the plug when the water level sensor was lowered down the one and a 1.3 cm (0.5 in) PVC. The water level sensor was successfully installed when an audible sound of the sensor hitting the bottom of the tube was heard, as well as when the cord and tube could not be lowered down any further. For the handmade drain gauge plots, the water level sensor was threaded down the 5.1 cm (2 in) PVC pipe until an audible sound of the sensor hitting the bottom of the bucket was heard, as well as when the cord for the water level sensor could not be lowered down any further.

Two soil water potential sensors were installed at each of the drain gauge plots. One of the soil water potential sensors was placed at the 10 cm depth and the other was placed below the 10cm sensor at the 50 cm depth. The location of the hole for the soil water potential sensors was set to be 1.5 m (5 ft) from the data logger and in a direction that did not obstruct the soil column that the drain gauge was buried in. Once the location was selected, a hole that was 50 cm deep and about 35.6 cm (14 in) diameter was dug out. The dirt dug out for the hole was separated by soil layers and was set aside to be filled back in later. In order to make a path connecting the soil water potential sensors to the data logger, a trench about 10.2 cm (4 in) deep and stretching from the data logger to the hole was created. The cords of the two soil water potential sensors were threaded through a 1.5 m (5 ft) long 2.5 cm (1 in) diameter PVC pipe, which was then placed in the trench. On one side of the wall of the soil water potential sensor hole, two pits – one 10 cm below the surface and the one 50 cm below the surface – were hollowed out to fit a sensor. The pits were slightly larger than the sensors to ensure there was dirt touching all sides of the sensors. The sensors were secured in the pits by packing dirt in any openings in the pits. The hole was then filled in with the separated layers of dirt and was packed in with a tamper. The trench was filled back in to completely cover the PVC pipe. Finally, the soil water potential sensor and water level sensor cords were plugged into the data logger. The ten cm depth soil water potential sensor was plugged into port one, the 50 cm depth soil water potential sensor was plugged into port two, and the water level sensor was plugged into port three. The data logger was connected to the laptop using a USB to stereo jack cord and the data logger was set up appropriately to begin logging every hour.

Appendix D: Collect Data and Water Samples

In order to collect the soil water potential, soil temperature, and water level data, a laptop with the ECH2O Utility program was connected to the data logger located at a drain gauge plot. Using a USB to stereo jack cord, the data logger was connected to the laptop, and the data for both soil water potential sensors and the water level sensor were downloaded. This process was repeated once a month or more frequently as needed.

Water samples were collected once a month from drain gauges that had any readable amount of water in the reservoir. In order to collect a water sample, a hand-vacuum pump was attached to a 1000 mL glass bottle via a 0.6 cm (0.25 in) diameter rubber tube. The tube was secured from the vacuum pump to a hole in a rubber stopper that was placed in the mouth of the bottle. The water sample line from the drain gauge was attached to a second hole in the rubber stopper. When the hand-vacuum pump filled the glass bottle to about the 900 mL mark, the rubber stopper was removed and a 500 mL sample of the water was poured into a labeled plastic sample bottle. After one sample was collected, this process was repeated and the collected water was then dumped into a 19 L (5 gal) bucket, which was disposed of outside of the drain gauge plot when the drain gauge had been emptied. When the drain gauge reservoir was emptied, the sample line was removed from the glass bottle and attached to the hand-pump, which cleared out any excess water droplets in the sample line. Finally, the sample line was detached from the hand-pump and the water sample bottle was labeled appropriately.

Appendix E: Soil Water Potential and Temperature Measurements

Graphs of hourly soil water potential and temperature measurements from drain gauge plots at all facilities from January 1, 2021 to December 31, 2021.

Cave Bay plot 101 CC1:

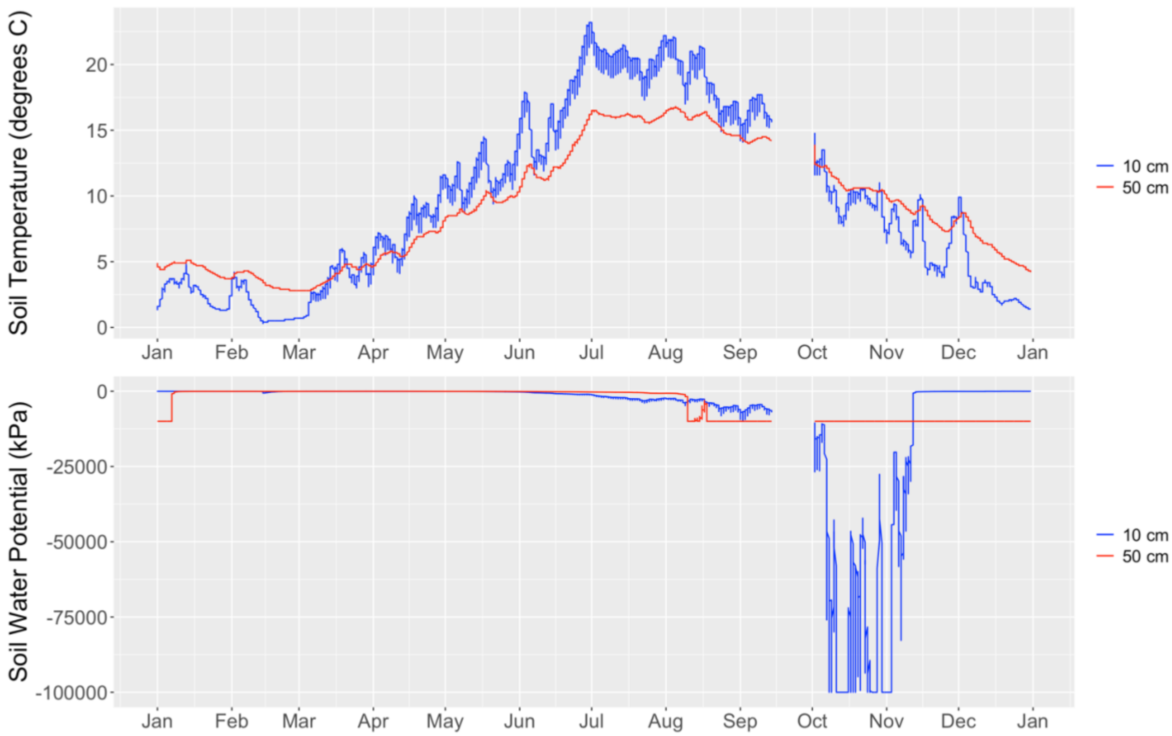

Cave Bay plot 106 CE1:

Cave Bay plot 107 CE2:

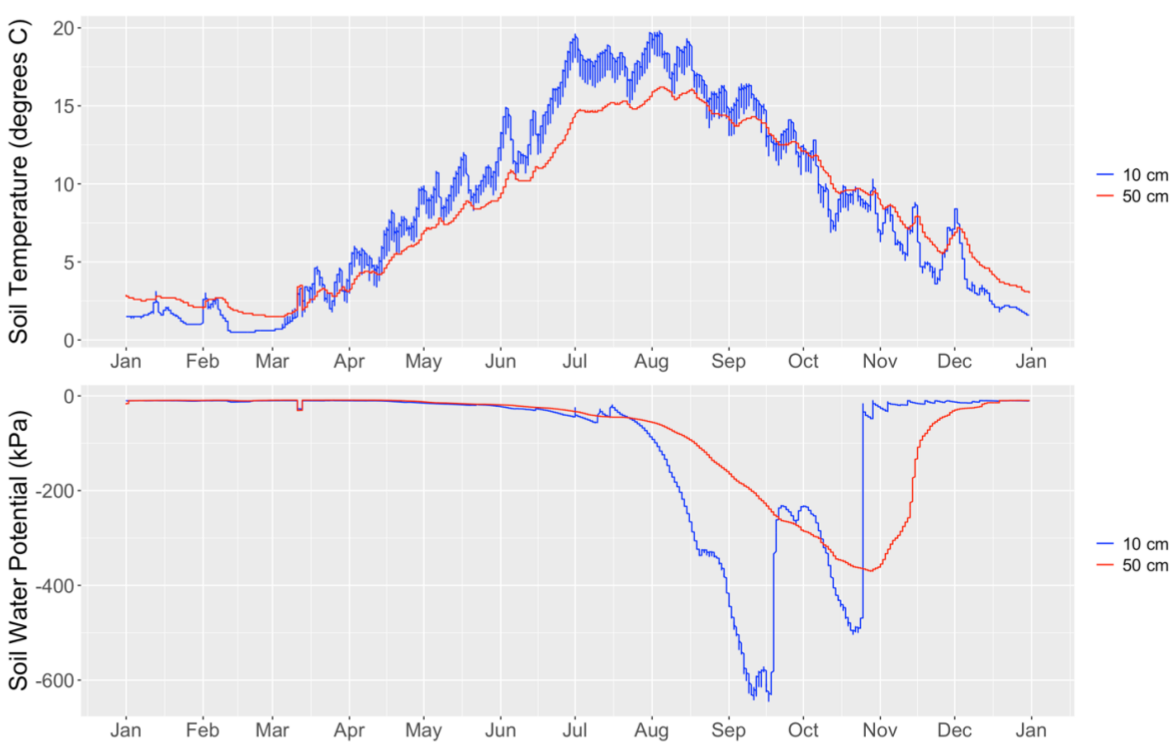

Heyburn State Park plot 201 HC1:

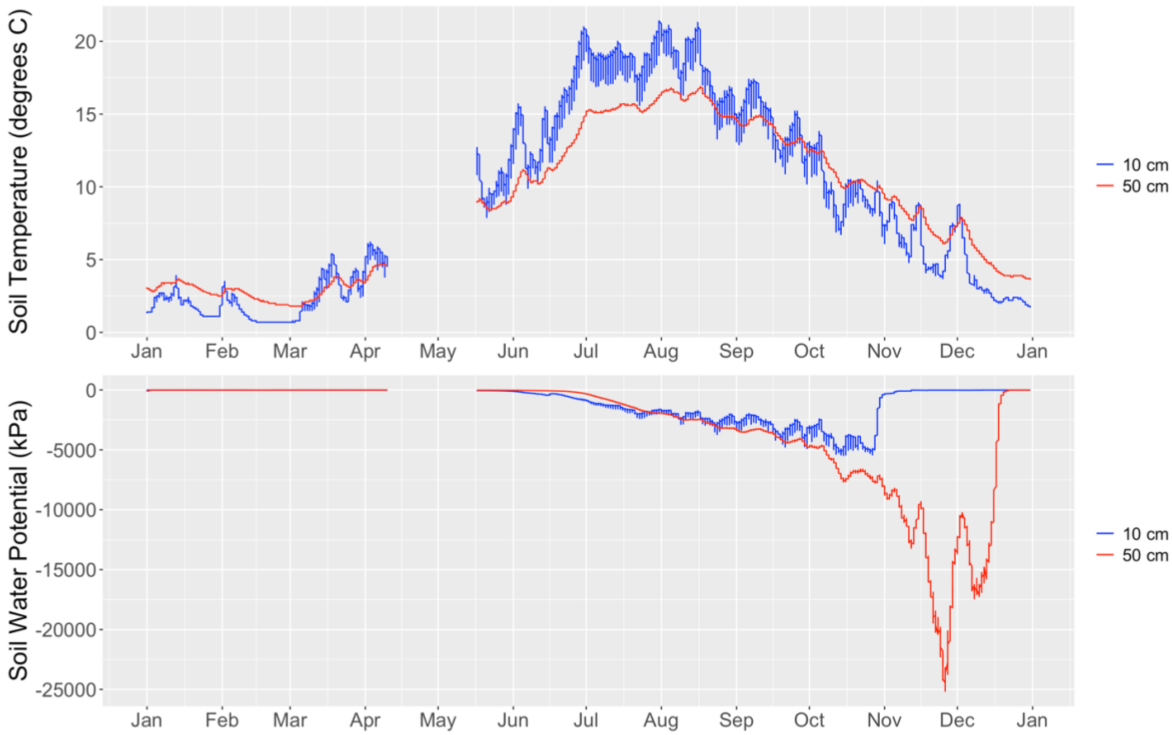

Heyburn State Park plot 208 HE3:

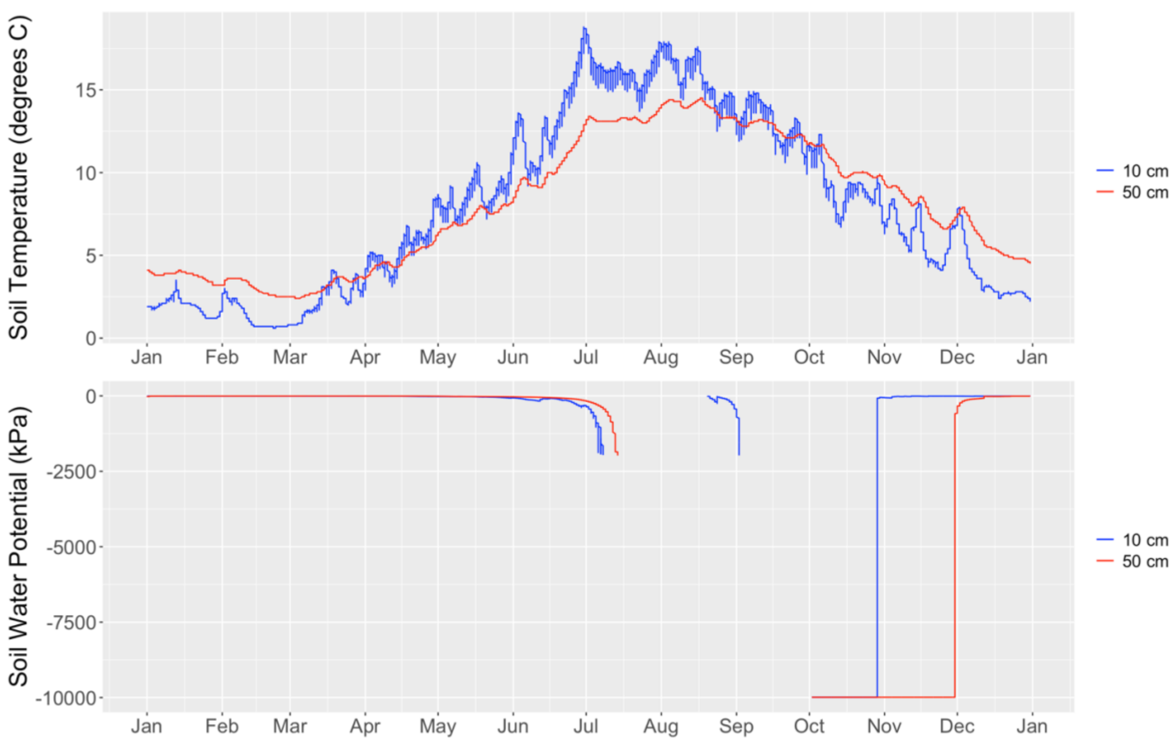

Heyburn State Park plot 209 HE4:

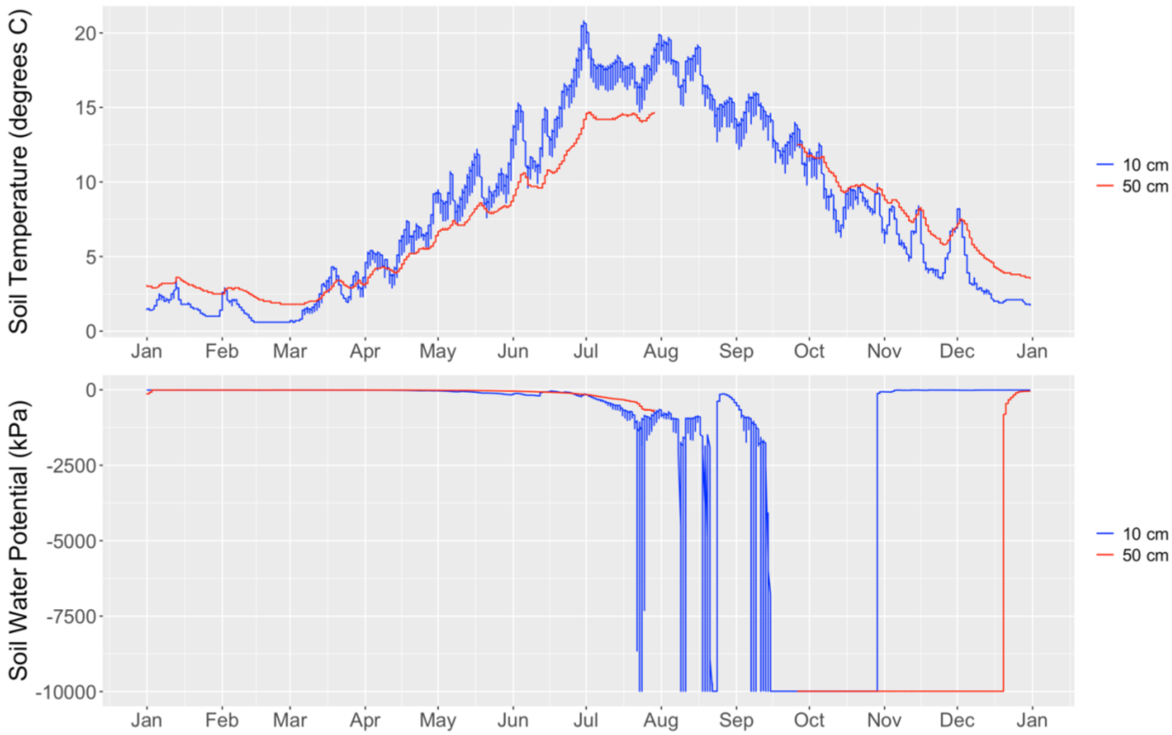

Ellisport Bay plot 302 EC2:

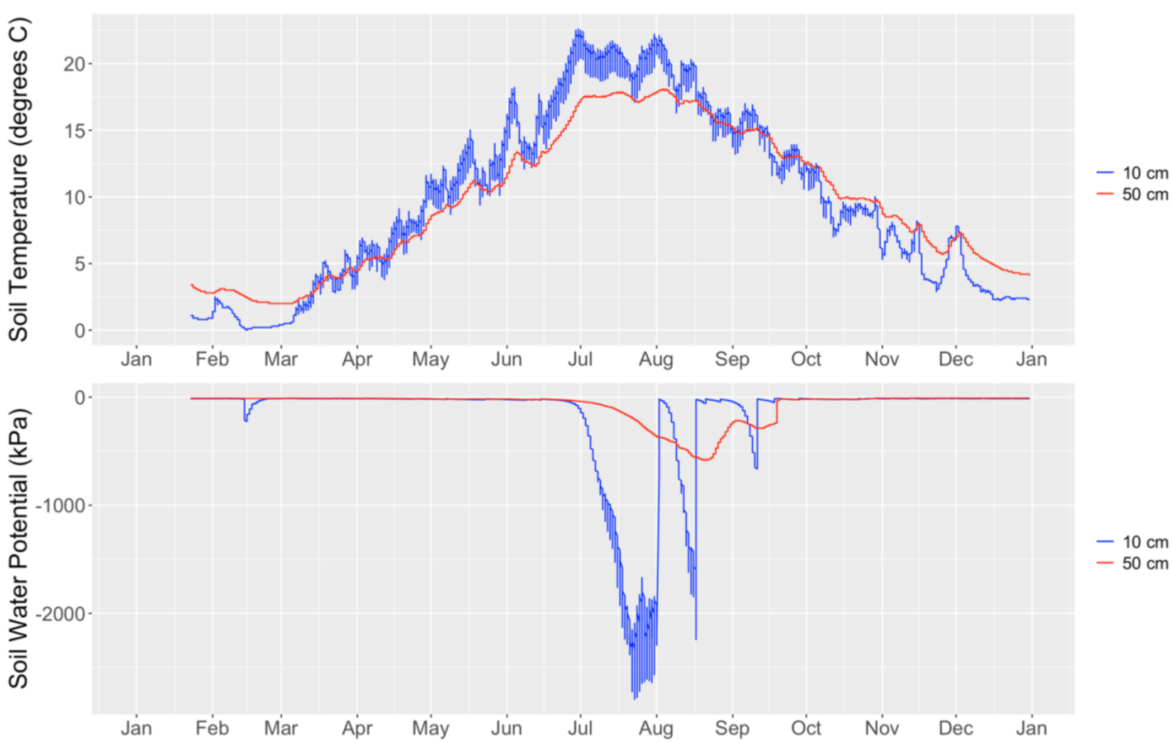

Ellisport Bay plot 306 EE1:

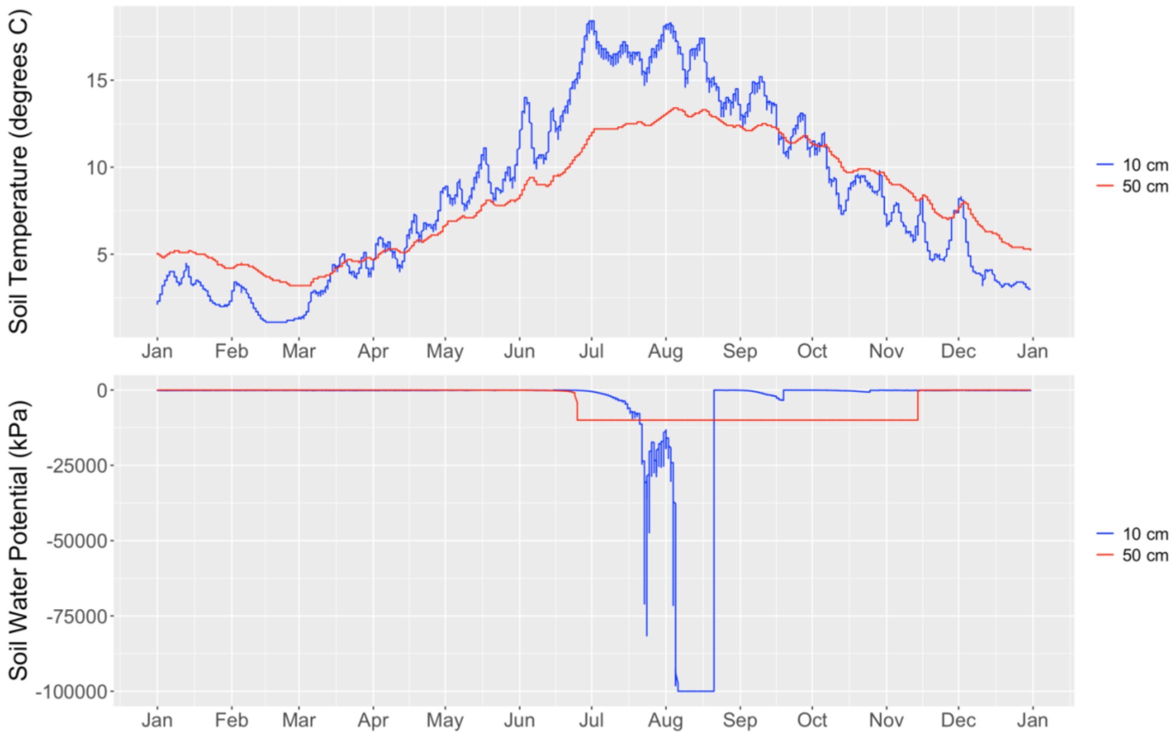

Ellisport Bay plot 307 EE2:

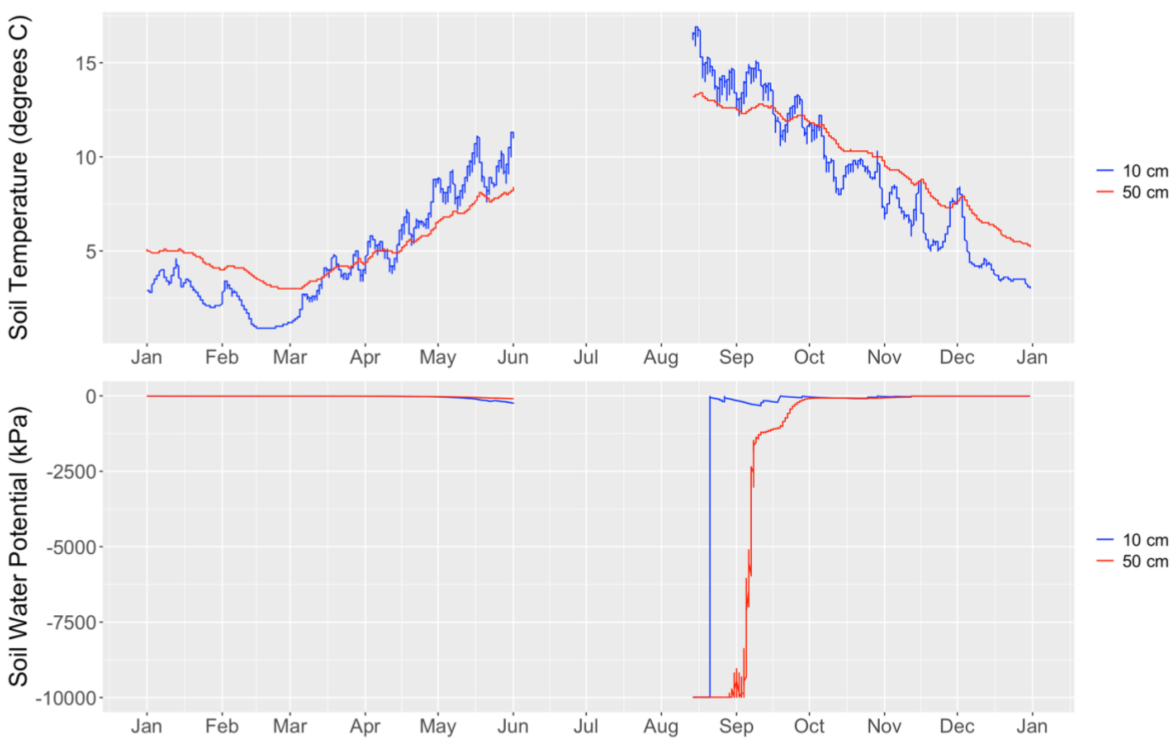

Bottle Bay plot 404 BC4:

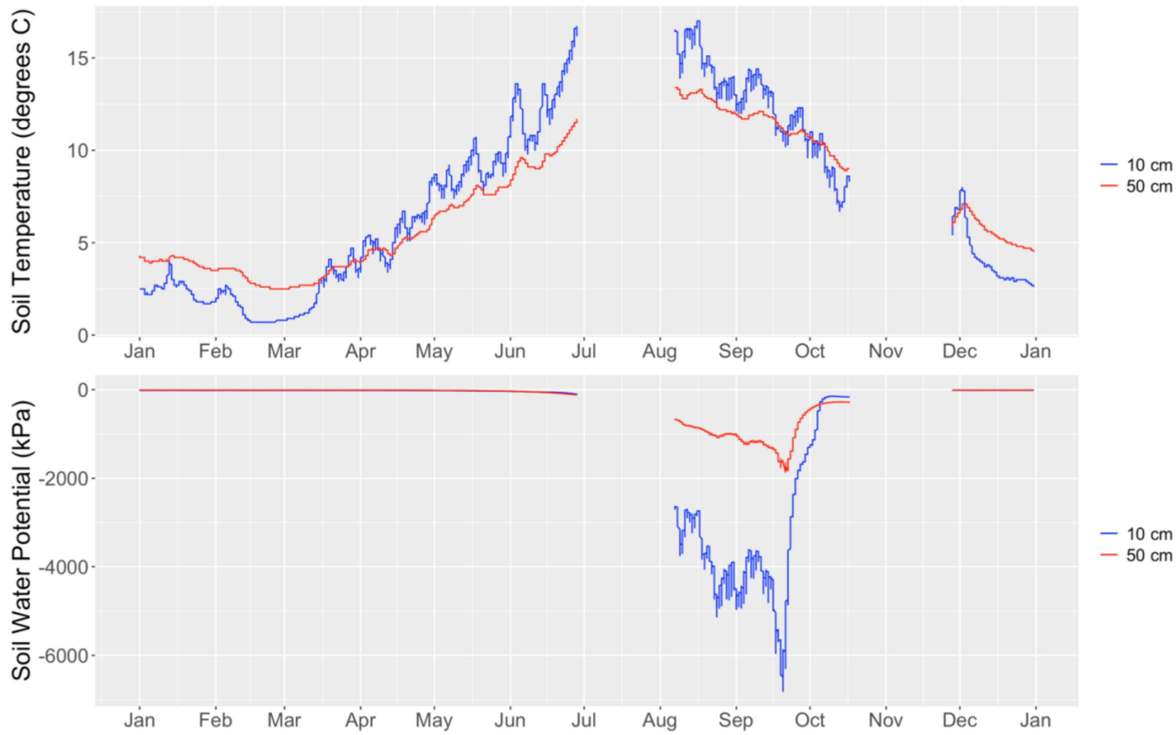

Bottle Bay plot 406 BE1:

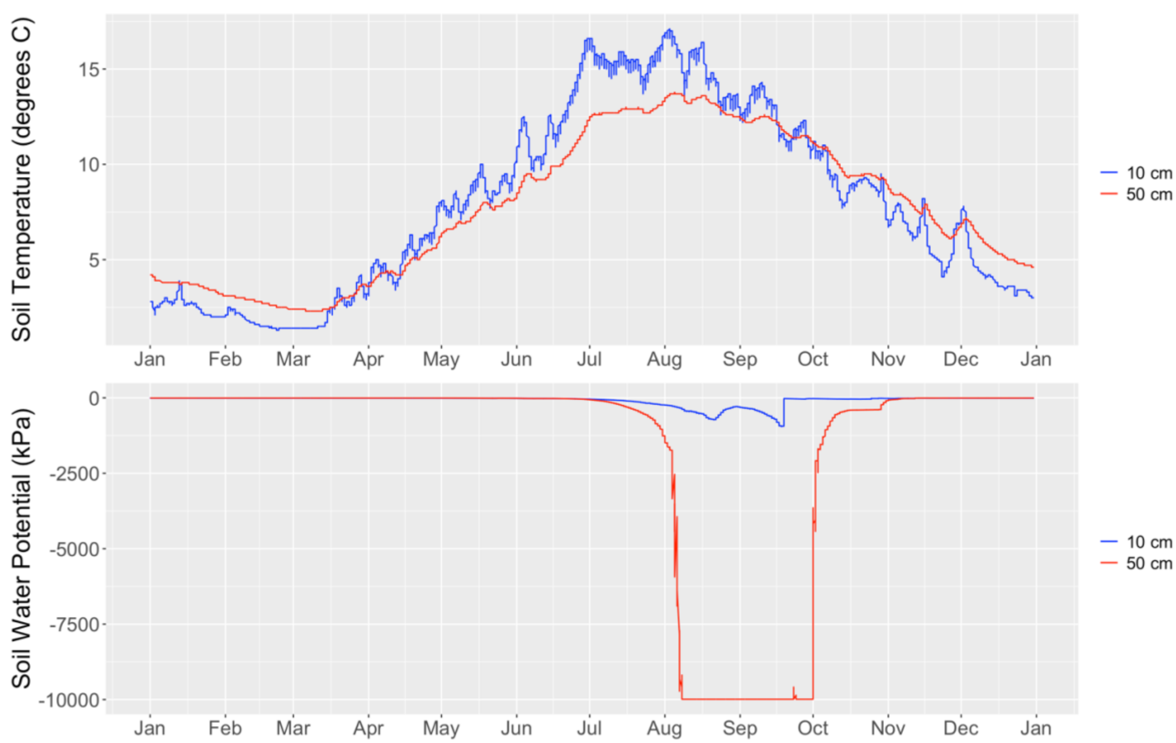

Bottle Bay plot 409 BE4:

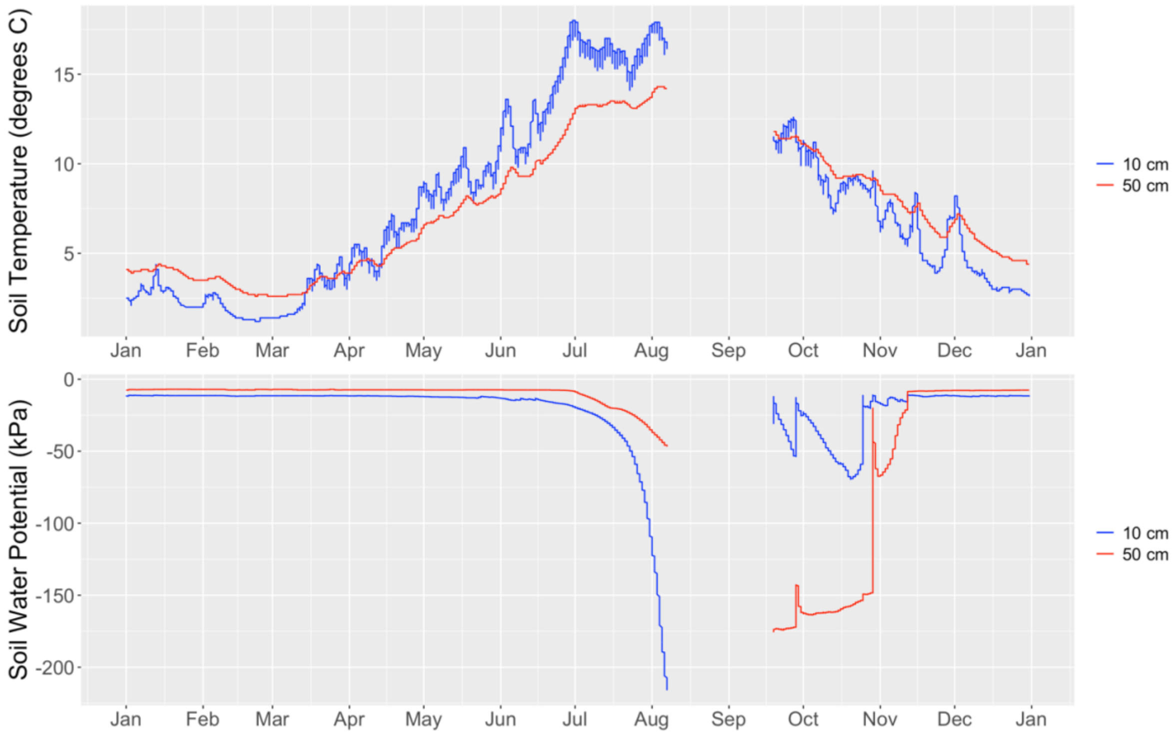

Garfield Bay plot 501 GC1:

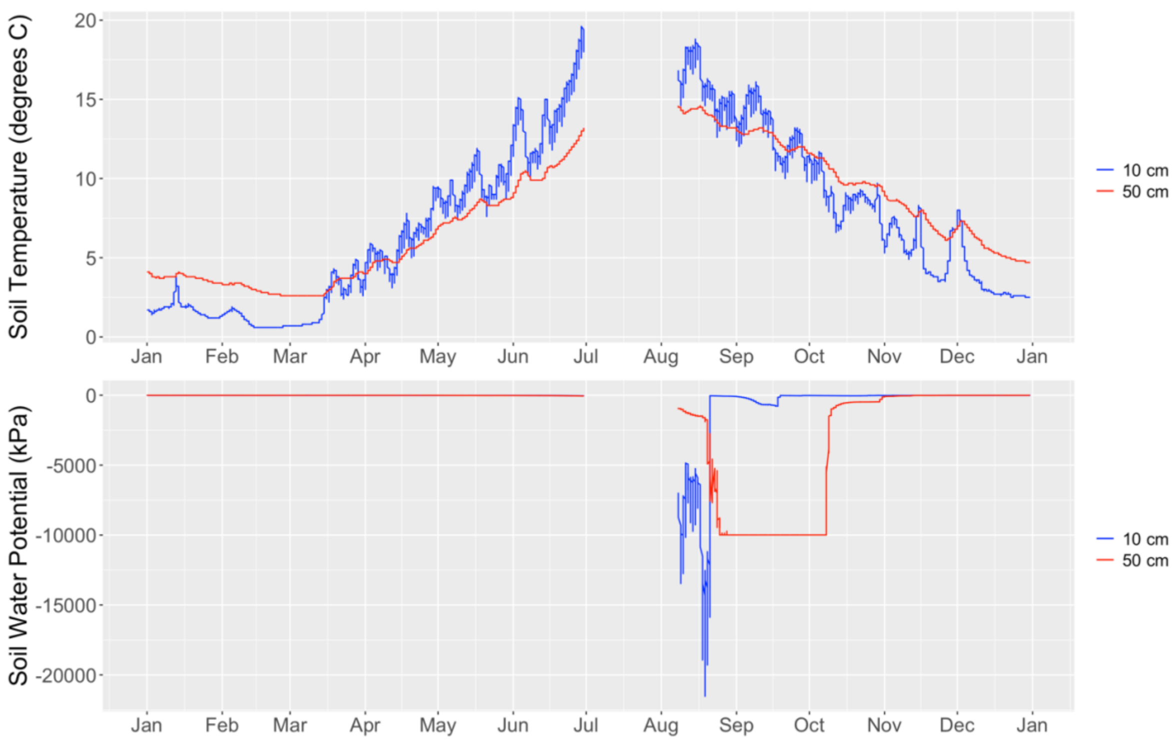

Garfield Bay 506 GE1:

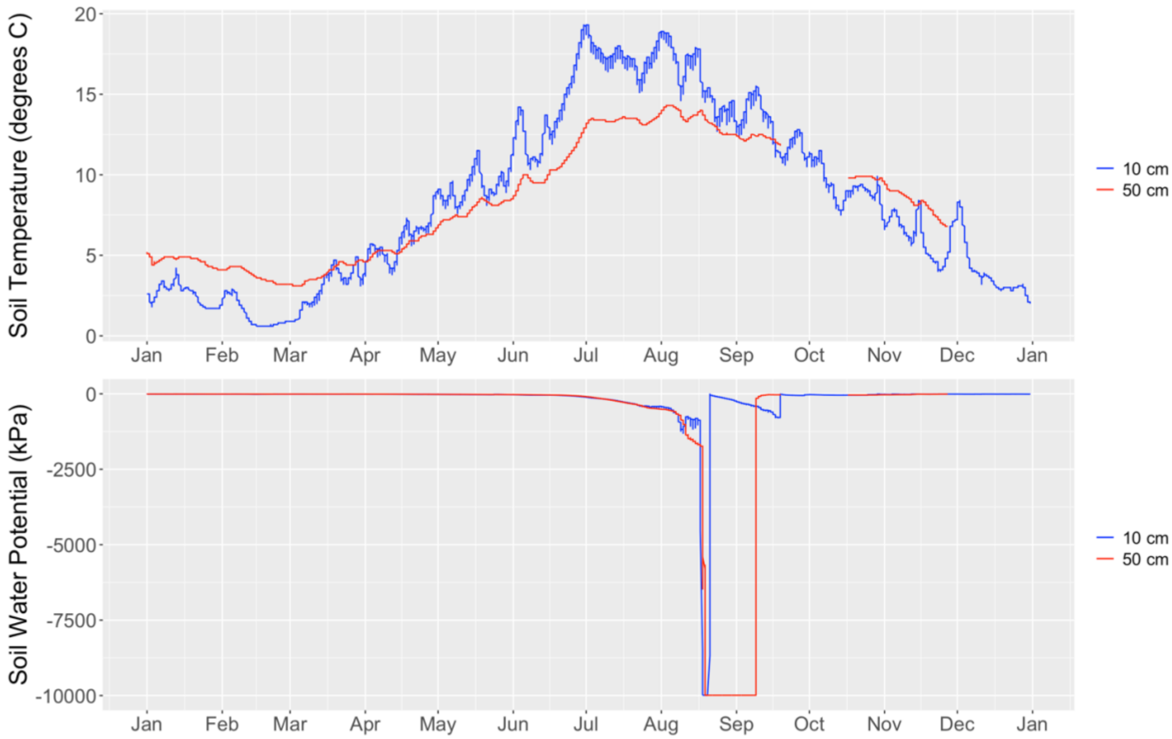

Garfield Bay plot 509 GE4:

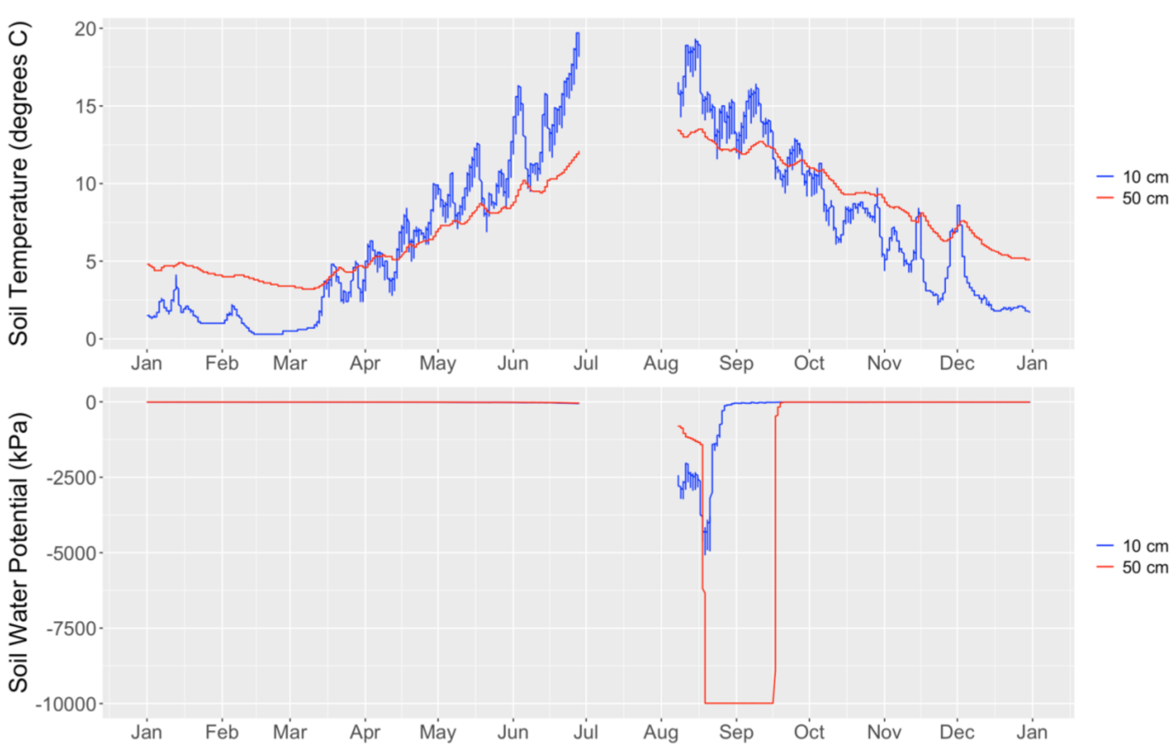

Appendix F: Irrigation Distribution Heat Maps

Plot-specific heat maps created using irrigation distribution data from irrigated plots. Black circles delineate the plot area, colored dots show locations of rain gauges, and black dots show locations of drain gauges. Cave Bay data not included because there was no verification that irrigation occurred during the rain gauge measurements. Heyburn State Park data not included because irrigation did not occur during the two-week measurement time.

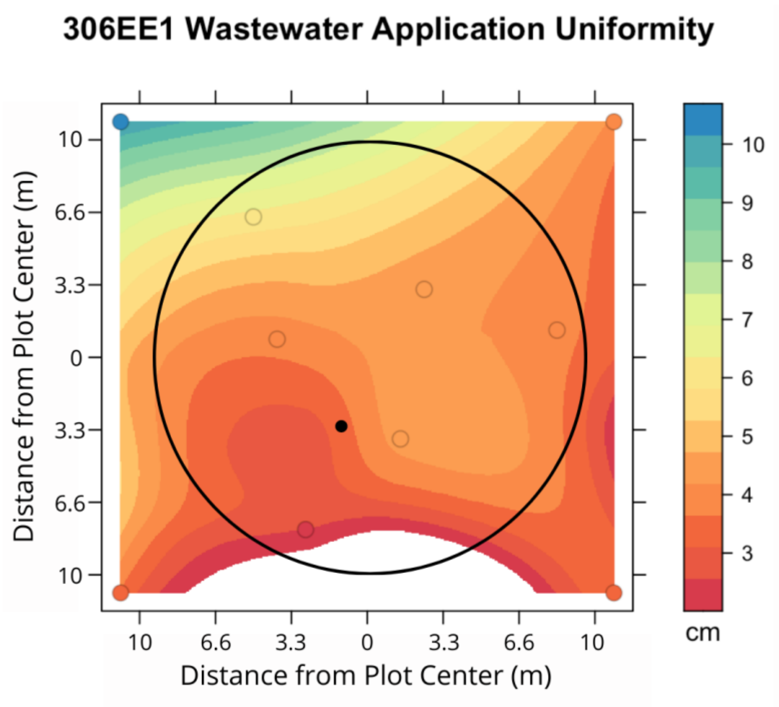

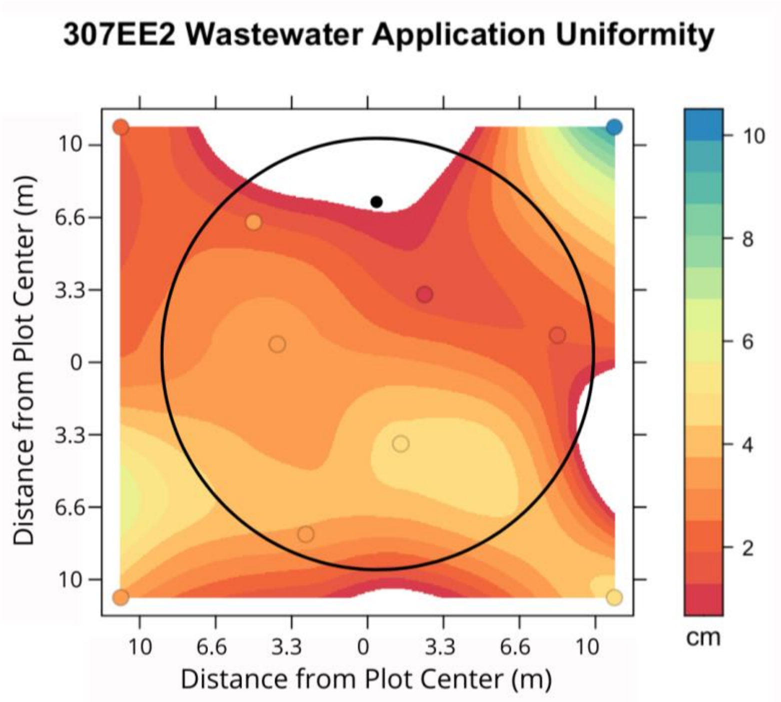

307EE2 Wastewater Application Uniformity
Distance from Plot Center (m)
10
6.6
3.3
0
3.3
6.6
10
Distance from Plot Center (m)
10
6.6
3.3
0
3.3
6.6
10
2
4
6
8
10
cm

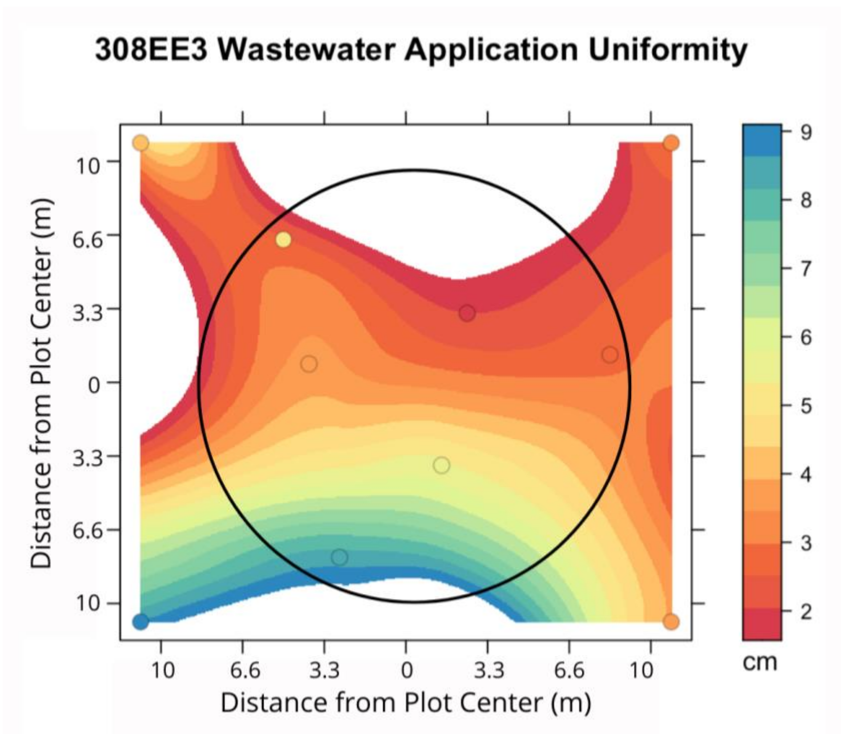

308EE3 Wastewater Application Uniformity
Distance from Plot Center (m)
10
6.6
3.3
0
3.3
6.6
10
Distance from Plot Center (m)
10
6.6
3.3
0
3.3
6.6
10
2
3
4
5
6
7
8
9
cm

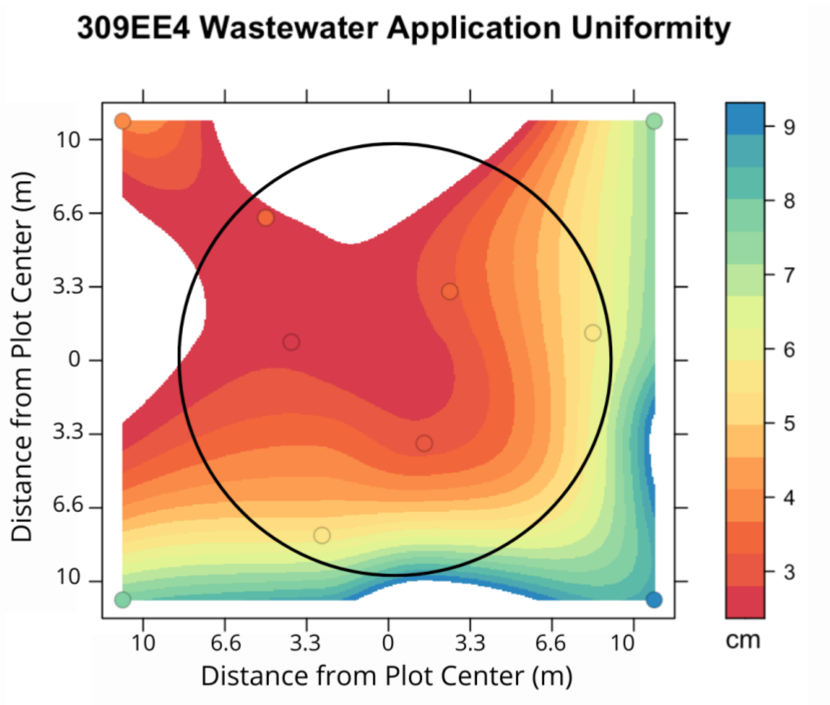
309EE4 Wastewater Application Uniformity
Distance from Plot Center (m)
10
6.6
3.3
0
3.3
6.6
10
Distance from Plot Center (m)
cm
9
8
7
6
5
4
3

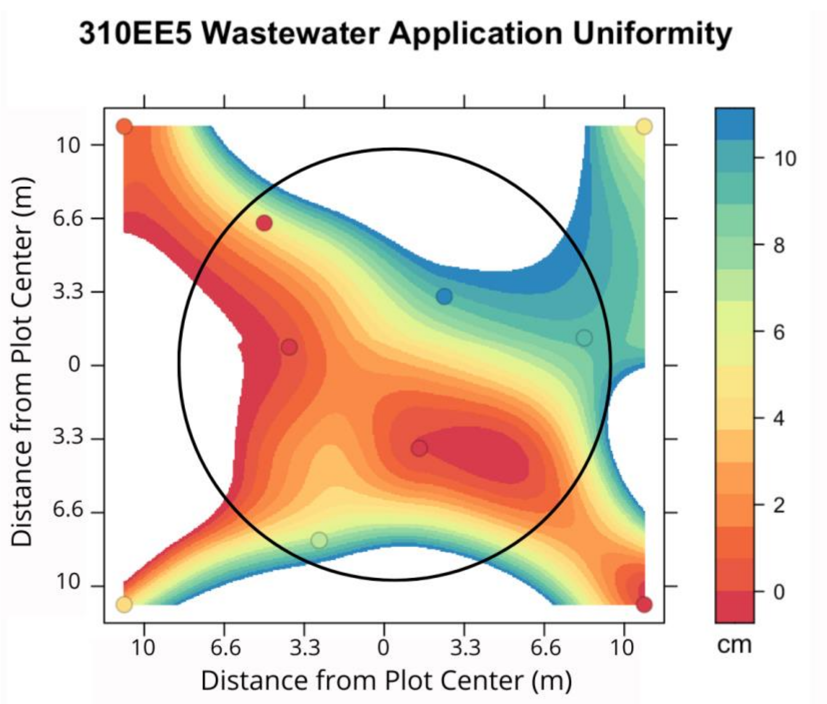
310EE5 Wastewater Application Uniformity
Distance from Plot Center (m)
10
6.6
3.3
0
3.3
6.6
10
Distance from Plot Center (m)
cm
10
8
6
4
2
0

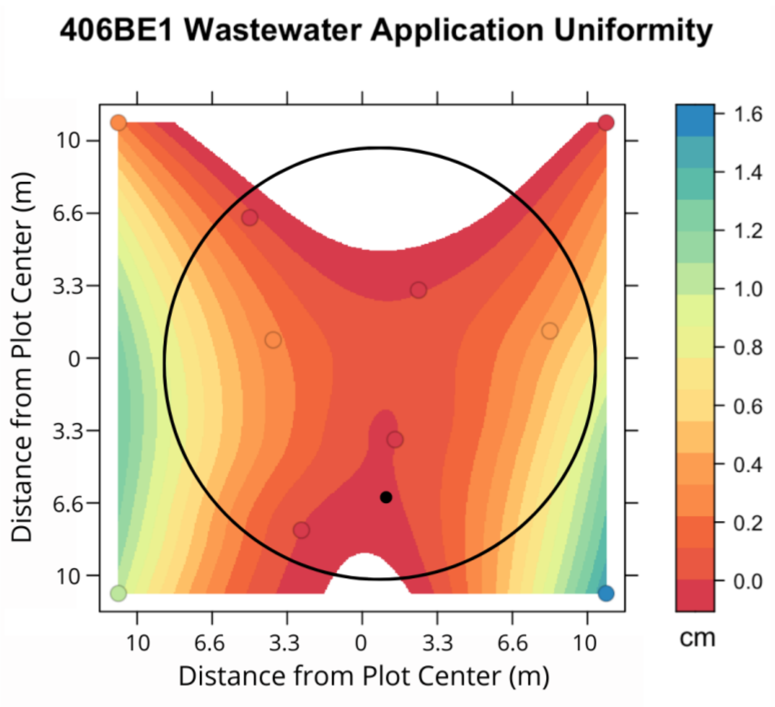
406BE1 Wastewater Application Uniformity
Distance from Plot Center (m)
10
6.6
3.3
0
3.3
6.6
10
Distance from Plot Center (m)
10
6.6
3.3
0
3.3
6.6
10
1.6
1.4
1.2
1.0
0.8
0.6
0.4
0.2
0.0
cm

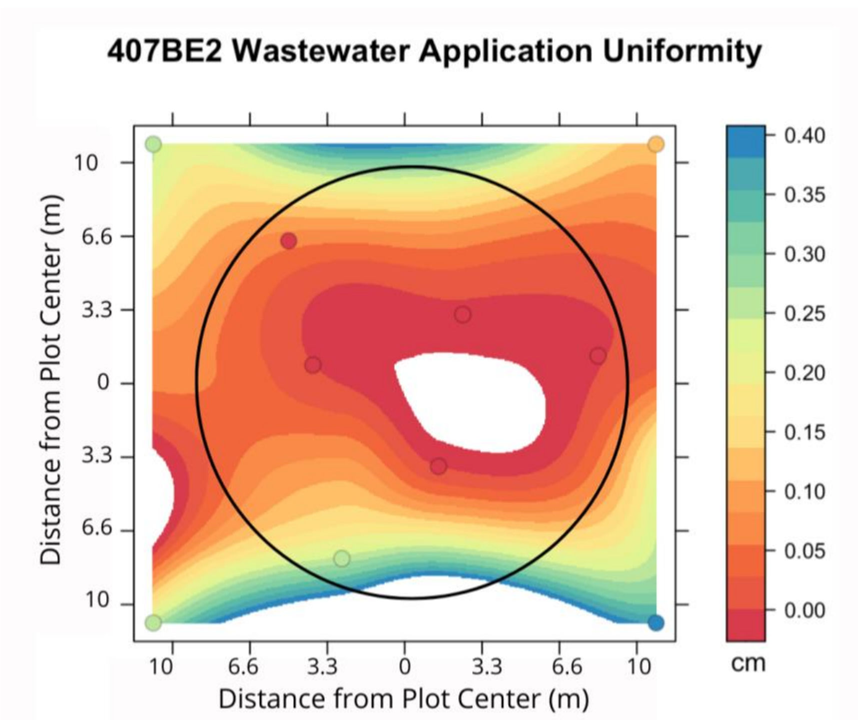
407BE2 Wastewater Application Uniformity
Distance from Plot Center (m)
10
6.6
3.3
0
3.3
6.6
10
Distance from Plot Center (m)
10
6.6
3.3
0
3.3
6.6
10
0.40
0.35
0.30
0.25
0.20
0.15
0.10
0.05
0.00
cm

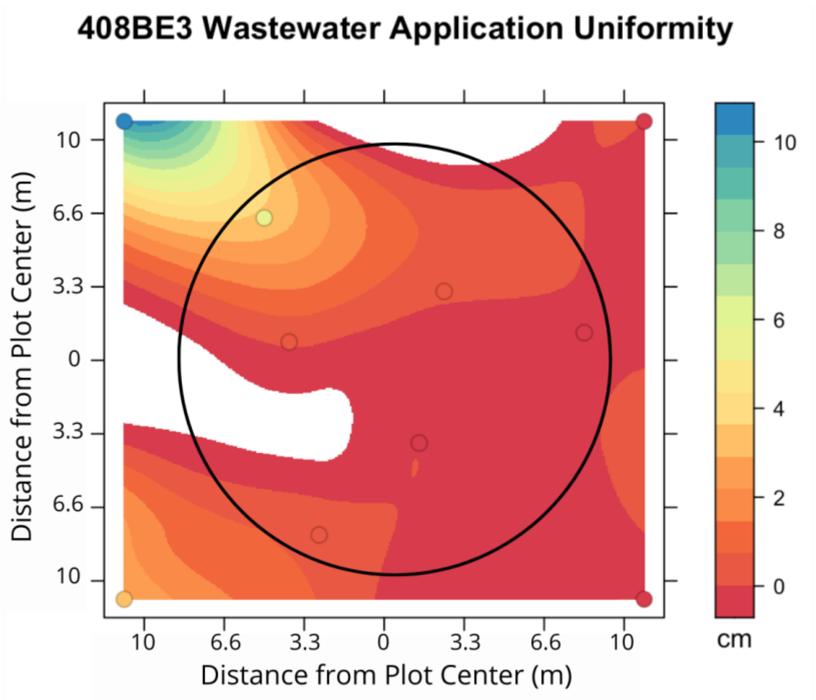
408BE3 Wastewater Application Uniformity
Distance from Plot Center (m)
10
6.6
3.3
0
3.3
6.6
10
Distance from Plot Center (m)
cm
10
8
6
4
2
0

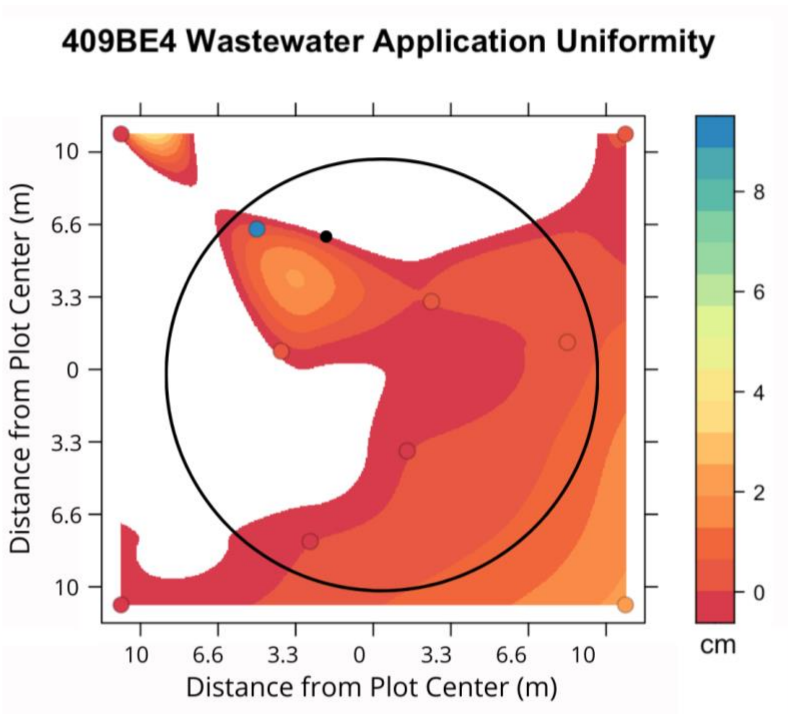
409BE4 Wastewater Application Uniformity
Distance from Plot Center (m)
10
6.6
3.3
0
3.3
6.6
10
Distance from Plot Center (m)
cm
8
6
4
2
0

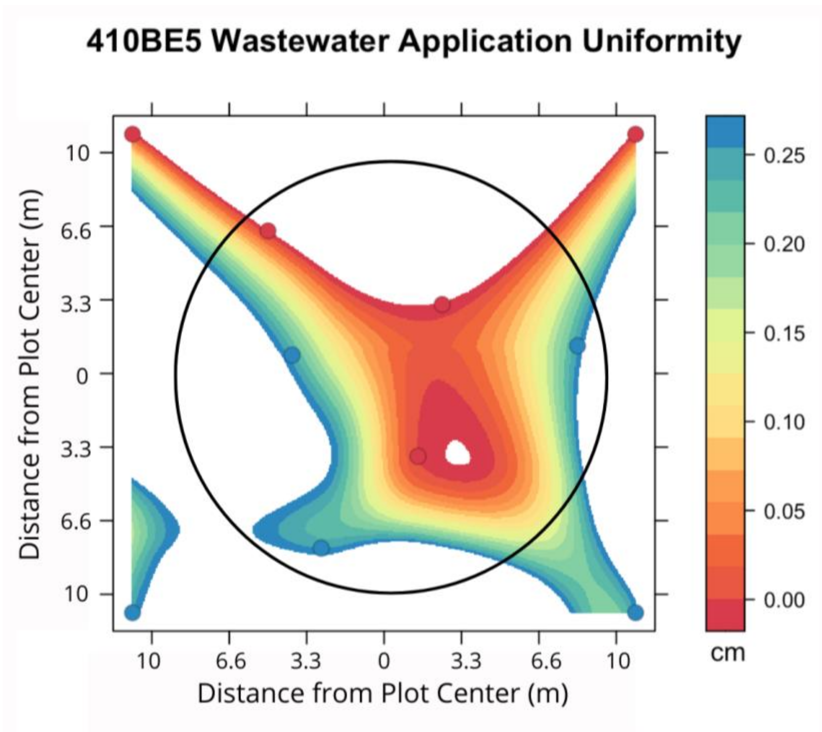
410BE5 Wastewater Application Uniformity
Distance from Plot Center (m)
10
6.6
3.3
0
3.3
6.6
10
Distance from Plot Center (m)
10
6.6
3.3
0
3.3
6.6
10
0.25
0.20
0.15
0.10
0.05
0.00
cm

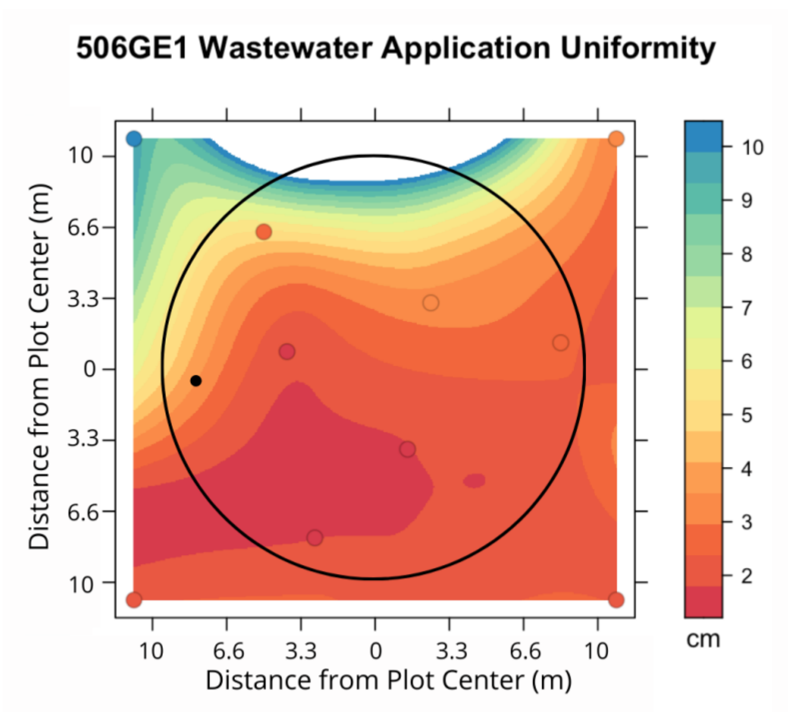
506GE1 Wastewater Application Uniformity
Distance from Plot Center (m)
10
6.6
3.3
0
3.3
6.6
10
Distance from Plot Center (m)
10
6.6
3.3
0
3.3
6.6
10
10
9
8
7
6
5
4
3
2
cm

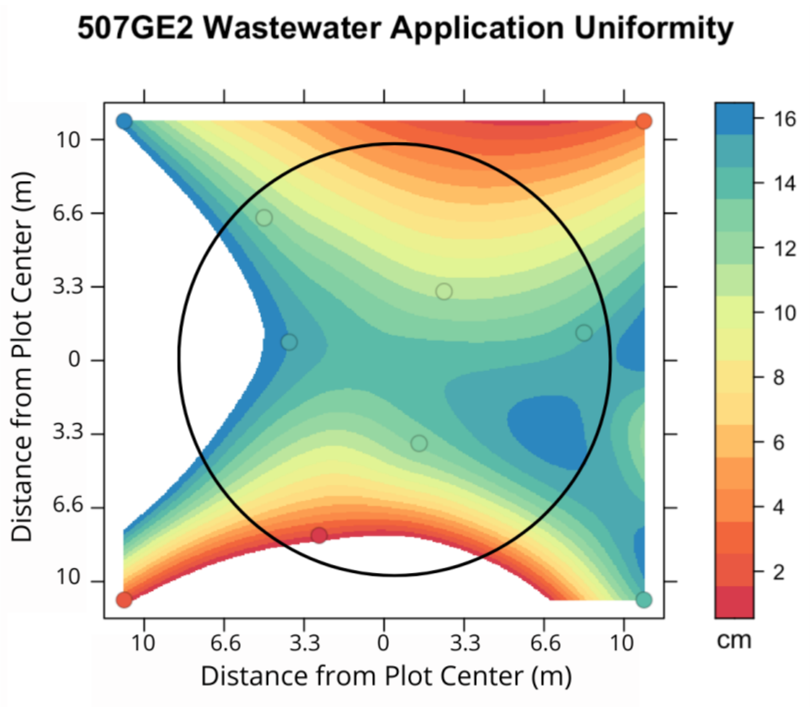
507GE2 Wastewater Application Uniformity
Distance from Plot Center (m)
10
6.6
3.3
0
3.3
6.6
10
Distance from Plot Center (m)
cm
16
14
12
10
8
6
4
2

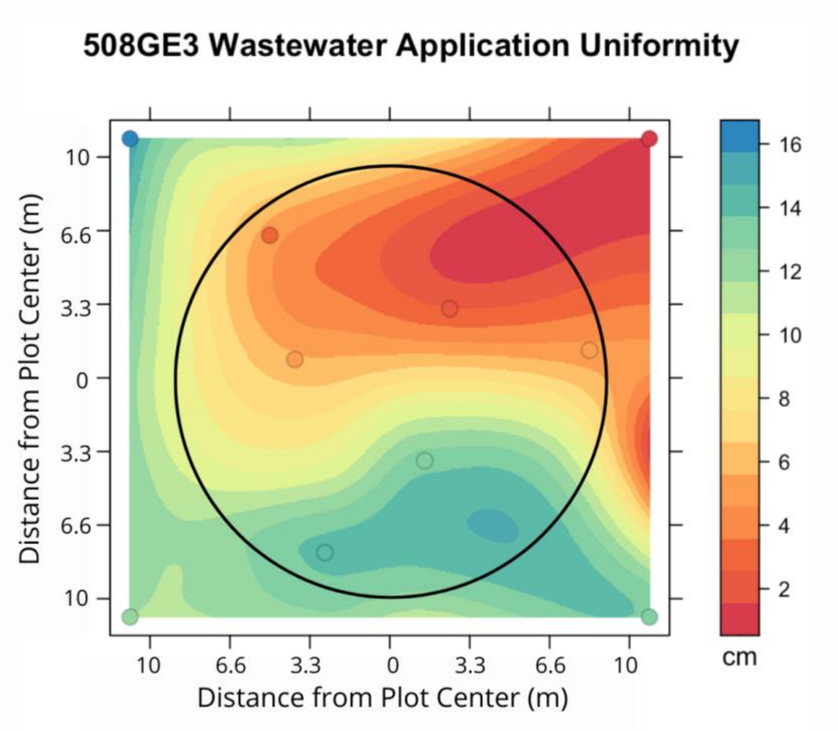
508GE3 Wastewater Application Uniformity
Distance from Plot Center (m)
10
6.6
3.3
0
3.3
6.6
10
Distance from Plot Center (m)
cm
16
14
12
10
8
6
4
2

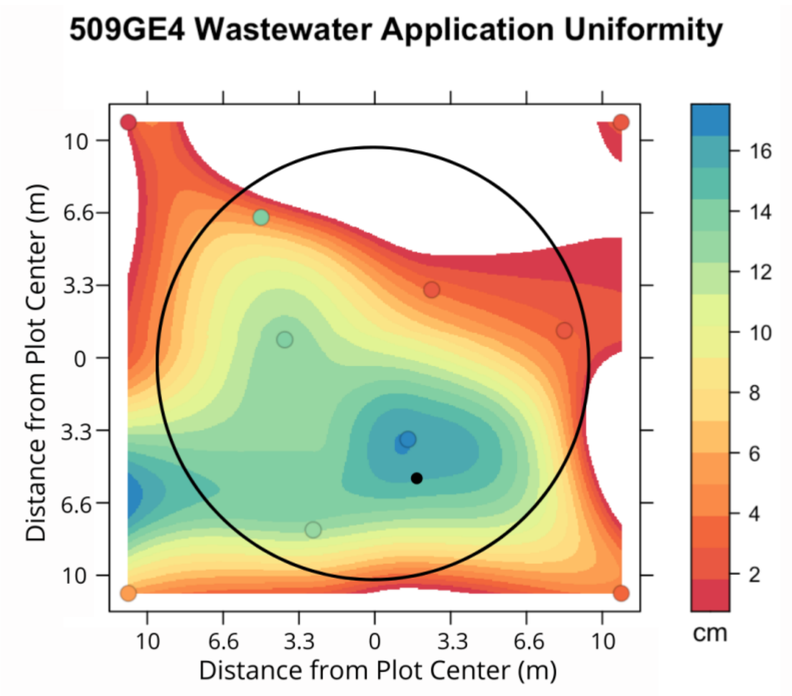
509GE4 Wastewater Application Uniformity
Distance from Plot Center (m)
Distance from Plot Center (m)
10
6.6
3.3
0
3.3
6.6
10
16
14
12
10
8
6
4
2
cm

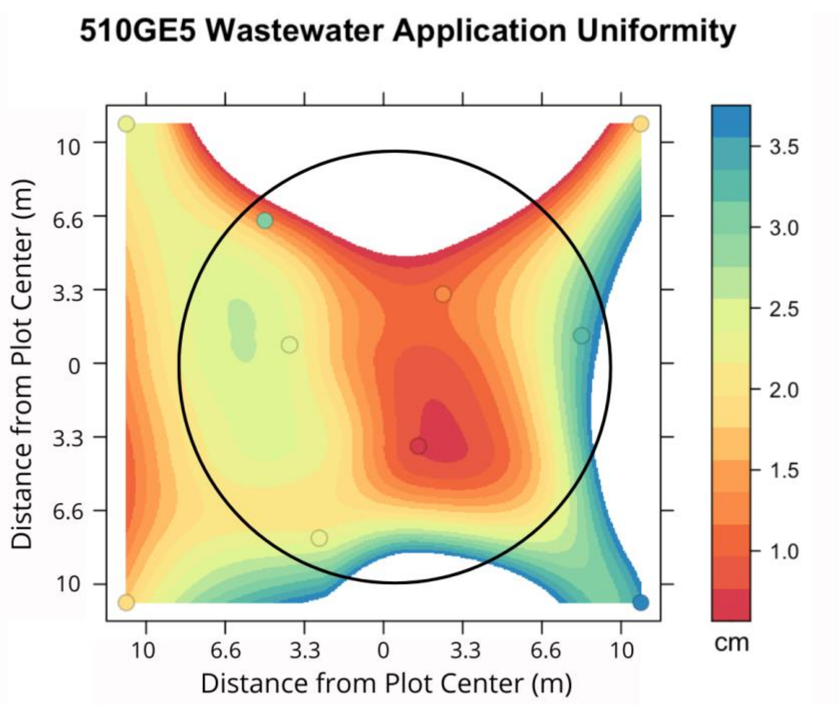
510GE5 Wastewater Application Uniformity
Distance from Plot Center (m)
Distance from Plot Center (m)
10
6.6
3.3
0
3.3
6.6
10
3.5
3.0
2.5
2.0
1.5
1.0
cm

Appendix G: Hydrus-1D and WEPP Analysis Table

Observed and predicted monthly drainage totals during the growing season with NSE, R^2, and RMSE values for Hydrus-1D and WEPP model runs of each drain gauge plot during the growing season without evapotranspiration and root water uptake. C represents a "control" non-irrigated plot and E represents an "effluent" irrigated plot. Values of "N/A" depict drain gauge plots with no observed drainage.

Facility	**Treatment**	**Observed Drainage**	**Predicted Drainage**		**NSE**		**R^2**		**RMSE**	
			Hydrus-1D	WEPP	Hydrus-1D	WEPP	Hydrus-1D	WEPP	Hydrus-1D	WEPP
Cave Bay	C	0	0	0	N/A	N/A	N/A	N/A	0	0
Heyburn State Park	C	0	0	0	N/A	N/A	N/A	N/A	0	0
	E	1.4	1.0	0.2	0.85	-0.31	0.93	0.001	0.15	0.45
	E	0	0	0	N/A	N/A	N/A	N/A	0	0
Ellisport Bay	C	51.1	40.9	42.6	0.65	0.59	0.75	0.64	2.73	3.24
	E	0	0	0	N/A	N/A	N/A	N/A	0	0
	E	0	0	0	N/A	N/A	N/A	N/A	0	0
Bottle Bay	C	0	0	0	N/A	N/A	N/A	N/A	0	0
	E	1	1	1.9	1.0	0.54	1.0	0.85	0.04	0.21
	E	0.2	0.1	0	0.69	-0.25	1.0	N/A	0.05	0.09
Garfield Bay	C	0	0	0	N/A	N/A	N/A	N/A	0	0
	E	6.2	6.5	6.2	0.99	0.97	0.99	0.97	0.19	0.39
	E	21.6	21.8	19.9	0.92	0.79	0.92	0.88	1.75	2.75

Literature Cited

Al-Jamal, M., Sammis, T., Mexal, J., Picchioni, G., & Zachritz, W. (2002). A growth-irrigation scheduling model for wastewater use in forest production. *Agricultural Water Management, 56*(1), 57-79.

Benson, M., Myers, B., & Raison, R. (1992). Dynamics of stem growth of Pinus radiata as affected by water and nitrogen supply. *Forest Ecology and Management, 52*(1-4), 117-137.

Birch, A. L., Emanuel, R. E., James, A. L., & Nichols, E. G. (2016). Hydrologic impacts of municipal wastewater irrigation to a temperate forest watershed. *Journal of environmental quality, 45*(4), 1303-1312.

Bond, W. J. (1998). Effluent irrigation—an environmental challenge for soil science. *Soil Research, 36*(4), 543-556.

Brister, G., & Schultz, R. (1981). *The response of a southern Appalachian forest to waste water irrigation* (0047-2425). Retrieved from

Brockway, D. G., Urie, D. H., Nguyen, P., & Hart, J. B. (1986). Wastewater and sludge nutrient utilization in forest ecosystems. *In: Cole, DW, Henry CL, Nutter, WL (eds.), The Forest Alternative for Treatment and Utilization of Municipal and Industrial Wastes. University of Washington Press, Seattle, Washington. Pp. 221-245.*

Brooks, E. S., Dobre, M., Elliot, W. J., Wu, J. Q., & Boll, J. (2016). Watershed-scale evaluation of the Water Erosion Prediction Project (WEPP) model in the Lake Tahoe basin. *Journal of Hydrology, 533*, 389-402.

Carlson, M. (1992). Municipal effluent irrigation of fast-growing hybrid poplar plantations near Vernon, British Columbia. *The Forestry Chronicle, 68*(2), 206-208.

Clark, M. (2020a). How to Build a Homemade Drain Gauge (part1). Retrieved from https://youtu.be/Hs-0WGmB5cw

Clark, M. (2020b). How to Build a Homemade Drain Gauge (part2). Retrieved from https://youtu.be/XkjlVgpBdiw

Clark, M. (2020c). Predicting Soil Hydraulic Conductivity with RETC. Retrieved from https://youtu.be/PssFBRm5h5Q

Cook, F., Kelliher, F., & McMahon, S. (1994). Changes in infiltration and drainage during wastewater irrigation of a highly permeable soil. *Journal of Environmental Quality, 23*(3), 476-482.

Cromer, R. (1980). Irrigation of radiata pine with waste water: a review of the potential for tree growth and water renovation. *Australian Forestry, 43*(2), 87-100.

Di, N., Wang, Y., Clothier, B., Liu, Y., Jia, L., Xi, B., & Shi, H. (2019). Modeling soil evaporation and the response of the crop coefficient to leaf area index in mature Populus tomentosa plantations growing under different soil water availabilities. *Agricultural and Forest Meteorology, 264*, 125-137.

Dimitriou, I., & Aronsson, P. (2011). Wastewater and sewage sludge application to willows and poplars grown in lysimeters–plant response and treatment efficiency. *biomass and bioenergy, 35*(1), 161-170.

Docktor, D., & Palmer, P. L. (1994). *Computation of the 1982 Kimberly-Penman and the Jensen-Haise Evapotranspiration Equations as Applied in the U.S. Bureau of Reclamation's Pacific*

Northwest AgriMet Program Computation of the 1982 Kimberly-Penman and the Jensen-Haise Evapotranspiration Equations as Applied in the U.S. Bureau of Reclamation's Pacific Northwest AgriMet Program U.S. Bureau of Reclamation

Drew, M., & Lynch, J. M. (1980). Soil anaerobiosis, microorganisms, and root function. *Annual Review of Phytopathology, 18*(1), 37-66.

Dun, S., Wu, J. Q., Elliot, W. J., Robichaud, P. R., Flanagan, D. C., Frankenberger, J. R., . . . Xu, A. C. (2009). Adapting the Water Erosion Prediction Project (WEPP) model for forest applications. *Journal of Hydrology, 366*(1-4), 46-54.

Elliot, W. J. (2013). Erosion processes and prediction with WEPP technology in forests in the Northwestern US. *Transactions of the ASABE, 56*(2), 563-579.

EPA. (2012). *Guidelines for Water Reuse*. (EPA/600/R-12/618). U.S. Environmental Protection Agency

Fan, J., Oestergaard, K. T., Guyot, A., Jensen, D. G., & Lockington, D. A. (2015). Spatial variability of throughfall and stemflow in an exotic pine plantation of subtropical coastal Australia. *Hydrological Processes, 29*(5), 793-804.

Feddes, R. A., Kowalik, P. J., & Zaradny, H. (1978). Simulation of Field Water Use and Crop Yield. *Centre for Agricultural Publishing and Documentation*.

Ferro, A. M., & Tammi, C. E. (2009). Field note: Irrigation of tree stands with groundwater containing 1, 4-dioxane. *International journal of phytoremediation, 11*(5), 425-440.

Gee, G. W., Zhang, Z., Ward, A. L., & Keller, J. M. (2004). Passive-wick water fluxmeters: theory and practice. *Supersoil, 2004*, 3rd.

Gessel, S., Miller, R., & Cole, D. (1990). Relative importance of water and nutrients on the growth of coast Douglas fir in the Pacific Northwest. *Forest Ecology and Management, 30*(1-4), 327-340.

Hall, F. (2018). Protocol for Deployment and Operation of Deep Soil Percolation Sampler. In (pp. 1-43): State of Idaho Department of Environmental Quality.

Hardie, M. A., Cotching, W. E., Doyle, R. B., Holz, G., Lisson, S., & Mattern, K. (2011). Effect of antecedent soil moisture on preferential flow in a texture-contrast soil. *Journal of Hydrology, 398*(3-4), 191-201.

Hoogland, J., Feddes, R. A., & Belmans, C. (1981). *Root water uptake model depending on soil water pressure head and maximum extraction rate.* Paper presented at the III International Symposium on Water supply and Irrigation in the open and under Protected Cultivation 119.

Hornberger, G. M., Germann, P. F., & Beven, K. J. (1991). Throughflow and solute transport in an isolated sloping soil block in a forested catchment. *Journal of hydrology, 124*(1), 81-99.

IDEQ. (2007). *Guidance for Reclamation and Reuse of Municipal and Industrial Wastewater*. Idaho Department of Environmental Quality

Isebrands, J. G., & Richardson, J. (2014). *Poplars and willows: trees for society and the environment*: CABI.

Jackson, R. B., Canadell, J., Ehleringer, J. R., Mooney, H., Sala, O., & Schulze, E.-D. (1996). A global analysis of root distributions for terrestrial biomes. *Oecologia, 108*(3), 389-411.

Jones, H. G. (2004). Irrigation scheduling: advantages and pitfalls of plant-based methods. *Journal of experimental botany, 55*(407), 2427-2436.

Kim, D. Y., & Burger, J. A. (1997). Nitrogen transformations and soil processes in a wastewater-irrigated, mature Appalachian hardwood forest. *Forest Ecology and Management, 90*(1), 1-11.

Kuhn, G. A. (2000). Wastewater management using hybrid poplar.

Lai, X., Liao, K., Feng, H., & Zhu, Q. (2016). Responses of soil water percolation to dynamic interactions among rainfall, antecedent moisture and season in a forest site. *Journal of Hydrology, 540*, 565-573.

Lee, S.-C., Black, T. A., Jassal, R. S., Christen, A., Meyer, G., & Nesic, Z. (2020). Long-term impact of nitrogen fertilization on carbon and water fluxes in a Douglas-fir stand in the Pacific Northwest. *Forest Ecology and Management, 455*, 117645.

Leuther, F., Schlüter, S., Wallach, R., & Vogel, H.-J. (2019). Structure and hydraulic properties in soils under long-term irrigation with treated wastewater. *Geoderma, 333*, 90-98.

Lew, R., Dobre, M., Srivastava, A., Brooks, E. S., Elliot, W. J., Robichaud, P. R., & Flanagan, D. C. (2022). WEPPcloud: An online watershed-scale hydrologic modeling tool. Part I. Model description. *Journal of Hydrology, 608*, 127603.

Magesan, G. (2001). AFTER IRRIGATION OF TWO FORESTED SOILS WITH MUNICIPAL WASTEWATER. *New Zealand Journal of Forestry Science, 31*(2), 188-195.

Matheny, A. M., Bohrer, G., Garrity, S. R., Morin, T. H., Howard, C. J., & Vogel, C. S. (2015). Observations of stem water storage in trees of opposing hydraulic strategies. *Ecosphere, 6*(9), 1-13.

Meissner, R., Rupp, H., Seeger, J., Ollesch, G., & Gee, G. (2010). A comparison of water flux measurements: passive wick-samplers versus drainage lysimeters. *European journal of soil science, 61*(4), 609-621.

METER. (2020). Drain Gauge G3 Lysimeter. Retrieved from https://www.metergroup.com/environment/products/drain-gauge-g3-lysimeter/

Molina, A. J., & del Campo, A. D. (2012). The effects of experimental thinning on throughfall and stemflow: A contribution towards hydrology-oriented silviculture in Aleppo pine plantations. *Forest Ecology and Management, 269*, 206-213.

Moriasi, D. N., Arnold, J. G., Van Liew, M. W., Bingner, R. L., Harmel, R. D., & Veith, T. L. (2007). Model evaluation guidelines for systematic quantification of accuracy in watershed simulations. *Transactions of the ASABE, 50*(3), 885-900.

Noguchi, S., Nik, A. R., Kasran, B., Tani, M., Sammori, T., & Morisada, K. (1997). Soil physical properties and preferential flow pathways in tropical rain forest, Bukit Tarek, Peninsular Malaysia. *Journal of Forest Research, 2*(2), 115-120.

NRC. (2012). *Water Reuse: Potential for Expanding the Nation's Water Supply Through Reuse of Municipal Wastewater*: The National Academies Press.

NRCS. (2022). Web Soil Survey. Retrieved from https://websoilsurvey.sc.egov.usda.gov/App/WebSoilSurvey.aspx

Pangle, R., Kavanagh, K., & Duursma, R. (2015). Decline in canopy gas exchange with increasing tree height, atmospheric evaporative demand, and seasonal drought in co-occurring inland Pacific Northwest conifer species. *Canadian Journal of Forest Research, 45*(8), 1086-1101.

Peters, T., & Hill, S. Irrigation Scheduler Mobile. Retrieved from http://weather.wsu.edu/is/

Petersen, M. R., & Hill, R. W. (1985). Evapotranspiration of small conifers. *Journal of irrigation and drainage engineering, 111*(4), 341-351.

PRISM. (2022). Time Series Values for Individual Locations. Retrieved from https://www.prism.oregonstate.edu/explorer/

Ramos, T., Šimůnek, J., Gonçalves, M., Martins, J., Prazeres, A., Castanheira, N., & Pereira, L. (2011). Field evaluation of a multicomponent solute transport model in soils irrigated with saline waters. *Journal of Hydrology, 407*(1-4), 129-144.

Schmidt, A., Mainwaring, D. B., & Maguire, D. A. (2020). Development of a tailored combination of machine learning approaches to model volumetric soil water content within a mesic forest in the Pacific Northwest. *Journal of Hydrology, 588*, 125044.

Singh, P., Deshbhratar, P., & Ramteke, D. (2012). Effects of sewage wastewater irrigation on soil properties, crop yield and environment. *Agricultural water management, 103*, 100-104.

Sparling, G., Barton, L., Duncan, L., McGill, A., Speir, T., Schipper, L., . . . Van Schaik, A. (2006). Nutrient leaching and changes in soil characteristics of four contrasting soils irrigated with secondary-treated municipal wastewater for four years. *Soil Research, 44*(2), 107-116.

Srivastava, A., Wu, J. Q., Elliot, W. J., & Brooks, E. S. (2015). Enhancements to the Water Erosion Prediction Project (WEPP) for Modeling Large Snow-Dominated Mountainous Forest Watersheds. In *Watershed Management 2015* (pp. 209-228).

Sutinen, R., Hänninen, P., & Venäläinen, A. (2008). Effect of mild winter events on soil water content beneath snowpack. *Cold Regions Science and Technology, 51*(1), 56-67.

Taiz, L., & Zeiger, E. (2002a). Water and Plant Cells. In *Plant Physiology* (3rd ed., pp. 33-46). Sunderland, MA, USA: Sinauer Associates Inc.

Taiz, L., & Zeiger, E. (2002b). Water Balance of Plants. In *Plant Physiology* (3rd ed., pp. 47-65). Sunderland, MA, USA: Sinauer Associates Inc.

USBR. (2022). AgriMet Weather Data. Retrieved from https://www.usbr.gov/pn/agrimet/h2ouse.html

Van Der Heijden, G., Legout, A., Pollier, B., Bréchet, C., Ranger, J., & Dambrine, E. (2013). Tracing and modeling preferential flow in a forest soil—Potential impact on nutrient leaching. *Geoderma, 195*, 12-22.

Vogeler, I. (2009). Effect of long-term wastewater application on physical soil properties. *Water, air, and soil pollution, 196*(1-4), 385-392.

Wang, J., Wang , G., & Wanyan, H. (2007). Treated wastewater irrigation effect on soil, crop and environment: Wastewater recycling in the loess area of China. *Journal of Environmental Sciences, 19*(9), 1093-1099.

Wang, L., Flanagan, D. C., & Cherkauer, K. A. (2017). Development of a coupled water quality model. *Transactions of the ASABE, 60*(4), 1153-1170.

Waring, R. H., Rogers, J. J., & Swank, W. T. (1980). Dynamic properties of forest ecosystems. In *Dynamic properties of forest ecosystems* (pp. 207-255): Cambridge University Press.

Waring, R. H., Running, S. W., Holbo, H. R., & Kline, J. R. (1979). *INTERNAL REPORT: MODELING WATER UPTAKE ON CONIFEROUS FOREST OREGON WATERSHED 10 SYNTHESIS*.

Warren, J., Meinzer, F., Brooks, J., & Domec, J. (2005). Vertical stratification of soil water storage and release dynamics in Pacific Northwest coniferous forests. *Agricultural and Forest Meteorology, 130*(1-2), 39-58.

WEPPcloud. (2022). WEPPcloud. Retrieved from https://wepp.cloud/weppcloud/

Wongkaew, A., Saito, H., Fujimaki, H., & Šimůnek, J. (2018). Numerical analysis of soil water dynamics in a soil column with an artificial capillary barrier growing leaf vegetables. *Soil Use and Management, 34*(2), 206-215.

Zhu, Y., Fox, R., & Toth, J. (2002). Leachate collection efficiency of zero-tension pan and passive capillary fiberglass wick lysimeters. *Soil Science Society of America Journal, 66*(1), 37-43.

Šimůnek, J., van Genuchten, M. T., & Šejna, M. (2008). Development and applications of the HYDRUS and STANMOD software packages and related codes. *Vadose Zone Journal, 7*(2), 587-600.